FEDERAL UNIVERSITY OF CEARA
TECHNOLOGY CENTER
DEPARTMENT OF ELECTRICAL ENGINEERING
GRADUATE PROGRAM IN ELECTRICAL ENGINEERING

RENÉ DESCARTES OLIMPIO PEREIRA

AUTO-TUNING CONTROL TECHNIQUES APPLIED TO A NEONATAL INCUBATOR

FORTALEZA

2016

RENÉ DESCARTES OLIMPIO PEREIRA

AUTO-TUNING CONTROL TECHNIQUES APPLIED TO A NEONATAL INCUBATOR

Dissertation presented to the Graduate Program in Electrical Engineering from Federal University of Ceara as a partial requirement to obtain the title of Master in Electrical Engineering. Concentration field: Electric Power Systems.

Supervisor: Prof. Dr. Bismark Claure Torrico
Co-supervisor: Prof. Dr. Fabrício Gonzalez Nogueira

FORTALEZA

2016

Dados Internacionais de Catalogação na Publicação
Universidade Federal do Ceará
Biblioteca Universitária
Gerada automaticamente pelo módulo Catalog, mediante os dados fornecidos pelo(a) autor(a)

P495a Pereira, René Descartes Olimpio.
Auto-tuning control techniques applied to a neonatal incubator / René Descartes Olimpio Pereira. – 2016.
143 f. : il. color.

Dissertação (mestrado) – Universidade Federal do Ceará, Centro de Tecnologia, Programa de Pós-Graduação em Engenharia Elétrica, Fortaleza, 2016.
Orientação: Prof. Dr. Bismark Claure Torrico.
Coorientação: Prof. Dr. Fabrício Gonzalez Nogueira.

1. auto-tuning. 2. PID control. 3. TITO processes. 4. dead-time compensator. 5. generalized predictive control. I. Título.

CDD 621.3

RENÉ DESCARTES OLIMPIO PEREIRA

AUTO-TUNING CONTROL TECHNIQUES APPLIED TO A NEONATAL INCUBATOR

Dissertation presented to the Graduate Program in Electrical Engineering from Federal University of Ceara as a partial requirement to obtain the title of Master in Electrical Engineering. Concentration field: Electric Power Systems.

Approved at Fortaleza, December 16, 2016.

EXAMINATION BOARD

Prof. Dr. Bismark Claure Torrico (Supervisor)
Federal University of Ceara

Prof. Dr. Fabrício Gonzalez Nogueira (Co-supervisor)
Federal University of Ceara

Prof. Dr. Julio Elias Normey-Rico
Federal University of Santa Catarina

Prof. Dr. Wilkley Bezerra Correia
Federal University of Ceara

Prof. Dr. Arthur Plínio de Souza Braga
Federal University of Ceara

This work is dedicated to my parents, Gabriel and Mércia.

ACKNOWLEDGEMENTS

To my Supervisor, Prof. Dr. Bismark Claure Torrico and my Co-supervisor, Prof. Dr. Fabrício Gonzalez Nogueira, for sharing their knowledge in process control theory and practice, for their guidance and suggestions to make this work possible and for giving me the opportunity to work in a research lab, the Research Group in Automation, Control and Robotics (GPAR).

To Prof. Dr. Julio Elias Normey-Rico, Prof. PhD Antonio Visioli and PhD Massimiliano (Max) Veronesi, for the opportunity to work on my first scientific journal article and for all the knowledge shared with me.

To all members of the examination board, for their attention and important contributions to improve this work.

To my family and friends, for their comprehension and support, manifested in different ways, that helped me to accomplish this work.

To the Fundação Cearense de Apoio ao Desenvolvimento Científico e Tecnológico (FUNCAP), for the financial support, by providing a scholarship.

“No one can build you the bridge on which you, and only you, must cross the river of life. There may be countless trails and bridges and demigods who would gladly carry you across; but only at the price of pawning and forgoing yourself. There is one path in the world that none can walk but you. Where does it lead? Don’t ask, walk!”

Friedrich W. Nietzsche

ABSTRACT

This work studies and proposes techniques of automatic tuning of controllers for single-input-single-output (SISO) and two-inputs-two-outputs (TITO) processes with dead time. Furthermore, it proposes a dead-time compensator (DTC) based on generalized predictive control (GPC) with anti-windup action. Firstly, generalities about the studied auto-tuning methodology are presented. The auto-tuning of proportional-integral-derivative (PID) controllers for SISO processes is studied e new methods for integrating and unstable processes are proposed. Following, it is proposed the auto-tuning of the simplified filtered Smith predictor, a robust dead-time compensator for stable, unstable and integrating SISO processes. The results for SISO processes are then extended for the auto-tuning of PID controllers for TITO processes. Finally, the GPC-based DTC with anti-windup action is presented. Its formulation can cope with stable, unstable and integrating SISO processes. Simulation results are presented, where studied and proposed methods are compared with other recent methods of the literature, highlighting their properties and advantages. Experimental results for stable SISO and TITO processes were obtained by applying the studied methods on the control of temperature and relative humidity of a neonatal incubator prototype and verify the effectiveness of the studied and proposed methods in a practical context.

Keywords: adaptive control; dead time; auto-tuning; PID control; TITO processes; dead-time compensator; generalized predictive control.

RESUMO

Este trabalho estuda e propõe técnicas de sintonia automática de controladores para processos de uma entrada e uma saída (SISO, do inglês single-input-single-output) e de duas entradas e duas saídas (TITO, do inglês two-input-two-output) com atraso de transporte. Além disso, ele propõe um compensador de atraso de transporte (DTC, do inglês dead-time compensator) baseado em controle preditivo generalizado (GPC, do inglês generalized predictive control) com ação anti-windup. Primeiramente, são apresentadas generalidades sobre a metodologia de sintonia automática estudada. A sintonia automática de controladores proporcional-integral-derivativos (PID) para processos SISO é estudada e novos métodos para processos integradores e instáveis são propostos. Em seguida, é proposta a sintonia automática do preditor de Smith filtrado simplificado, um compensador de atraso de transporte robusto para processos SISO estáveis, instáveis e integradores. Os resultados para processos SISO são então estendidos para a sintonia automática de controladores PID para processos TITO. Finalmente, o DTC baseado em GPC com ação anti-windup é apresentado. Sua formulação pode lidar com processos SISO estáveis, instáveis e integradores. São apresentados resultados de simulações, onde os métodos estudados e propostos são comparados com outros métodos recentes da literatura, destacando suas propriedades e vantagens. Resultados experimentais para processos SISO e TITO estáveis foram obtidos aplicando os métodos estudados no controle de temperatura e umidade relativa de um protótipo de incubadora neonatal e verificam a eficácia dos métodos estudados e propostos em um contexto prático.

Palavras-chave: controle adaptativo; atraso de transporte; sintonia automática; controle PID; processos TITO; compensador de atraso de transporte; controle preditivo generalizado.

LIST OF FIGURES

LIST OF TABLES

LIST OF ABBREVIATIONS AND ACRONYMS

SISO	single input single output
TITO	two inputs two outputs
PI	proportional integral
PID	proportional integral derivative
I-P	integral proportional
I-PD	integral proportional derivative
FVT	final value theorem
DTC	dead-time compensator
SP	Smith predictor
FSP	filtered Smith predictor
SFSP	simplified filtered Smith predictor
MSP	modified Smith predictor
MPC	model predictive control
GPC	generalized predictive control
LQI	linear quadratic integral
FOPDT	first order plus dead time
UFOPDT	unstable first order plus dead time
IPDT	integrator plus dead time
IFOPDT	integrating first order plus dead time
IAE	integrated absolute error
SIMC	simple internal model control
SP	set-point
LD	load disturbance
2DOF	two degree of freedom

RGA	relative gain array
US	undershoot
CARIMA	controlled auto regressive integral moving average
FIR	finite impulse response

LIST OF SYMBOLS

t	time
$r(t)$	set-point
$e(t)$	error
$u(t)$	control signal
$d(t)$	input disturbance
$j(t)$	process input
$y(t)$	process variable
s	complex frequency
$P(s)$	Laplace transform of the process model
$R(s)$	Laplace transform of the set-point
$E(s)$	Laplace transform of the error
$U(s)$	Laplace transform of the control signal
$D(s)$	Laplace transform of the input disturbance
$J(s)$	Laplace transform of the process input
μ	process gain
τ	time constant of the first-order process model
θ	apparent dead time of the first-order process model
θ_0	original dead time of the high-order process model
$q(s)$	Laplace transform of the denominator polynomial of the high-order process model
$m(s)$	neglected time constants of a first-order model reduction
τ_k	k-th time constant of the high-order process model
T_0	relation between time constants and dead time for stable processes
T_0'	relation between time constants and dead time for unstable processes

A_r	magnitude of the set-point step change
$e_{su}(t)$	virtual signal for stable processes after a set-point step change
$e_{uu}(t)$	virtual signal for unstable processes after a set-point step change
$e_{iu}(t)$	virtual signal for integrating processes after a set-point step change
A_d	magnitude of the step load disturbance
$e_{sj}(t)$	virtual signal for stable processes after a step load disturbance
$e_{uj}(t)$	virtual signal for unstable processes after a step load disturbance
$e_{ij}(t)$	virtual signal for integrating processes after a step load disturbance
$\Delta y(t)$	variation of the process variable
NB	noise band
$C(s)$	Laplace transform of the controller
K_p	proportional gain of the PID controller
T_i	integral time of the PID controller
T_d	derivative time of the PID controller
$C_i(s)$	Laplace transform of the integral term of the PID controller
$C_{pd}(s)$	Laplace transform of the proportional-derivative terms of the PID controller
$E_{su}(s)$	Laplace transform of e_{su}
$E_{uu}(s)$	Laplace transform of e_{uu}
$E_{iu}(s)$	Laplace transform of e_{iu}
$E_{sj}(s)$	Laplace transform of e_{sj}
$E_{uj}(s)$	Laplace transform of e_{uj}
$E_{ij}(s)$	Laplace transform of e_{ij}
IE	integral of the error
IU	integral of the control signal
IY	integral of the process variable
IJ	integral of the process input

IE_{su}	integral of $e_{su}(t)$
IE_{uu}	integral of $e_{uu}(t)$
IE_{iu}	integral of $e_{iu}(t)$
IE_{sj}	integral of $e_{sj}(t)$
IE_{uj}	integral of $e_{uj}(t)$
IE_{ij}	integral of $e_{ij}(t)$
ν	integration variable
DIE_f	double integral of the filtered error
DIJ	double integral of the process input
DIE_{sj}	double integral of $e_{sj}(t)$
DIE_{uj}	double integral of $e_{uj}(t)$
DIE_{ij}	double integral of $e_{ij}(t)$
γ	auto-tuning constant for the PID controller
K_P	proportional gain of the PID controller after the re-tuning
T_I	integral time of the PID controller after the re-tuning
T_D	derivative time of the PID controller after the re-tuning
Γ	auto-tuning constant for the PID controller after the re-tuning
IAE_a	actual integrated absolute error
IAE_{sp}	target integrated absolute error for a set-point step change
IAE_{ld}	target integrated absolute error for a step load disturbance
SPPI	set-point performance index
LDPI	load disturbance performance index
τ_c	desired closed-loop time constant
$P_n(s)$	Laplace transform of the nominal process model
$G_n(s)$	Laplace transform of the delay-free process model
μ_m	process gain of the nominal process model

τ_m	time constant of the nominal first-order process model
θ_m	apparent dead time of the nominal first-order process model
$F(s)$	Laplace transform of the reference filter
$F_r(s)$	Laplace transform of the robustness filter
$H_{yr}(s)$	continuous-time transfer function from the set-point to the process variable
$H_{yd}(s)$	continuous-time transfer function from the disturbance input to the process variable
$F_{eq}(s)$	Laplace transform of the equivalent reference filter
$C_{eq}(s)$	Laplace transform of the equivalent controller
k_c	proportional gain of the primary controller of the SFSP
k_r	reference gain of the SFSP
$\bar{H}_{yr}(s)$	continuous-time desired closed-loop transfer function from the set-point to the process variable
b_i	continuous-time numerator parameters of the robustness filter of the SFSP
α	time constant of the robustness filter of the SFSP
$e_f(t)$	filtered error
IE_f	integral of the filtered error
ϕ	auto-tuning constant of the SFSP for stable and unstable processes
Φ	auto-tuning constant of the SFSP for stable and unstable processes after the re-tuning
ψ	auto-tuning constant of the SFSP for integrating processes
Ψ	auto-tuning constant of the SFSP for integrating processes after the re-tuning
$\mathbf{P}(s)$	matrix transfer function of the process model
$P_{ij}(s)$	transfer function of the i-th row and j-column of the matrix transfer function of the process model
μ_{ij}	process gain of $P_{ij}(s)$
$q_{ij}(s)$	denominator polynomial of the high-order process model of $P_{ij}(s)$

$\tau_{ij,k}$	k-th time constant of the high-order process model of $P_{ij}(s)$
θ_{ij}	dead time of $P_{ij}(s)$
T_{ij}^{0}	relation between time constants and dead time for stable TITO processes
$\mathbf{C}(s)$	matrix transfer function of the controller
$\mathbf{C}_j(s)$	transfer function of the j-th row and j-column of the matrix transfer function of the controller
K_{Pj}	proportional gain of the PID controller $\mathbf{C}_j(s)$
T_{Ij}	integral time of the PID controller $\mathbf{C}_j(s)$
T_{Dj}	derivative time of the PID controller $\mathbf{C}_j(s)$
$r_j(t)$	j-th set-point
$e_j(t)$	j-th error
$u_j(t)$	j-th control signal
$y_j(t)$	j-th process variable
$R_j(s)$	Laplace transform of the j-th set-point
$E_j(s)$	Laplace transform of the j-th error
$U_j(s)$	Laplace transform of the j-th control signal
$Y_j(s)$	Laplace transform of the j-th process variable
$E_{j,n}(s)$	Laplace transform of the j-th error due to the n-th set-point step change
$IE_{j,n}(s)$	integral of $E_{j,n}(s)$
A_{sn}	magnitude of the n-th set-point step change
A_{un}	steady-state values of the output of the controllers $\mathbf{C}_j(s)$ due to the n-th set-point step change
$v(t)$	virtual signal for TITO processes related to $y_1(t)$
$w(t)$	virtual signal for TITO processes related to $y_2(t)$
$V(s)$	Laplace transform of $v(t)$
$W(s)$	Laplace transform of $w(t)$
$IV_n(s)$	integral of $v(t)$ due to the n-th set-point step change

$IW_n(s)$	integral of $w(t)$ due to the n-th set-point step change
$\tilde{P}_{ij}(s)$	FOPDT transfer function of the i-th row and j-column of the matrix transfer function of the identified process model
$\tilde{\mu}_{ij}$	process gain of $\tilde{P}_{ij}(s)$
$\tilde{\tau}_{ij}$	time constant of $\tilde{P}_{ij}(s)$
$\tilde{\theta}_{ij}$	dead time of $\tilde{P}_{ij}(s)$
λ_i	desired closed-loop time constant of the i-th control loop
t_s	settling time
z	z-transform operator
q	discrete-time operator
$P(z)$	z-transform of the nominal process model
$G(z)$	z-transform of the nominal delay-free process model
d	discrete-time dead time of the nominal process model
$A(z)$	discrete-time denominator polynomial of the nominal CARIMA process model of order n_a
$B(z)$	discrete-time numerator polynomial of the nominal CARIMA process model of order n_b
$C(z)$	discrete-time disturbance polynomial of the nominal CARIMA process model of order n_c
Δ	discrete-time integrator
$e(t)$	discrete-time white noise
J	cost function
Δu	control increment
ω	vector of future references
$\lambda(j)$	control weight
N	prediction horizon window
N_u	control horizon window

$\mathbf{Y}$	output prediction matrix
$\Delta\mathbf{U}$	control increment prediction matrix
$\mathbf{W}$	reference prediction matrix
$\mathbf{Q}$	control weight matrix
$\mathbf{U}$	control prediction matrix
$\mathbf{M}$	auxiliary matrix of dimension N_u x N_u
$\bar{\mathbf{U}}$	control vector of dimension N_u x 1
$F_j(z)$	discrete-time polynomial of order n_a
$f_{j,n}$	n-th coefficient of $F_j(z)$, where $n = 0,\ 1, ...,\ n_a$
$\tilde{F}_k(z)$	discrete-time polynomial of order n_a
$\tilde{f}_{k,n}$	n-th coefficient of $\tilde{F}_k(z)$, where $n = 0,\ 1, ...,\ n_a$
$E_j(z)$	discrete-time polynomial of order $k-d-1$
e_n	n-th coefficient of $E_j(z)$, where $n = 0,\ 1, ...,\ k-d-1$
$\tilde{E}_k(z)$	discrete-time polynomial of order $k-1$
$\tilde{e}_n$	n-th coefficient of $\tilde{E}_k(z)$, where $n = 0,\ 1, ...,\ k-1$
$G_j(z)$	discrete-time polynomial of order $k-d-1$
h_n	n-th coefficient of $G_j(z)$, where $n = 1,\ 2, ...,\ k-d$
$\tilde{G}_j(z)$	discrete-time polynomial of order n_b-1
$\tilde{g}_n$	n-th coefficient of $\tilde{G}_j(z)$, where $n = 0,\ 1, ...,\ n_b-1$
$\mathbf{G}$	dynamic matrix
$\mathbf{f}$	free response matrix
$\tilde{\mathbf{G}}$	matrix of polynomials $G_j(z)$ of dimension N x 1
$\mathbf{F}$	matrix of polynomials $F_j(z)$ of dimension N x 1
$\tilde{\mathbf{F}}$	matrix of polynomials $\tilde{F}_k(z)$ of dimension N x 1
$\mathbf{H}$	auxiliary matrix
$\mathbf{b}$	auxiliary matrix

k_0	the element of the first row and first column of $(\mathbf{G}^T\mathbf{G}+\mathbf{M}^T\mathbf{Q}\mathbf{M})^{-1}\mathbf{M}^T\mathbf{Q}$
$\mathbf{k}_1$	the first row of $(\mathbf{G}^T\mathbf{G}+\mathbf{M}^T\mathbf{Q}\mathbf{M})^{-1}\mathbf{G}^T$
k_r	the sum of the elements of $\mathbf{k}_1$
$P_0(z)$	discrete-time polynomial of the DTC-GPC formulation
$P_1(z)$	discrete-time polynomial of the DTC-GPC formulation
$P_2(z)$	discrete-time polynomial of the DTC-GPC formulation
$P_3(z)$	discrete-time polynomial of the DTC-GPC formulation
$P_4(z)$	discrete-time polynomial of the DTC-GPC formulation
$P_5(z)$	discrete-time polynomial of the DTC-GPC formulation
$P_6(z)$	discrete-time polynomial of the DTC-GPC formulation
$T(z)$	discrete-time filter of the DTC-GPC formulation
α_i	tuning parameters of the $C(z)$ polynomial
$R(z)$	z-transform of the set-point
$U(z)$	z-transform of the control signal
$U_{sat}(z)$	z-transform of the constrained control signal
$Q(z)$	z-transform of the disturbance
$V(z)$	z-transform of the measurement noise
$Y(z)$	z-transform of the process variable
$H_{yr}(z)$	discrete-time transfer function from the set-point to the process variable
$H_{yq}(z)$	discrete-time transfer function from the disturbance input to the process variable
$H_{uv}(z)$	discrete-time transfer function from the measurement noise to the control signal
ω	frequency
$I_r(z)$	robustness index
$\Delta P(z)$	norm-bound multiplicative uncertainty
T_s	sampling period
$S(z)$	expression for implementation of the DTC-GPC

CONTENTS

1 INTRODUCTION

The automatic tuning (auto-tuning) of a controller is a technique that computes controller parameters in an automated way when the process model parameters are unknown. The first significant progresses in this field occurred in the nineteen-seventies, when the growing availability of digital computers stimulated the development of several techniques (KEYES; KAYA, 1989). Today, with increasingly computational resources available, several problems were solved, there is a wide theory behind it, and a growing number of practical applications. In the process control industry, such developments made an user-initiated auto-tuning function one of the most desired features of an industrial controller (CONTROL ENGINEERING, 2006).

Model predictive control (MPC) is also a control technique that over the last decades had great impact on the process control industry. Being based on the concepts of optimal control, stochastic control, finite control horizon, and others, it can easily deal with constraints. Furthermore, its formulation can handle processes with dead time (CAMACHO; BORDONS, 2007).

1.1 State of the art

1.1.1 The auto-tuning methodology

The auto-tuning methods studied and proposed in this work are based on a methodology that has been applied to different types of controllers and processes in the last years. Such methodology was applied to proportional-integral-derivative (PID) controllers for stable processes in (VERONESI; VISIOLI, 2009; VERONESI; VISIOLI, 2010a; VERONESI; VISIOLI, 2012) and for integrating processes based on integrating-first-order-plus-dead-time (IFOPDT) models in (VERONESI; VISIOLI, 2010b), to cascade PID controllers in (VERONESI; VISIOLI, 2011b), to TITO PID controllers in (VERONESI; VISIOLI, 2011a; PEREIRA; TORRICO, 2015; PEREIRA et al., 2017) and to dead-time compensators for stable, integrating and unstable processes in (NORMEY-RICO et al., 2014; PEREIRA et al., 2016).

The studied and proposed auto-tunings are applicable to controllers manually tuned (roughly tuned), based on an inconsistent model, or acting over time-varying plants (self-tuning). It consists of: (i) a closed-loop identification of a new model after a set-point step change or a step load disturbance, (ii) a performance assessment and (iii) the re-tuning of the controller.

In this work, such methodology is applied to PID controllers and to the simplified filtered Smith predictor (SFSP) for SISO stable, unstable and integrating processes described by first-order-plus-dead-time (FOPDT), unstable-first-order-plus-dead-time (UFOPDT) and integrating-plus-dead-time (IPDT) models, respectively. In the MIMO case, the methodology is applied to decentralized PID controllers for TITO processes.

The auto-tuning procedure can be applied after a set-point step change (for SISO and TITO processes) or a step load disturbance (for SISO processes), when the system reaches the steady-state. The identification method is based on the analysis of the closed-loop system signals that converge to zero at the steady-state. Those signals exhibit the characteristic that its integrals or its double integrals have a non-zero finite value at the steady-state. Therefore, by applying the final value theorem (FVT), relations between these integrals and the process model parameters can be obtained.

1.1.2 Auto-tuning of PID controllers for SISO processes

The auto-tuning of PID controllers for stable processes was first presented by (VERONESI; VISIOLI, 2009; VERONESI; VISIOLI, 2012) and is studied in this work. In addition, some modifications for the unstable and integrating cases are proposed. The integrating case differs from (VERONESI; VISIOLI, 2010b) in terms of the identified model, as an IPDT model is considered herein, while in the mentioned work an integrating-first-order-plus-dead-time (IFOPDT) model is taken into account. Therefore, both formulations are different.

Modifications in the auto-tuning methodology of several works presented by Veronesi and Visioli are also proposed in this work. For instance, the formulations take in account that any tuning rule can be chosen to re-tune the PID controller. In addition, the formulations were expressed as compact as possible, in order to simplify the computations and evidence their similarities between different processes and even different controllers. For cases where smoother responses for set-point changes are required, formulations for the integral-proportional-derivative (I-PD) controller were also proposed.

1.1.3 Auto-tuning of the simplified filtered Smith predictor

Over the last decades, the study of dead-time processes has been widely considered, regarding its importance for both academia and industry. Within this context, the Smith predictor (SP) (SMITH, 1957), described as the first dead-time compensator (DTC) proposed in the literature, plays an important role.

Many modifications regarding the SP structure have been proposed over the last decades, as in (MATAUŠEK; MICIC, 1996), to deal with integrating processes and, as in (MATAUŠEK; RIBIĆ, 2012), to deal with stable, integrating and unstable processes. The filtered Smith predictor (FSP) includes a robustness filter, which makes the proposed structure able to deal with stable, integrating and unstable processes, as it improves closed-loop robustness properties (NORMEY-RICO, 2007; NORMEY-RICO; CAMACHO, 2009). High frequencies noise attenuation is dealt in (SANTOS; BOTURA; NORMEY-RICO, 2010) and the study of SISO processes with multiple dead times can be found in (NORMEY-RICO et al., 2014) and (TORRICO; CORREIA; NOGUEIRA, 2016). The simplified FSP (SFSP) was proposed in (TORRICO et al., 2013)

for stable, unstable and integrating first-order models, which considers the controller and the reference filter as simple gains, easing the tuning procedure by making it more intuitive.

Following this idea, this work investigates simple tuning rules, when the auto-tuning methodologies proposed by (VERONESI; VISIOLI, 2009; VERONESI; VISIOLI, 2010a; VERONESI; VISIOLI, 2010b; VERONESI; VISIOLI, 2011b; VERONESI; VISIOLI, 2011a; VERONESI; VISIOLI, 2012; NORMEY-RICO et al., 2014) are applied. The proposed identification method is an extension of the methodology presented in (NORMEY-RICO et al., 2014) for the FSP auto-tuning and is presented for the three cases mentioned earlier (FOPDT, UFOPDT and IPDT models) for both set-point step changes and step load disturbances. Simulation results show a significant improvement when the system to be controlled is subjected to parameter uncertainties.

1.1.4 Auto-tuning of PID controllers for TITO processes

PID controllers are largely employed in industry because of their relative simplicity and the satisfactory performance they provide for a wide range of processes. For such a class of controller, many tuning rules and auto-tuning methods have been proposed in the past, especially for SISO systems (ÅSTRÖM; HÄGGLUND, 2006). However, many industrial plants are actually MIMO systems, and the interactions between the variables make the design of the controller more difficult. In this context, although Model-based Predictive Control has been proven to be effective and has been therefore applied successfully in many MIMO systems applications, the simplest option still remains the use of decentralized PID controllers. In any case, because of the above mentioned coupling between the variables, the tuning of the controller parameters is more difficult than in the SISO case (WANG et al., 2008; WANG; NIE, 2012) and, therefore, auto-tuning techniques are useful. Considering the analysis of the most common case, that is, of TITO processes, different methods have been proposed in the literature. For example, in (WANG; HUANG; GUO, 2000) the evaluation of open-loop step tests (one for each input) has been proposed to identify the process model. Based on it, a decoupler can then be suitably determined and then a sequential tuning method is implemented for decentralized PID controllers (note that in this case the overall controller is actually centralised). Regarding proposed closed-loop techniques, they are usually related to relay-feedback techniques. In particular, simultaneous (PALMOR; HALEVI; KRANSNEY, 1995; HALEVI; PALMOR; EFRATI, 1997; WANG et al., 1997) and sequential ones (SHEN; YU, 1994; SHIU; HWANG, 1998; MARCHETTI; SCALI; ROMAGNOLI, 2002) have been devised. Another closed-loop approach, based on finite frequency response data, has been proposed in (GILBERT et al., 2003). In this case, it is assumed that the feedback controllers have been already (possibly roughly) tuned and, then, a square wave excitation input is applied to one set-point at a time.

Indeed, it can be noted that all these kinds of closed-loop methods require special experiments, which can be costly in terms of time and material, that is, the identification part

of the auto-tuning technique is not based on simple operating data. An exception is the work of (LI et al., 2005), which proposes the use of closed-loop step responses and linear regression equations to obtain four individual single open-loop systems with the same input signal. Then, the parameters of a first- or second-order-plus-dead-time model can be obtained directly. However, only simulations examples are used to test the method.

This work proposes to analyse and experimentally test a new auto-tuning technique, based on extended versions of (VERONESI; VISIOLI, 2011a) and (PEREIRA; TORRICO, 2015), which uses simple closed-loop data, that is, the process model is obtained by analysing the closed-loop response of the control system when a sequence of set-point step signals (one at a time for each reference input) is applied during normal process operation. Indeed, decentralized PID controllers have to be in place during the experiment and the only condition is that they stabilize the system. In the proposed method, the controller tuning is done without any manual operator interference. In practice, the operator has just to give the command to start the auto-tuning procedure (this can also be done automatically, in a self-tuning context, if a performance assessment method is also employed).

At this point, it is important to highlight that this work mainly deals with the identification part of the re-tuning, and that no new PID tuning method is proposed. The method can only be applied to non-singular TITO processes, i.e., processes with non-singular transfer-function matrix, which means that it is not singular for any positive finite frequency on the real axis.

The identification method, which is one of the principal contributions of the work, is actually an extension to TITO processes of a methodology that has already been proven to be effective for different SISO processes and for different control structures (VERONESI; VISIOLI, 2009; VERONESI; VISIOLI, 2010a; VERONESI; VISIOLI, 2010b; VERONESI; VISIOLI, 2011b; VERONESI; VISIOLI, 2011a). Once a process model, based on FOPDT transfer functions, is estimated, the PID parameters can be determined, for example, by applying one of the many tuning rules available in literature (see, for example, (LUYBEN, 1986; VAZQUEZ; MORILLA; DORMIDO, 1999)). Here, it is suggested the use of the tuning rule proposed in (LEE et al., 2004), which is based on the internal model control (IMC) design (MORARI; ZAFIRIOU, 1989) and on a Maclaurin series expansion. The main features of this method are its analytical formula basis (so that no iterations are required) and the trade-off between aggressiveness and robustness (and control effort), that can be handled by the designer by selecting the desired dominant time constant of the closed-loop system. In any case, a default value can be fixed by taking into account the estimation technique employed.

It is worth mention that, in any case, the identified model can be exploited for the design of any kind of controller, starting from simple PI controllers (which can be appropriate if the noise level is critical) to more complex ones (see, for example, (LIU; ZHANG; GU, 2005; LIU; ZHANG; GU, 2006; WANG et al., 1997)).

In terms of a general comparison the proposed method has some advantages over the ones

which use least squares approach, because these methods are strongly dependent on the tuning of the PID controllers, as the frequency content of the input signal, that depends on the PID tuning, could not be sufficient to excite the overall dynamics of the process (LIU; WANG; HUANG, 2013). Others more complex methodologies, such as evolutionary algorithms (LIU; WANG; HUANG, 2013) are not suitable for an on-line and fast identification. Concerning decentralised relay based methods (WANG et al., 1997), in general, they are not always applicable (as stated in (LIU; WANG; HUANG, 2013)), while for the sequential relay feedback there might be many iterations before convergence. As already mentioned, the method presented in (LI et al., 2005) has similar qualities as the one proposed in this work, and thus, it was selected for the comparative simulation study, where the advantages of the proposed approach are highlighted.

In order to validate the proposed new method and to show its effectiveness, some simulation examples and experiments on a neonatal incubator prototype are presented. The experiments aim to improve the control of temperature and relative humidity in the interior of the neonatal incubator. This experimental part, with the practical implementation of the automatic modelling and PID tuning, is also an important contribution of the work, as most of the previous works were only tested in simulation.

1.1.5 Anti-windup dead-time compensator based on generalized predictive control

Many industrial processes are characterized by the presence of dead time. It occurs, for example, in the time required to transport mass, energy or information. Dead times can also be caused by processing time or by accumulation of time lags in dynamic systems in series. Therefore, many control methods used in industry consider dead time as an integral part of the dynamics of process models (NORMEY-RICO, 2007).

DTCs are a special type of controllers that incorporates a prediction of the process output. For instance, as important works at the last few years, we can mention the following. In (NORMEY-RICO; CAMACHO, 2009), a modified SP (MSP) allows to decouple the disturbance rejection and the set-point tracking and can deal with unstable plants. In (ONO et al., 2010a; ONO et al., 2010b), a discrete MSP based on linear-quadratic-integral (LQI) control method is proposed and applied to integrating and unstable processes. In (MATAUŠEK; RIBIĆ, 2012), a MSP is proposed and proven to be a PID controller in series with a second order filter, dealing with stable, integrating and unstable processes; the tuning is made by means of constrained optimization and the controller has anti-windup action. In (RIBIĆ; MATAUŠEK, 2012), a DTC proportional-integral-derivative (DTC-PID) controller with anti-windup action is proposed and tuned by constrained optimization; it can deal with stable, integrating and unstable processes.

Besides the already mentioned works of (MATAUŠEK; RIBIĆ, 2012; RIBIĆ; MATAUŠEK, 2012), the following works present DTCs with anti-windup action. In (TAN; LEE; LEU, 2001) a predictive PI controller capable of dead-time compensation is presented with an anti-windup action. In (ZHANG; JIANG, 2008), it is proposed an anti-windup controller based on an MSP

for integrating processes.

Model predictive control (MPC) is based on predictions and, over the years, this technique has been widely used to deal with dead-time problems. Therefore, this work proposes a GPC based DTC with anti-windup action.

1.2 Published works related to this dissertation

An article was published in a Qualis CAPES "A1" scientific journal:

- René D. O. Pereira, Massimiliano Veronesi, Antonio Visioli, Julio E. Normey-Rico, Bismark C. Torrico. Implementation and test of a new autotuning method for PID controllers of TITO processes. *Control Engineering Practice*, v. 58, p. 171–185, 2017. DOI: 10.1016/j.conengprac.2016.10.010.

Other three papers were presented in international conferences:

- René D. O. Pereira, Bismark C. Torrico. New automatic tuning of multivariable PID controller applied to a neonatal incubator. In: *8th International Conference on Biomedical Engineering and Informatics (BMEI)*. Shenyang, CHN: 2015. DOI: 10.1109/BMEI.2015.7401572.

- René D. O. Pereira, Francisco V. Andrade, Bismark C. Torrico, Wilkley B. Correia. Automatic tuning of a dead-time compensator for stable, integrating and unstable processes. In: *2016 IEEE Biennial Congress of Argentina (ARGENCON)*. Buenos Aires, ARG: 2016. DOI: 10.1109/ARGENCON.2016.7585358.

- Bismark C. Torrico, Francisco V. Andrade, René D. O. Pereira, and Fabricio G. Nogueira. Anti-windup dead-time compensation based on generalized predictive control. In: *2016 American Control Conference (ACC)*. Boston, USA: 2016, DOI: 10.1109/ACC.2016.7526524.

1.3 Motivation

It is increasingly necessary in the industry to simplify and accelerate the commissioning of control loops, without the need of special and long experiments. Simple and effective auto-tuning procedures are some of the solutions that can be applied to meet this need. And to achieve that, simpler identification methods need to be employed by the new auto-tuning methods. At the actual context, auto-tuning techniques are mainly based on identification methods that present heavy computational costs. The control of processes that dynamically change with time also needs to be addressed by these new methods and the computational cost is a key aspect that affects the control performance. The performance assessment of control loops is also useful to verify the necessity of re-tuning the controller.

Another issue that can be pointed out under the control theory context is the presence of dead time in several industrial processes. Related studies show that the dead time contributes to deterioration of the control system performance.

1.4 Objectives

The main objective of this work is to investigate new techniques of auto-tuning of controllers and of MPC for processes with dead time, applying them in the control of relative humidity and temperature of a neonatal incubator prototype.

The work proposes auto-tuning methods for PID controllers and the SFSP, in the SISO case. It also studies an auto-tuning method of PID controllers for TITO processes. Finally, it proposes a DTC based on GPC.

1.4.1 Specific objectives

- To propose, for SISO PID controllers, auto-tuning methods for unstable and integrating processes;
- To make, for SISO PID controllers, a new interpretation of the auto-tuning method from (VERONESI; VISIOLI, 2009) for stable process;
- To propose, for the SFSP, an auto-tuning method for stable, unstable and integrating processes;
- To study and further investigate an auto-tuning method for PID controllers for stable TITO processes;
- To propose a GPC-based DTC with a formulation considering the presence of dead time and with an anti-windup action, for stable, unstable and integrating processes.

1.5 Organization of the work

The text is organised as follows. First, some generalities of the studied auto-tuning methodology are defined and a method to estimate the apparent dead time from a step response is presented in Chapter 2. In Chapter 3, it is presented the auto-tuning method for PID controllers, where the approach for stable processes proposed in (VERONESI; VISIOLI, 2009; VERONESI; VISIOLI, 2010a; VERONESI; VISIOLI, 2012) is analysed and approaches for unstable and integrating processes are proposed. Chapter 4 is an extended version of (PEREIRA et al., 2016) and presents the auto-tuning of the SFSP. Chapter 5 is a modified version of (PEREIRA et al., 2017) and deals with the auto-tuning of PID controllers for TITO processes. In Chapter 6, an extended version of (TORRICO et al., 2016), the proposed GPC-based DTC is presented. Finally,

in Chapter 7 some relevant features of the studied methodologies are highlighted and future works are discussed.

2 AUTO-TUNING GENERALITIES

This chapter is dedicated to present some important concepts and definitions related to the studied auto-tuning methodology. They appear in almost all cases where this methodology is applied.

The auto-tuning procedure is based on closed-loop experiments. In the SISO case it can be applied after a set-point step change response or after a step load disturbance response. In the MIMO case it can be applied after a sequence of set-point step changes responses at each input. The responses need to reach the steady-state, as the mathematical approach of the method is based on the FVT.

The auto-tuning methodology uses the FVT to obtain relations between parameters of first-order models and integrals of signals. Such signals in the steady-state tend to zero and, therefore, their integrals have a finite value. After the closed-loop experiment, by means of mathematical expressions, two parameters are identified, the process gain and the sum of the time constant and the dead time. Estimating the dead time, the time constant can be then computed.

The auto-tuning can be applied to closed-loop systems that where roughly (manually) tuned or to plants with parameters uncertainties or plants where the parameters changed with time. The method can use operational data from a response initiated by an operator command or can use data stored from past responses without interference in the current state of the control system. After the identification a performance assessment is made to determine the necessity of an new tuning. The method leaves free the choice for the tuning rules. The procedure can be repeated until a desired level of performance is achieved, but generally the first auto-tuning is sufficient to achieve a good performance.

In the next sections important definitions are presented. First, the models to be identified and some useful signals are defined. The topic of model reduction is then presented and some important variables are defined. Finally, the apparent dead-time estimation method used by the auto-tuning method is studied.

2.1 Models and signals

For sake of simplicity, it is assumed that if the process $P(s)$ is stable, it can be properly approximated by a FOPDT model, as presented below:

$$P(s) = \frac{\mu e^{-\theta s}}{\tau s + 1}, \tag{2.1}$$

where μ is the process gain, τ is the time constant and θ is the apparent dead time.

Similarly, if $P(s)$ is an unstable process, it is assumed that an UFOPDT model can

properly approximate it. That model is given by

$$P(s) = \frac{\mu e^{-\theta s}}{\tau s - 1}. \tag{2.2}$$

For integrating processes, it is assumed that $P(s)$ can be properly approximated by a IPDT model, defined as:

$$P(s) = \frac{\mu e^{-\theta s}}{s}. \tag{2.3}$$

Next, important signals present in the formulations are defined. Among them are the so called "virtual signals", that have the common characteristic of converging to zero at the steady-state. They can be computed after a set-point step change or after a step load disturbance.

Figure 1 – Feedback control scheme.

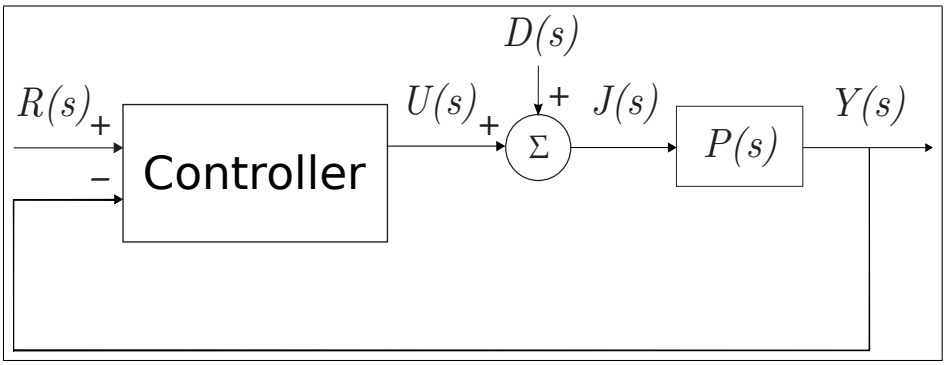

Source: The author.

2.1.1 Set-point step change

The set-point of the closed-loop system considered is $r(t)$. When a set-point step change occurs, such that:

$$r(t) = \begin{cases} 0, & t < 0 \\ A_r, & t \geq 0 \end{cases} \tag{2.4}$$

where A_r is the magnitude of the step, its transfer function is

$$R(s) = \frac{A_r}{s}. \tag{2.5}$$

For stable processes like (2.1) the final value of the output variable $y(t)$ is

$$\lim_{t \to +\infty} y(t) = \mu u(\infty). \tag{2.6}$$

Therefore, the following variable is defined:

$$e_{su}(t) = \mu u(t) - y(t). \tag{2.7}$$

It can be seen that its final value tends to zero at the steady-state.

For unstable processes like (2.2) the final value of the output variable $y(t)$ is

$$\lim_{t\to+\infty} y(t) = -\mu u(\infty). \tag{2.8}$$

The following variable, equivalent to (2.7), is then defined:

$$e_{uu}(t) = -\mu u(t) - y(t). \tag{2.9}$$

The final value of $e_{uu}(t)$ tends to zero at the steady-state.

The final value of the output variable $y(t)$ for integrating process like (2.3) can be computed as

$$\lim_{t\to+\infty} y(t) = \mu \int_0^{\infty} u(t)dt. \tag{2.10}$$

The following virtual signal is then defined:

$$e_{iu}(t) = \mu \int_0^{t} u(\nu)d\nu - y(t). \tag{2.11}$$

One can see that at the steady-state its value equals zero. Its integral, therefore, converges to a finite value.

2.1.2 *Step load disturbance*

The input of process $P(s)$ is given by

$$j(t) = u(t) + d(t). \tag{2.12}$$

In the case when a step load disturbance occurs, such that:

$$d(t) = \begin{cases} 0, & t < 0 \\ A_d, & t \geq 0 \end{cases} \tag{2.13}$$

where A_d is the magnitude of the step, its transfer function is

$$D(s) = \frac{A_d}{s}. \tag{2.14}$$

In an experiment, a step load disturbance can be added to the control signal by means of an algorithm.

For stable processes, the final value of $y(t)$ is zero and can be computed by

$$\lim_{t\to+\infty} y(t) = \mu j(\infty), \tag{2.15}$$

where $j(\infty) = 0$. Defining the following variable as

$$e_{sj}(t) = \mu j(t) - y(t), \tag{2.16}$$

its value in the steady-state equals zero. Its integral, as can be computed, also equals zero.

The final value of $y(t)$ for unstable processes is

$$\lim_{t\to+\infty} y(t) = -\mu\, j(\infty), \tag{2.17}$$

where $j(\infty) = 0$. The following variable is defined as

$$e_{uj}(t) = -\mu\, j(t) - y(t). \tag{2.18}$$

In the steady-state its value equals zero. Its integral also equals zero.

For an integrating process, applying the FVT to the output variable $y(t)$ results

$$\lim_{t\to+\infty} y(t) = \mu \int_0^{\infty} j(t)dt. \tag{2.19}$$

Defining the variable below as

$$e_{ij}(t) = \mu \int_0^{t} j(\nu)d\nu - y(t), \tag{2.20}$$

it can be seen that its final value is zero. As can be computed, its integral is also zero.

2.2 Model reduction and the "half rule"

A linear, time-invariant, continuous-time, nth-order process, can be modelled as

$$P(s) = \frac{\mu e^{-\theta_0 s}}{q(s)}, \tag{2.21}$$

where, for stable processes,

$$q(s) = \prod_{k=1}^{n} (\tau_k s + 1) \tag{2.22}$$

and μ is the process gain, τ_k $(k = 1, 2, ..., n)$ are time constants and θ_0 is the original dead time of the model.

Following the model reduction method proposed in (SKOGESTAD, 2003), for high-order processes as those described by (2.21) it is possible to obtain an equivalent FOPDT model fitting (2.1).

Consider the following first-order Taylor approximation of a dead time L in form of transfer function:

$$e^{-Ls} = \frac{1}{e^{Ls}} \approx \frac{1}{Ls+1}. \tag{2.23}$$

It can be observed that a (small) time constant can be approximated as a dead time.

Now consider only the neglected time constants of a first-order model reduction as

$$m(s) = \prod_{k=2}^{n} (\tau_k s + 1). \tag{2.24}$$

Thus, the expression below can be derived:

$$\frac{e^{-\theta_0 s}}{m(s)} \approx e^{-(\theta_0+\tau_2+\ldots+\tau_n)}. \tag{2.25}$$

The approximation above, in terms of control, is conservative, i.e., slower in terms of tuning. A dead time deteriorates more the control performance than a lag of equal magnitude (SKOGESTAD; POSTLETHWAITE, 1996). This is more evident when approximating the largest of the neglected lags.

A less conservative (faster in terms of tuning) approach is given by the simple "half rule" (SKOGESTAD, 2003). It states that the largest neglected time constant (τ_2) has its half value added to the the original dead time (θ_0) and to the smallest retained time constant (τ_1). From (2.23), the other neglected time constants ($\tau_3, \tau_4, \ldots, \tau_n$) are added also to the original dead time.

Consequently, the expressions for the first-order time constant τ and for the apparent dead time θ result

$$\tau = \tau_1 + \frac{\tau_2}{2}, \tag{2.26}$$

$$\theta = \theta_0 + \frac{\tau_2}{2} + \sum_{k=3}^{n} \tau_k. \tag{2.27}$$

Defining the variable T_0 as the sum of the time constants and the dead time of a model, one gets

$$T_0 = \sum_{k=1}^{n} \tau_k + \theta_0 = \tau + \theta, \tag{2.28}$$

which is often referred to in expressions related to the studied auto-tuning methodology, as in (VERONESI; VISIOLI, 2009; VERONESI; VISIOLI, 2010a; VERONESI; VISIOLI, 2010b; VERONESI; VISIOLI, 2011b; VERONESI; VISIOLI, 2011a; VERONESI; VISIOLI, 2012; NORMEY-RICO et al., 2014; PEREIRA et al., 2016).

Similarly, unstable processes can be represented by (2.21), where

$$q(s) = (\tau_1 s - 1) \prod_{k=2}^{n} (\tau_k s + 1). \tag{2.29}$$

Multiplying both numerator and denominator of (2.21) by -1 results

$$P(s) = \frac{-\mu e^{-\theta_0 s}}{-q(s)}, \tag{2.30}$$

where

$$-q(s) = (-\tau_1 s + 1) \prod_{k=2}^{n} (\tau_k s + 1), \tag{2.31}$$

is a well suited representation of the model denominator for model reduction by the "half rule". The desired denominator for the UFOPDT model is

$$-q(s) = (-\tau s + 1). \tag{2.32}$$

Applying the "half rule" one gets

$$\tau = \tau_1 + \frac{\tau_2}{2}, \tag{2.33}$$

$$\theta = \theta_0 + \frac{\tau_2}{2} + \sum_{k=3}^{n} \tau_k. \tag{2.34}$$

The sum of time constants and dead time for the unstable case is then given by

$$T_0' = \sum_{k=3}^{n} \tau_k + \theta_0 - \tau_1 = \theta - \tau. \tag{2.35}$$

These are the model reduction expressions to obtain an UFOPDT model and of T_0', a variable present in the unstable processes case auto-tuning formulation.

Consider now an integrating process represented by (2.21), where

$$q(s) = s \prod_{k=1}^{n} (\tau_k s + 1). \tag{2.36}$$

The apparent dead-time expression for model reduction, as in (SKOGESTAD, 2003), to obtain an IPDT model is

$$\theta = \theta_0 + \sum_{k=1}^{n} \tau_k. \tag{2.37}$$

In the studied methodology, differently from the stable and unstable cases, the parameter θ of the IPDT model is estimated directly by an numerical expression.

2.3 Estimation of the dead time

As is proposed in (VERONESI; VISIOLI, 2009), after a set-point step change the apparent dead time θ can be estimated as the time interval between the set-point step change and the instant when the output variable $y(t)$ attains 2% of the step magnitude A_r, i.e., when $\Delta y(t) = 0.02A_r$.

After a step load disturbance the apparent dead time θ can be obtained (as in (VERONESI; VISIOLI, 2012)) as the time interval between the instant by which a step load disturbance is applied and the instant by which the output variable $y(t)$ attains 2% of the corresponding

final value of $y(t)$ produced by an input step of magnitude A_d, i.e., when $\Delta y(t) = 0.02\mu A_d$. A procedure for detection of abrupt load disturbances is proposed in (VERONESI; VISIOLI, 2008).

Nevertheless, in a practical context, a noise band *NB* equal to the measurement noise can be defined (ÅSTRÖM et al., 1993). Hence, the apparent dead time θ can be estimated as the time interval until $\Delta y(t) \geq NB$.

It is worth noting that a slow controller can cause an overestimation of the dead time. Therefore, if the operator has previous knowledge of the system (sort of controller, controller parameters, usual settling time, etc.), the level of 2% or the *NB* level can be reduced accordingly to obtain better estimated values of the apparent dead time θ.

3 AUTO-TUNING OF PID CONTROLLERS FOR SISO PROCESSES

This chapter is organized as follows. Section 3.1 presents the considered PID controllers. Sections 3.2 and 3.3 present the estimation of model parameters for stable, unstable and integrating processes considering set-point step changes and step load disturbances. Section 3.4 describes the tuning process. In Section 3.5 the performance assessment method is presented. Section 3.6 shows simulation results for each process case. The neonatal incubator prototype is presented in Section 3.7. In Section 3.8 experimental results in the relative humidity control of the neonatal incubator are presented and in Section 3.9 some important details are discussed.

3.1 The PID controller

The studied PID control system is shown in Fig. 2, where $C(s)$ and $P(s)$ are the PID controller and the process, respectively.

Figure 2 – The PID controller scheme.

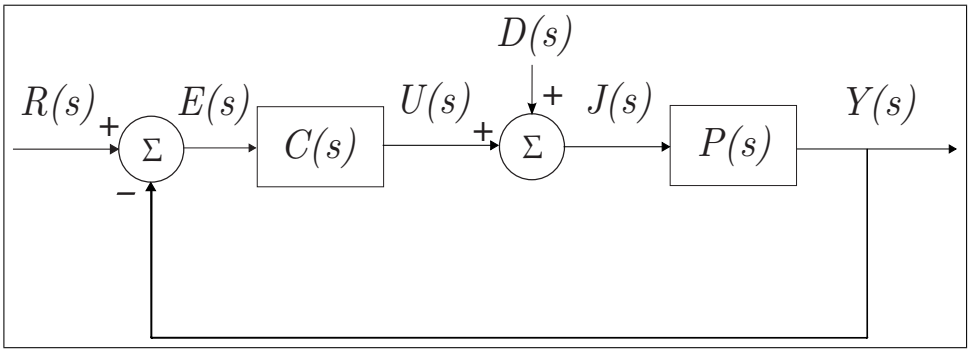

Source: The author.

In this work, the PID controller can be expressed in its ideal ("non-interacting") form as

$$C(s) = K_p \left(1 + \frac{1}{T_i s} + T_d s\right) \tag{3.1}$$

or in the series ("interacting") form as

$$C(s) = K_p \left(1 + \frac{1}{T_i s}\right)(T_d s + 1), \tag{3.2}$$

where K_p is the proportional gain, T_i is the integral time and T_d is the derivative time. The formulation that follows can be applied to both ideal and series forms.

In addition, a formulation for the I-PD controller is also devised in this work.

3.1.1 The I-PD controller

The I-PD controller is a modified version of the PID controller that has a smoother response after a set-point change. It is most used for practical applications where the overshoot is not acceptable and to prevent the control signals applied of wearing the actuators. Its control scheme is shown in Fig. 3.

Figure 3 – The I-PD controller scheme.

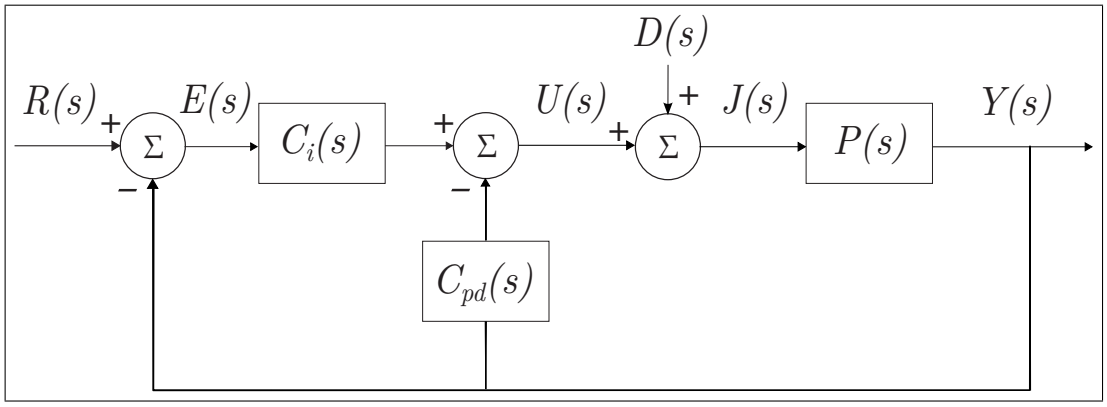

Source: The author.

In the I-PD controller structure the integral term multiply the error signal $e(t)$ while the proportional and derivative terms multiply the process output $y(t)$. The expression for its control signal $u(t)$ is shown below:

$$U(s) = C_i(s)E(s) - C_{pd}(s)Y(s), \tag{3.3}$$

where,

$$C_i(s) = \frac{K_p}{T_i s} \tag{3.4}$$

and

$$C_{pd}(s) = K_p + K_p T_d s. \tag{3.5}$$

Substituting $E(s) = R(s) - Y(s)$, (3.3) can be expressed as

$$U(s) = C_i(s)R(s) - C(s)Y(s), \tag{3.6}$$

where

$$C(s) = C_i(s) + C_{pd}(s) = K_p\left(1 + \frac{1}{T_i s} + T_d s\right) \tag{3.7}$$

is the ideal PID controller expression.

For set-point tracking the expressions for $Y(s)$ and $U(s)$ are

$$Y(s) = \frac{P(s)C_i(s)}{1 + C(s)P(s)}R(s) \tag{3.8}$$

and

$$U(s) = \frac{C_i(s)}{1 + C(s)P(s)} R(s). \tag{3.9}$$

For load disturbances, when $r(t) = 0$, it is obtained

$$Y(s) = \frac{P(s)}{1 + C(s)P(s)} D(s) \tag{3.10}$$

and

$$J(s) = \frac{1}{1 + C(s)P(s)} D(s). \tag{3.11}$$

Note that, when the derivative time T_d is zero, the controller results in an I-P controller.

3.2 Estimation of model parameters

3.2.1 Stable processes

3.2.1.1 Set-point step change

In the steady-state the error $e(t)$ equals zero. Applying the FVT to the integral of $e(t)$, it can be obtained that

$$IE = \int_0^\infty e(t)dt = \lim_{s \to 0} E(s) = \lim_{s \to 0} \frac{1}{1 + C(s)P(s)} R(s). \tag{3.12}$$

Substituting (2.1), (2.5) and (3.1) in the expression above, one gets

$$IE = \frac{\gamma A_r}{\mu}, \tag{3.13}$$

where

$$\gamma = \frac{T_i}{K_p}. \tag{3.14}$$

It is worth noting that the constant γ appears often in the formulations of the studied method applied to PID control.

The process gain can be then given by

$$\mu = \frac{\gamma A_r}{IE}. \tag{3.15}$$

By applying the FVT to the integral of the virtual signal $e_{su}(t)$ (2.7), it is obtained

$$IE_{su} = \int_0^\infty e_{su}(t)dt = \lim_{s \to 0} E_{su}(s) = \lim_{s \to 0} [\mu - P(s)]U(s) = \lim_{s \to 0} [\mu - P(s)]C(s) \lim_{s \to 0} E(s). \tag{3.16}$$

Substituting in the expression above (2.1), (3.1) and (3.13), and applying the l'Hôpital's rule to the first limit, results

$$IE_{uu} = T_0 A_r, \tag{3.17}$$

then

$$T_0 = \frac{IE_{su}}{A_r}. \tag{3.18}$$

Therefore, from (2.28) the time constant is

$$\tau = T_0 - \theta. \tag{3.19}$$

3.2.1.2 *Step load disturbance*

The output variable $y(t)$, in the steady-state, equals zero. Applying the FVT to the integral of $y(t)$ results

$$IY = \int_0^\infty y(t)dt = \lim_{s\to 0} Y(s) = \frac{P(s)}{1+C(s)P(s)} D(s). \tag{3.20}$$

Substituting (2.1), (2.14) and (3.1) in the expression above, one gets

$$IY = \gamma A_d. \tag{3.21}$$

Therefore, the magnitude of the step load disturbance is

$$A_d = \frac{IY}{\gamma}. \tag{3.22}$$

As the controller acts to reject the disturbance, it can be seen that the variable $j(t)$ goes to zero at steady-state. Applying the FVT to the integral of $j(t)$ it can be obtained that

$$IJ = \int_0^\infty j(t)dt = \lim_{s\to 0} J(s) = \lim_{s\to 0} \frac{1}{1+C(s)P(s)} D(s). \tag{3.23}$$

Substituting (2.1), (2.14) and (3.1) in (3.23), then

$$IJ = \frac{\gamma A_d}{\mu} \tag{3.24}$$

and the process gain results

$$\mu = \frac{\gamma A_d}{IJ}. \tag{3.25}$$

By applying the FVT to the double integral of $e_{sj}(t)$ results

$$DIE_{sj} = \int_0^\infty \int_0^t e_{sj}(\nu)d\nu dt = \lim_{s\to 0} \frac{E_{sj}(s)}{s} = \lim_{s\to 0} \frac{[\mu - P(s)]}{s} \lim_{s\to 0} J(s). \tag{3.26}$$

Substituting (2.1) and (3.24) in the expression above and applying the l'Hôpital's rule, it is obtained

$$DIE_{sj} = T_0 \gamma A_d \tag{3.27}$$

and

$$T_0 = \frac{DIE_{sj}}{\gamma A_d}. \tag{3.28}$$

Therefore, the time constant is

$$\tau = T_0 - \theta. \tag{3.29}$$

3.2.2 *Unstable processes*

The formulations for the unstable case and for the stable case are alike. Therefore, for sake of simplicity, some expressions are straight through following the stable case.

3.2.2.1 *Set-point step change*

Applying the FVT to the integral of $e(t)$, the expression (3.12) can be obtained. Substituting (2.2), (2.5) and (3.1) in that expression, one gets

$$IE = -\frac{\gamma A_r}{\mu} \tag{3.30}$$

and then the process gain can be given by

$$\mu = -\frac{\gamma A_r}{IE}. \tag{3.31}$$

By applying the FVT to the integral of $e_{uu}(t)$, it is obtained

$$IE_{uu} = \int_0^\infty e_{uu}(t)dt = \lim_{s\to 0} E_{uu}(s) = \lim_{s\to 0} -[\mu + P(s)]U(s) = \lim_{s\to 0} -[\mu + P(s)]C(s) \lim_{s\to 0} E(s). \tag{3.32}$$

Substituting in expression (3.32) the expressions (2.2), (3.1) and (3.30), and applying the l'Hôpital's rule to the first limit, results

$$IE_{uu} = T_0' A_r \tag{3.33}$$

and

$$T_0' = \frac{IE_{uu}}{A_r}. \tag{3.34}$$

Therefore, from (2.35), the time constant is

$$\tau = \theta - T_0'. \tag{3.35}$$

3.2.2.2 Step load disturbance

Applying the FVT to the integral of $y(t)$ results in (3.20). Substituting (2.2), (2.5) and (3.1) in that expression, the magnitude of the step load disturbance, as in the stable case, is

$$A_d = \frac{IY}{\gamma}. \tag{3.36}$$

Applying the FVT to the integral of $j(t)$ one obtains expression (3.23). Substituting (2.2), (2.5) and (3.1) in that expression results

$$IJ = -\frac{\gamma A_d}{\mu} \tag{3.37}$$

and the process gain results

$$\mu = -\frac{\gamma A_d}{IJ}. \tag{3.38}$$

By applying the FVT to the double integral of $e_{uj}(t)$ (2.18) results

$$DIE_{uj} = \int_0^\infty \int_0^t e_{uj}(\nu) d\nu dt = \lim_{s\to 0} \frac{E_{uj}(s)}{s} = \lim_{s\to 0} \frac{-[\mu + P(s)]}{s} \lim_{s\to 0} J(s). \tag{3.39}$$

Substituting (2.2) and (3.37) in expression (3.39) and applying the l'Hôpital's rule, one gets

$$DIE_{uj} = T_0' \gamma A_d, \tag{3.40}$$

then

$$T_0' = \frac{DIE_{uj}}{\gamma A_d}. \tag{3.41}$$

Therefore, the time constant is

$$\tau = \theta - T_0'. \tag{3.42}$$

3.2.3 *Integrating processes*

3.2.3.1 Set-point step change

For integrating processes like (2.3), in the steady-state, the control signal $u(t)$ has the final value equals zero. Therefore, the integral of $u(t)$ converge to a finite value. Applying the FVT to that integral one gets

$$IU = \int_0^\infty u(t) dt = \lim_{s\to 0} U(s) = \lim_{s\to 0} \frac{C(s)}{1 + C(s)P(s)} R(s). \tag{3.43}$$

Substituting (2.3), (2.5) and (3.1) in the expression above, results

$$IU = \frac{A_r}{\mu} \tag{3.44}$$

and the process gain is

$$\mu = \frac{A_r}{IU}. \tag{3.45}$$

Applying the FVT to the integral of $e_{iu}(t)$ (2.11):

$$IE_{iu} = \int_0^\infty e_{iu}(t)dt = \lim_{s\to 0} E_{iu}(s) = \lim_{s\to 0}\left[\frac{\mu}{s} - P(s)\right]\lim_{s\to 0} U(s). \tag{3.46}$$

Substituting (2.3) and (3.44) in (3.46) and solving the first limit expression by applying the l'Hôpital's rule, it is obtained

$$IE_{iu} = \theta A_r. \tag{3.47}$$

Therefore, the apparent dead time results

$$\theta = \frac{IE_{iu}}{A_r}. \tag{3.48}$$

3.2.3.2 *Step load disturbance*

At steady-state the value of the output variable $y(t)$ is zero. Therefore, its integral has a finite value. Applying the FVT to the integral of $y(t)$ results

$$IY = \int_0^\infty y(t)dt = \lim_{s\to 0} Y(s) = \frac{P(s)}{1+C(s)P(s)}D(s) \tag{3.49}$$

Replacing (2.3), (2.14) and (3.1) in the above equation, it is obtained

$$IY = \gamma A_d. \tag{3.50}$$

Therefore, the magnitude of the step load disturbance results

$$A_d = \frac{IY}{\gamma}. \tag{3.51}$$

The value of the variable $j(t)$ at the steady-state is zero. But applying the FVT to its integral, it also tends to zero. Therefore, taking the double integral of $j(t)$ and applying the FVT, it is obtained

$$DIJ = \int_0^\infty \int_0^t j(v)dvdt = \lim_{s\to 0}\frac{J(s)}{s} = \lim_{s\to 0}\frac{1}{s}\frac{1}{1+C(s)P(s)}D(s). \tag{3.52}$$

Substituting (2.3), (2.14) and (3.1) in (3.52) one gets

$$DIJ = \frac{\gamma A_d}{\mu}. \tag{3.53}$$

Therefore, the process gain is given by

$$\mu = \frac{\gamma A_d}{DIJ}. \tag{3.54}$$

Applying the FVT to the double integral of $e_{ij}(t)$ (2.20) results

$$DIE_{ij} = \int_0^\infty \int_0^t e_{ij}(\nu) d\nu dt = \lim_{s\to 0} \frac{E_{ij}(s)}{s} = \lim_{s\to 0} \frac{\mu - sP(s)}{s} \lim_{s\to 0} \frac{J(s)}{s}. \tag{3.55}$$

Substituting (2.3) and (3.53) in (3.55) and using the l'Hôpital's rule in the first limit expression, it is obtained

$$DIE_{ij} = \theta \gamma A_d. \tag{3.56}$$

The apparent dead time then results

$$\theta = \frac{DIE_{ij}}{\gamma A_d}. \tag{3.57}$$

3.3 Estimation of model parameters: The I-PD controller case

3.3.1 Stable processes

3.3.1.1 Set-point step change

Applying the FVT to the integral of $e(t)$, it can be obtained

$$IE = \lim_{s\to 0} [R(s) - Y(s)] = \lim_{s\to 0} \left[1 - \frac{P(s)C_i(s)}{1 + C(s)P(s)}\right] R(s). \tag{3.58}$$

Substituting (2.5), (2.1), (3.4) and (3.7) in the expression above and using the l'Hôpital's rule to compute the limit, one gets

$$IE = T_i A s \left(1 + \frac{1}{\mu K_p}\right) \tag{3.59}$$

and the process gain is

$$\mu = \frac{\gamma A_r}{IE - T_i A_r}. \tag{3.60}$$

Applying the FVT to the integral of $e_{su}(t)$, results

$$IE_{su} = \lim_{s\to 0} \frac{[\mu - P(s)]C_i(s)}{1 + C(s)P(s)} R(s). \tag{3.61}$$

Substituting in that expression (2.5), (2.1), (3.4) and (3.7), and applying the l'Hôpital's rule, results

$$IE_{uu} = T_0 A_r, \tag{3.62}$$

the same as in the PID controller case. Therefore, T_0 and the time constant τ can be computed as in (3.18) and (3.19), respectively.

3.3.1.2 Step load disturbance

The expressions for $Y(s)$ and $J(s)$ are identical to those of the PID controller case. Therefore, the formulation is the same as in that case and is omitted.

3.3.2 Unstable processes

3.3.2.1 Set-point step change

Applying the FVT to the integral of $e(t)$, it is obtained (3.58). Substituting (2.5), (2.2), (3.4) and (3.7) in that expression and using the l'Hôpital's rule to compute the limit, the process gain results

$$\mu = -\frac{\gamma A_r}{IE - T_i A_r}. \tag{3.63}$$

Applying the FVT to the integral of $e_{uu}(t)$, results

$$IE_{uu} = \lim_{s\to 0} -\frac{[\mu + P(s)]C_i(s)}{1 + C(s)P(s)} R(s). \tag{3.64}$$

Substituting (2.5), (2.2), (3.4) and (3.7) in that expression and applying the l'Hôpital's rule, one gets

$$IE_{uu} = T_0' A_r, \tag{3.65}$$

as in the PID controller case, resulting that T_0' and time constant τ are expressed by (3.34) and (3.35), respectively.

3.3.2.2 Step load disturbance

The expressions for $Y(s)$ and $J(s)$ are identical to those of the PID controller case. Therefore, the formulation remains the same and is also omitted.

3.3.3 Integrating processes

3.3.3.1 Set-point step change

Applying the FVT to the integral of $u(t)$ results

$$IU = \lim_{s\to 0} \frac{C_i(s)}{1 + C(s)P(s)} R(s). \tag{3.66}$$

Substituting (2.5), (2.3), (3.4) and (3.7) in the expression above, results, as in the PID controller case,

$$IU = \frac{A_r}{\mu}. \tag{3.67}$$

Therefore, the expression of the process gain μ is the same as in (3.45).

Following the same steps as in Section 3.2.3.1, the apparent dead time θ results the same as in the PID controller case.

3.3.3.2 Step load disturbance

The expressions for $Y(s)$ and $J(s)$, as can be seen from (3.10) and (3.11) respectively, are the same as in the PID controller case. Therefore, the formulation for this case is identical to that of the PID controller case.

3.4 Tuning

After a new process model is identified, the performance of the actual system response needs to be assessed by computing a performance index. For this, chosen tuning rules have to be applied to the new model in order to compute a target performance that is compared with the actual performance.

In (VERONESI; VISIOLI, 2009; VERONESI; VISIOLI, 2010a; VERONESI; VISIOLI, 2010b) the chosen tuning rule was the Skogestad Internal Model Control (SIMC) tuning rule (SKOGESTAD, 2003). Nevertheless, any tuning rules based on FOPDT, IPDT or UFOPDT models can be used to re-tune the PID controller. The choice is based on the objective of the controller, for either set-point tracking or disturbance rejection. Therefore, the most suitable tuning rule of those can be chosen to meet system requirements.

After applying the chosen tuning rule, the new parameters of the PID controller result as K_P, T_I, T_D and in the constant $\Gamma = T_I/K_P$.

3.5 Performance assessment

The performance assessment of the controller, as in (VERONESI; VISIOLI, 2009), is based on the integrated absolute error (IAE) performance index, expressed as

$$IAE = \int_0^\infty |e(t)|dt. \tag{3.68}$$

The IAE was chosen because its minimization results generally in low overshoot and reduced settling time (SHINSKEY, 1994).

The performance of a control system can be assessed by comparing the actual performance of the system with a target performance. The actual integrated absolute error IAE_a value is computed after a set-point step change or a step load disturbance. After the identification, the corresponding target integrated absolute error can then be computed assuming that the identified model suitably represents the plant. Next, analytic expressions for the target indexes are devised for each identification case. Later, the performance indexes proposed by (VERONESI; VISIOLI, 2009) are defined.

3.5.1 Set-point step change

Considering a monotonic response of the output variable after a set-point step change, the target IAE can be computed as

$$IAE_{sp} = \int_0^\infty e(t)dt = \lim_{s\to 0} E(s). \tag{3.69}$$

For stable processes the target IAE, in the PID controller case, is

$$IAE_{sp} = \frac{\Gamma A_r}{\mu} \tag{3.70}$$

and in the I-PD controller case one gets

$$IAE_{sp} = T_I A_r \left(1 + \frac{1}{\mu K_P}\right). \tag{3.71}$$

For unstable processes, in the PID controller case, the target IAE is the same as for stable processes:

$$IAE_{sp} = \frac{\Gamma A_r}{\mu} \tag{3.72}$$

and in the I-PD controller case results

$$IAE_{sp} = T_I A_r \left(1 - \frac{1}{\mu K_P}\right). \tag{3.73}$$

For integrating processes, the target IAE can be computed, in the PID controller case, as in (VERONESI; VISIOLI, 2010b):

$$IAE_{sp} = 0.43125 T_I A_r \tag{3.74}$$

and in the I-PD controller case as

$$IAE_{sp} = T_I A_r. \tag{3.75}$$

3.5.2 Step load disturbance

For regulation tasks the target IAE is obtained by

$$IAE_{ld} = \int_0^\infty |e(t)|dt = |\lim_{s\to 0} Y(s)|. \tag{3.76}$$

The target IAE in both PID and I-PD controller cases for stable, unstable and integrating processes is given by the same expression:

$$IAE_{ld} = |\Gamma A_d|. \tag{3.77}$$

3.5.3 Performance indexes

The Set-Point Performance Index (SPPI) (VERONESI; VISIOLI, 2009) can then be defined below as the ratio between the target and the actual IAE values:

$$SPPI = \frac{IAE_{sp}}{IAE_a}. \tag{3.78}$$

Similarly, the Load Disturbance Performance Index (LDPI) (VERONESI; VISIOLI, 2009) is defined as

$$LDPI = \frac{IAE_{ld}}{IAE_a}. \tag{3.79}$$

Theoretically, the performance of the PID controller is satisfactory when the performance index value is equal to 1. Nevertheless, in a practical context, it has been found from a large number of simulations that a PID controller can be considered well tuned when that value is greater than 0.6 (VERONESI; VISIOLI, 2009). But certainly, if tighter performance is required, that value must be higher.

3.6 Simulation results

The chosen examples are stable, unstable and integrating processes presented in (NORMEY-RICO; CAMACHO, 2009) and (GARCÍA; ALBERTOS, 2008). For better responses, I-P controllers were used in both simulations. For each case, model uncertainties were added considering that the initial model was incorrectly estimated or that the parameters of the plant changed. The same tuning rules are used for initial tuning and for re-tuning the controller. In the same simulation are performed both the auto-tunings based on the set-point (SP) step change as on the step load disturbance (LD). Its responses are then plotted in the same figure with the initial tuning response for comparison. As I-P controllers have slower set-point step change responses than others sorts of PID controllers and as considered about the dead-time estimation in Section 2.3, for set-point step change cases the dead time was estimated as the time when the output reaches $\Delta y(t) = 0.005A_r$, i.e.,using a level of 0.5%. As the I-P controller characteristic of load disturbance responses is maintained the same as a PI controller, the estimated dead time for such cases remains as the time when the output reaches $\Delta y(t) = 0.02\mu A_d$.

3.6.1 Stable process

The expression below represents the model for temperature control in a heat exchanger (NORMEY-RICO; CAMACHO, 2009):

$$P_1(s) = \frac{0.12e^{-3s}}{6s+1} \tag{3.80}$$

It was chosen the SIMC tuning rule presented in (SKOGESTAD, 2003) and, for a FOPDT model, a PI controller can be obtained. The proportional gain K_p and the integral time T_i are

computed as below:

$$K_p = \frac{\tau}{\mu(\tau_c + \theta)}, \tag{3.81}$$

$$T_i = min\{\tau, 4(\tau_c + \theta)\}, \tag{3.82}$$

where τ_c is the desired closed-loop time constant of the system and is a tuning parameter chosen such that $\tau_c < \theta$ results in higher performance and $\tau_c > \theta$ results in robust responses. A suitable trade-off can also be obtained by choosing $\tau_c = \theta$ (SKOGESTAD, 2003), being explored in this example. The value of τ_c can be chosen freely, but from Eq. 3.81 one must have $-\theta < \tau_c < \infty$ to get a positive and non-zero controller gain. Another conservative and simpler choice is also to make $T_i = \tau$.

The uncertainties applied to the nominal model were $+40\%$ for the process gain, $+50\%$ for the time constant and $+60\%$ for the dead time. At $t = 275$, a step load disturbance of magnitude -4 is applied and then estimated as $A_d = -4$. The output and control signal responses are shown in Fig. 4 and the estimated parameters and performance indexes are presented in Table 1.

Figure 4 – Set-point and load disturbance step responses for process $P_1(s)$ with the initial tuning and with the auto-tunings of I-P controllers.

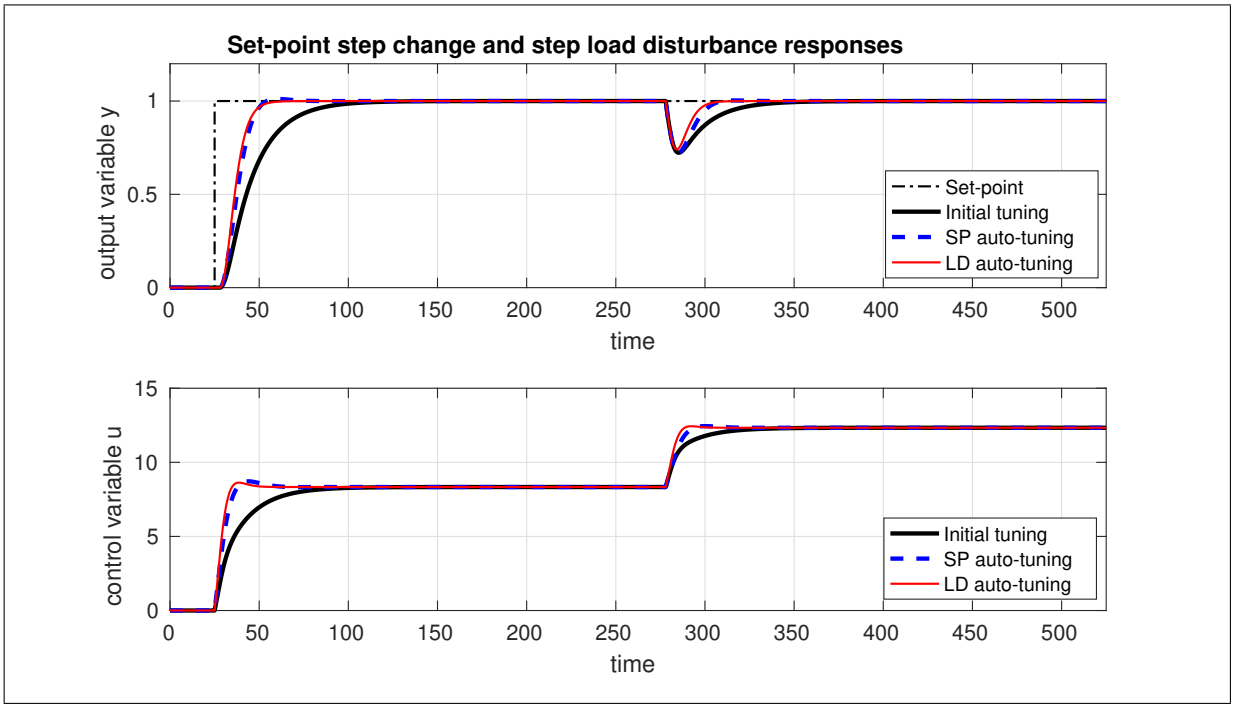

Source: The author.

From Fig. 4 and Table 1, it can be seen that, in both auto-tunings cases, the estimated parameters were next to the correct values and the responses presented better SPPI and LDPI than the initial tuning.

Table 1 – Parameters and indexes for process $P_1(s)$ with I-P controllers.

	μ	T_0	τ	θ	SPPI	LDPI
Initial tuning	0.17	13.80	9.00	4.80	0.58	0.49
SP auto-tuning	0.12	9.00	4.90	4.10	0.98	0.79
LD auto-tuning	0.12	9.02	5.72	3.30	1.06	1.00

3.6.2 *Unstable process*

The second example is a model of concentration control in an unstable reactor (NORMEY-RICO; CAMACHO, 2009).

$$P_2(s) = \frac{3.433e^{-20s}}{103.1s - 1}. \tag{3.83}$$

It was chosen the SIMC tuning rule (SKOGESTAD, 2003) that, for UFOPDT models, is applicable to a PI controller. The rules are:

$$K_p = \frac{\tau}{\mu(\tau_c + \theta)}, \tag{3.84}$$

$$T_i = \tau. \tag{3.85}$$

For this example, a faster response was desirable. Therefore, by testing, it was chosen $\tau_c = 0.3\theta$.

The uncertainties were $+20\%$ for the process gain, $+30\%$ for the time constant and $+70\%$ for the dead time. At $t = 1700$, a step load disturbance of magnitude -0.1 is applied, that is estimated as $A_d = -0.1$. The output and control signal responses are in Fig. 5 and the estimated parameters and performance indexes are in Table 2.

Table 2 – Parameters and indexes for process $P_2(s)$ with I-P controllers.

	μ	T_0'	τ	θ	SPPI	LDPI
Initial tuning	4.12	100.03	134.03	34.00	0.65	0.40
SP auto-tuning	3.43	83.10	110.60	27.50	0.83	0.64
LD auto-tuning	3.43	83.78	105.98	22.20	0.95	0.87

The responses of the auto-tunings were faster and presented smaller overshoots. Even so the SPPI had an acceptable value, it was improved to even better values in both cases of the auto-tunings. The LDPI in both cases were improved to better and acceptable values.

3.6.3 *Integrating process*

The integrating process below is presented in (GARCÍA; ALBERTOS, 2008).

$$P_3(s) = \frac{0.1e^{-8s}}{s(s+1)(0.5s+1)(0.1s+1)}. \tag{3.86}$$

Figure 5 – Set-point and load disturbance step responses for process $P_2(s)$ with the initial tuning and with the auto-tunings of I-P controllers.

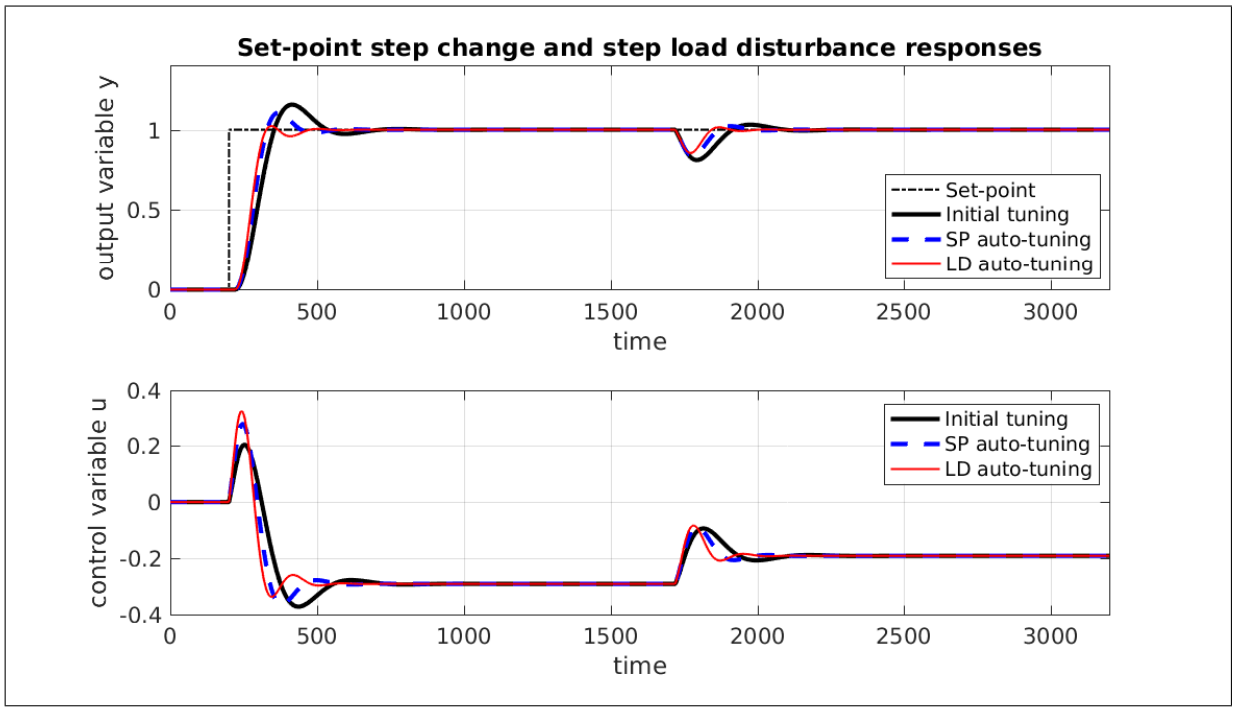

Source: The author.

A IPDT model for that process is

$$P_n(s) = \frac{0.1e^{-9.6s}}{s}. \tag{3.87}$$

The SIMC tuning rule (SKOGESTAD, 2003) was chosen and for an IPDT model a PI controller is obtained. The rules are:

$$K_p = \frac{1}{\mu(\tau_c + \theta)}, \tag{3.88}$$

$$T_i = 4(\tau_c + \theta). \tag{3.89}$$

To obtain faster responses, by testing, it was chosen for this simulation $\tau_c = 0.5\theta$.

The uncertainties are $+20\%$ for the process gain and $+70\%$ for the dead time. At $t = 1100$, a step load disturbance of magnitude -0.15 is applied, that is estimated exactly as $A_d = -0.15$. The output and control signal responses are seen in Fig. 6 and the estimated parameters and performance indexes are presented in Table 3.

What can be seen from Fig. 6 and Table 3 is that the both auto-tunings estimated consistent parameters and presented better responses than the initial tuning, improving considerably the SPPI and the LDPI.

Figure 6 – Set-point and load disturbance step responses for process $P_3(s)$ with the initial tuning and with the auto-tunings of I-P controllers.

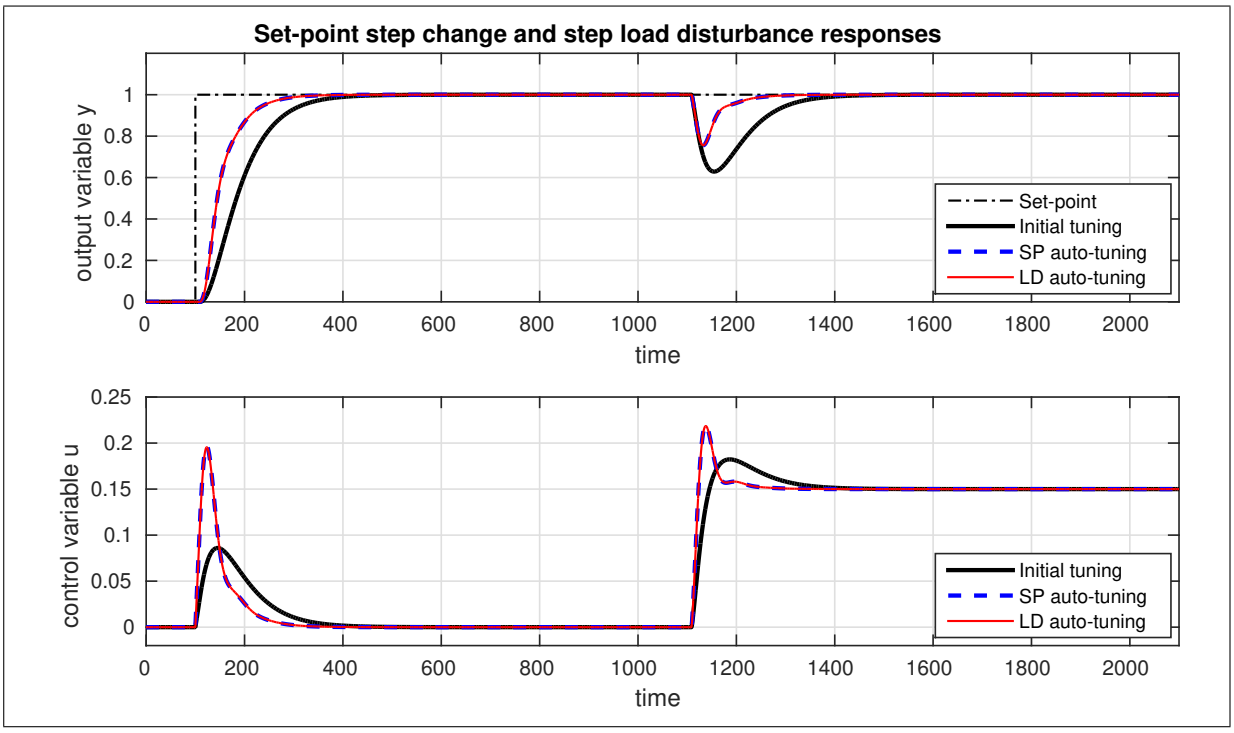

Source: The author.

Table 3 – Parameters and indexes for process $P_3(s)$ with I-P controllers.

	μ	θ	SPPI	LDPI
Initial tuning	0.12	16.32	0.59	0.29
SP auto-tuning	0.10	9.60	1.00	1.01
LD auto-tuning	0.10	9.63	1.00	1.00

It can be noted also that for this particular case where the model do not have a time constant that the dead time is estimated directly by a mathematical expression. That results in almost identical models for both cases of auto-tunings. Unlikely from the cases of stable and unstable processes, where an empirical rule is used to estimate the dead time and the dead time depends on the speed of the controller response.

3.7 The neonatal incubator prototype

The studied and proposed methods, are applied to control the temperature and the humidity of a neonatal incubator prototype. In general, neonatal incubators are used in the care of a premature or ill newborn infants which can loose heat and water easily (KAREN, 1994). Thus, a properly control of the temperature and the relative humidity are associated with safety and comfort. From control standpoint the control of a neonatal incubator is challenging because

it is a coupled TITO process with multiple time delays.

The general overview of the neonatal incubator prototype used is presented in Fig. 7. The neonate is supposed to be in the dome, where also are located the temperature and the relative humidity sensors. Right below, separated only by two openings (air input and output), there is a reservoir where a fan, a heating resistor and an ultrasonic humidifier are located. They are used to recirculate the air, to control the temperature, and to control the relative humidity, respectively.

Figure 7 – The neonatal incubator prototype.

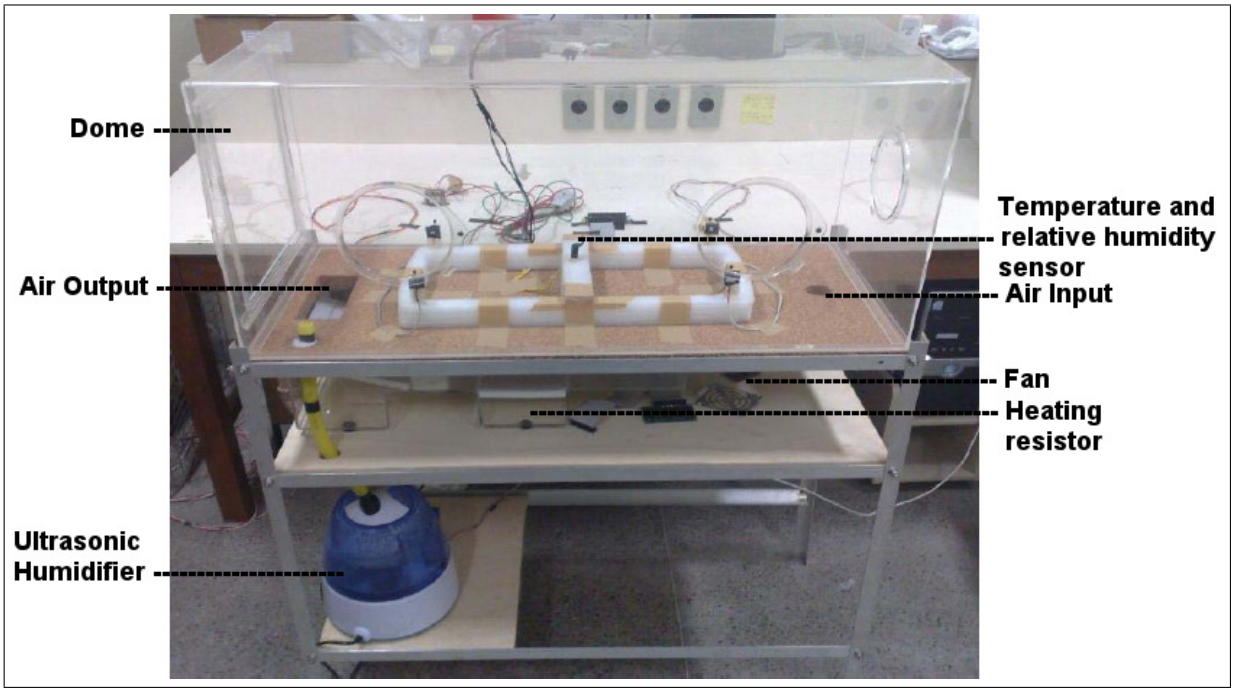

Source: The author.

The power delivered to the heating resistor is controlled by the duty cycle of a switching power supply. The humidifier is controlled using a circuit based on a light dependent resistor. The control inputs are ranged between 0 and 100%. The modelling of a neonatal incubator is presented in (CAVALCANTE et al., 2010), where it is shown that a TITO model made by FOPDT transfer functions as in (5.25) can be used. It is important to note that, in the present work, we used the same neonatal incubator as in (CAVALCANTE et al., 2010), but over the years its hardware has changed. Therefore, the models presented in the two works are different.

3.8 Experimental results

For faster experiments, it was chosen to control the relative humidity loop of the neonatal incubator. The experiments were performed using PI controllers. The controllers were discretised using Tustin approximation, where the sampling time was $T_s = 0.2$ min.

For the initial tuning the PI controller parameters were $K_p = 1.45$ and $T_i = 5.59$. Initially, the relative humidity was controlled in 50%. A set-point (SP) step change of $A_r = 15\%$ was

applied at $t = 0$ and a step load disturbance (LD) of $A_d = -20\%$ was applied at $t = 60$ min.

Obtaining the apparent dead times as described in Section 2.3 and applying (3.15), (3.18) and (3.19) to the set-point step change data and (3.22), (3.25), (3.28) and (3.29) to the step load disturbance data, results in the estimated parameters as in Table 4. The step load disturbance was estimated as $A_d = -21.16$.

Table 4 – Estimated parameters of the experiment with a PI controller.

	μ	T_0	τ	θ
SP auto-tuning	0.48	7.54	6.94	0.6
LD auto-tuning	0.50	11.97	10.57	1.40

The performance indexes were then computed as

$$\begin{aligned} SPPI &= 0.28, \\ LDPI &= 0.69. \end{aligned} \tag{3.90}$$

Note that the computed SPPI is smaller than 0.6, meaning that the controller needs to be re-tuned. The LDPI is still greater than 0.6, the acceptable value for the performance indexes. But even so, that index can be improved.

As validation of the models, Fig. 8 shows a comparison between the experimental and simulation results using the initial controller tuning. The simulations were performed with the models identified by each case, as in Table 4.

In Fig. 9 are shown simulations using the models identified by each case with the initial tuning and with the tuning obtained by the respective auto-tuning. As can be seen, the responses with the auto-tuning were improved in relation to the responses with the initial tuning.

From the two auto-tunings, the SP auto-tuning is the one that presents better performance, therefore, it was chosen to be experimentally implemented. Fig. 10 shows the comparison of the two experiments, with the initial tuning and with the SP auto-tuning. As can be seen, the responses with the auto-tuning are better both for the set-point step change and for the step-load disturbance.

The computed performance indexes for the experiment with the auto-tuning are

$$\begin{aligned} SPPI &= 0.83, \\ LDPI &= 1.57. \end{aligned} \tag{3.91}$$

Comparing this results with those in (3.90), one can see that that indexes were improved to much higher values. The LDPI index presents a value much higher than 1, meaning that the IAE of the experimental response was smaller than that computed as the target IAE_{ld}.

Figure 8 – Relative humidity responses and control signals of the experiment and of the validation simulations with PI controllers with the initial tuning.

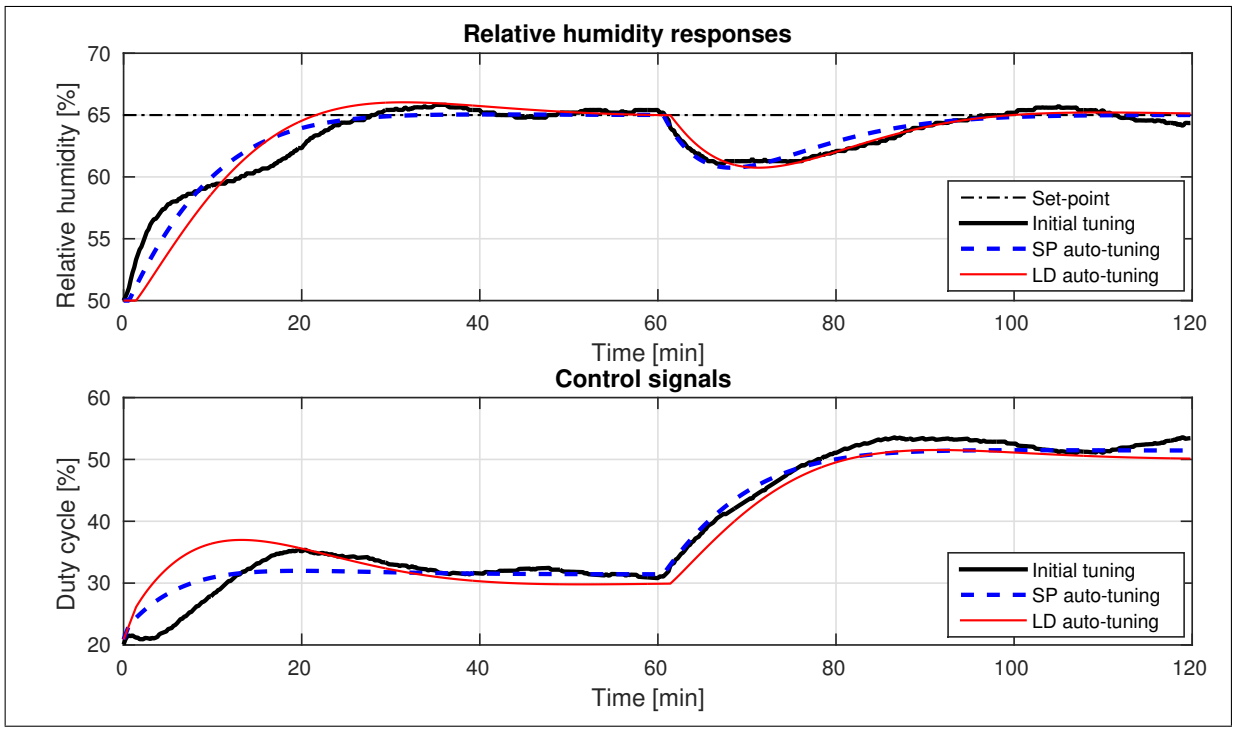

Source: The author.

Figure 9 – Relative humidity responses and control signals of the simulations with PI controllers with the initial tuning and with the auto-tuning considering the identified models.

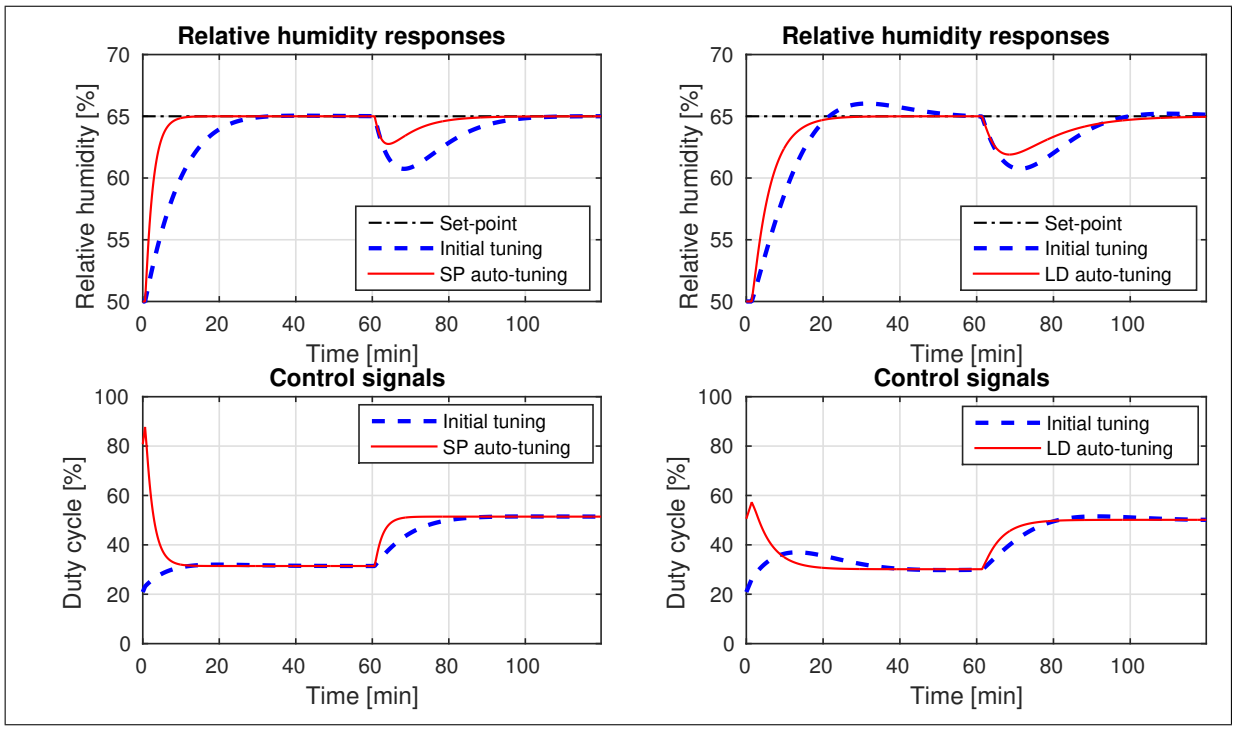

Source: The author.

Figure 10 – Relative humidity responses and control signals of the experiments with PI controllers with the initial tuning and with the auto-tuning.

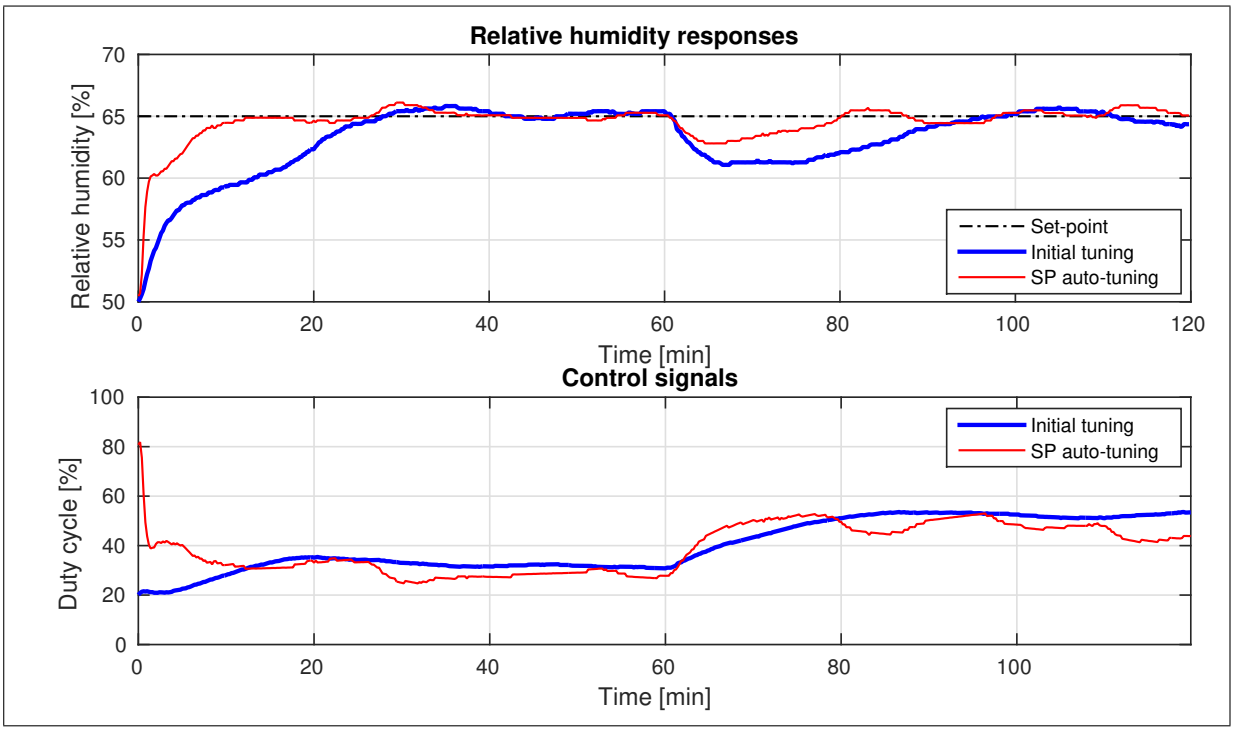

Source: The author.

3.9 Discussion

In this chapter the studied auto-tuning methodology was applied to PID controllers and their variation of I-PD controllers. The simulations gave emphasis to I-P controllers as that sort of controller is particularly largely used in the industry because of their characteristic of set-point step changes with smoother responses and smoother variation of the control signal, avoiding wearing the actuators. It was shown that the formulation of the estimation of model parameters is the same for step load disturbances and is different only for the set-point step change case.

It is important to note that in the simulations with the set-point step change auto-tuning for stable and unstable processes cases, the dead times were overestimated. Even when the level of the magnitude of the set-point step change when the dead time is computed was reduced to 0.5%. That happened due to the slower responses of the I-P controllers. A solution to that problem is to repeat the auto-tuning until a faster response is achieved. Also, a new method for the dead-time estimation can be studied, to eliminate the dependence of the estimated dead time on the speed of the controller response.

The experiments showed that the auto-tuning method is robust to the presence of measurement noise. The set-point step change based auto-tuning presented better results than the step load disturbance case. By analyzing the results, it is possible that the former case can cope better with measurement noise than the latter. To solve this problem a step load disturbance with

bigger magnitude needs to be applied, in order to get a bigger signal-to-noise ratio.

4 AUTO-TUNING OF THE SIMPLIFIED FILTERED SMITH PREDICTOR

This chapter is organized as follows. Section 4.1 describes the Simplified FSP for the continuous-time case. Section 4.2 presents the identification method of the auto-tuning. Section 4.3 describes the simple tuning rules. In Section 4.4 the performance assessment used by the proposed method is presented. Section 4.5 shows simulation results for each process case. In Section 4.6 experimental results in the relative humidity control of the neonatal incubator are presented and in Section 4.7 some important details are discussed.

4.1 The continuous-time SFSP

The FSP structure has lately become one of the most popular DTC structures to deal with stable, unstable and integrating systems (NORMEY-RICO; CAMACHO, 2009), whose block diagram is shown in Fig. 11, where the nominal plant model is written as $P_n(s) = G_n(s)e^{-\theta_m s}$, $G_n(s)$ is the delay-free model and θ_m is the nominal dead time. The nominal model $P_n(s)$ is known a priori and is expressed as

$$P_n(s) = \frac{\mu_m e^{-\theta_m s}}{\tau_m s + 1} \tag{4.1}$$

for stable processes, as

$$P_n(s) = \frac{\mu_m e^{-\theta_m s}}{\tau_m s - 1} \tag{4.2}$$

for unstable processes and as

$$P_n(s) = \frac{\mu_m e^{-\theta_m s}}{s} \tag{4.3}$$

for integrating processes.

If model uncertainties are not taken into account, then $P_n(s) = P(s)$, leading to the closed-loop transfer functions for set-point tracking and disturbance rejection, respectively:

$$H_{yr}(s) = \frac{Y(s)}{R(s)} = \frac{F(s)C(s)P_n(s)}{1 + C(s)G_n(s)}, \tag{4.4}$$

$$H_{yd}(s) = \frac{Y(s)}{D(s)} = P_n(s)\left[1 - \frac{F(s)C(s)P_n(s)F_r(s)}{1 + C(s)G_n(s)}\right], \tag{4.5}$$

where $R(s)$, $Y(s)$ and $D(s)$ are the Laplace transform of the desired set-point $r(t)$, the output $y(t)$ and the load disturbance $d(t)$, respectively.

Figure 11 – FSP structure.

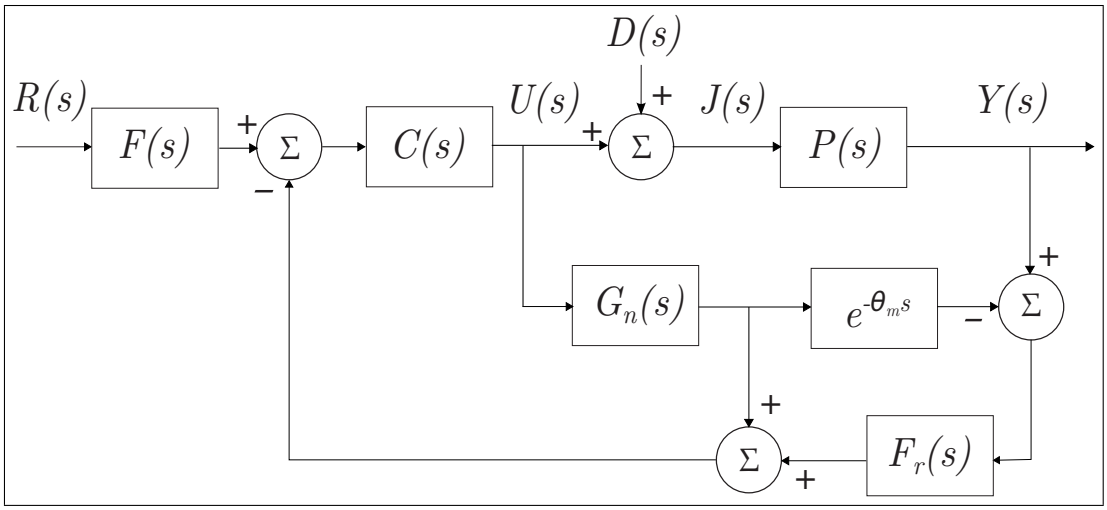

Source: The author.

Alternatively, the FSP structure can be rewritten by applying block manipulations to the diagram in Fig. 11 to obtain a classical 2-DOF structure as the one shown in Fig. 12, where

$$C_{eq}(s) = \frac{C(s)F_r(s)}{1 + G_n(s)C(s)(1 - F_r(s)e^{-\theta_m s})} \tag{4.6}$$

and

$$F_{eq} = \frac{F(s)}{F_r(s)}. \tag{4.7}$$

Figure 12 – Classical 2-DOF structure.

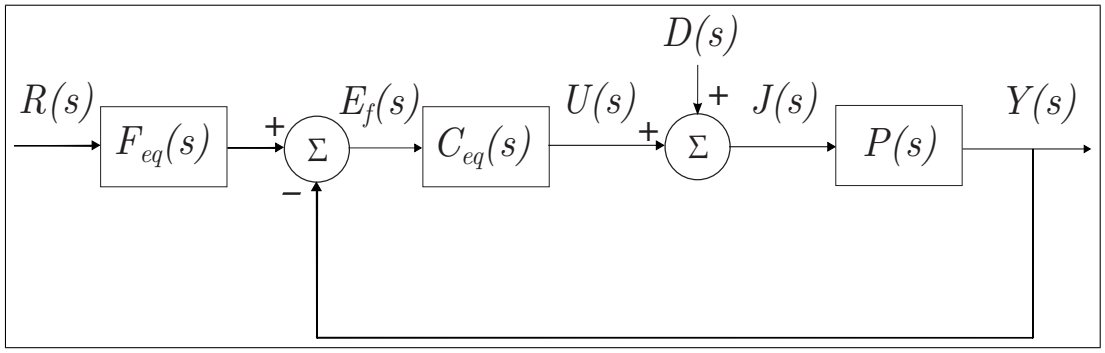

Source: The author.

As usual for a 2-DOF controller, F_{eq} is designed in order to assure

$$\lim_{s \to 0} F_{eq}(s) = 1. \tag{4.8}$$

In addition, in order to assure zero steady-state error for steplike set-point reference tracking, one might consider an integrator (a pole at $s = 0$) for the $C_{eq}(s)$ controller.

Simple tuning rules for the FSP controller were proposed in (TORRICO et al., 2013), applicable for first-order discrete-time processes, where the feedback controller $C(s)$ and the reference filter $F(s)$ are reduced to simple gains k_c and k_r, respectively, and are tuned for a desired step response. The filter $F_r(s)$ is tuned considering both steplike disturbance rejection at steady state and the trade-off between robustness and disturbance rejection. Such ideas constitute the so called SFSP.

4.1.1 Tuning of C(s) and F(s)

Following the ideas in (TORRICO et al., 2013), the design of $C(s) = k_c$ and $F(s) = k_r$ is made by first specifying the desired closed-loop response for set-point tracking and then finding their respective expressions to match that response. Therefore, it is desirable a first-order response following a dead time, resulting in the desired closed-loop transfer function:

$$\bar{H}_{yr}(s) = \frac{e^{-\theta_m s}}{\tau_c s + 1}, \tag{4.9}$$

where τ_c is the desired closed-loop time constant of the control system and it is a tuning parameter of the FSP.

For stable processes represented by a FOPDT model, equating (4.9) and (4.4) it is obtained

$$\frac{e^{-\theta_m s}}{\tau_c s + 1} = \frac{\frac{k_r k_c \mu_m}{k_c \mu_m + 1}}{\frac{\tau_m}{k_c \mu_m + 1} s + 1} e^{-\theta_m s}, \tag{4.10}$$

resulting in the expressions

$$k_c = \frac{1}{\mu_m}\left(\frac{\tau_m}{\tau_c} - 1\right) \tag{4.11}$$

and

$$k_r = \frac{\tau_m}{\tau_m - \tau_c}. \tag{4.12}$$

For the case of unstable processes described by an UFOPDT model, when equating (4.9) and (4.4) one gets

$$\frac{e^{-\theta_m s}}{\tau_c s + 1} = \frac{\frac{k_r k_c \mu_m}{k_c \mu_m - 1}}{\frac{\tau_m}{k_c \mu_m - 1} s + 1} e^{-\theta_m s}, \tag{4.13}$$

resulting in

$$k_c = \frac{1}{\mu_m}\left(\frac{\tau_m}{\tau_c} + 1\right) \tag{4.14}$$

and

$$k_r = \frac{\tau_m}{\tau_m + \tau_c}. \tag{4.15}$$

For an IPDT model describing integrating processes results

$$\frac{e^{-\theta_m s}}{\tau_c s+1} = \frac{k_r}{\frac{1}{k_c\mu_m}s+1}e^{-\theta_m s}, \tag{4.16}$$

obtaining

$$k_c = \frac{1}{\mu_m \tau_c}, \tag{4.17}$$

and

$$k_r = 1. \tag{4.18}$$

4.1.2 Tuning of $F_r(s)$

The robustness filter $F_r(s)$ can be written in continuous-time as

$$F_r(s) = \frac{b_1 s+b_2}{(\alpha s+1)^2}. \tag{4.19}$$

In this case, b_1 and b_2 are designed such as $C_{eq}(s)$ meet the conditions: (i) to exhibit a pole at $s=0$ in order to guarantee step disturbance rejection at steady state; (ii) to cancel the pole related to the τ_m time constant on the closed-loop transfer function for disturbance rejection $H_{yd}(s)$, which implies internal stability for unstable processes. The filter pole α is a tuning parameter set for faster or slower disturbance rejection dynamics. Some algebraic manipulations on (4.6) allow to write

$$C_{eq}(s) = \frac{F_r(s)}{G_n(s)\left(\frac{1+C(s)G_n(s)}{C(s)G_n(s)} - F_r(s)e^{-\theta_m s}\right)}. \tag{4.20}$$

Consider that the FOPDT and UFOPDT models can be rearranged, respectively, as

$$P_n(s) = \frac{\mu' e^{-\theta s}}{s+a} \tag{4.21}$$

and

$$P_n(s) = \frac{\mu' e^{-\theta s}}{s-a}. \tag{4.22}$$

Thus, in order to reach conditions (i) and (ii), for the stable and unstable cases ($a \neq 0$), one might have

$$\left[\frac{1+C(s)G_n(s)}{C(s)G_n(s)} - F_r(s)e^{-\theta_m s}\right]\Bigg|_{s=0} = 0, \tag{4.23}$$

$$\left[\frac{1+C(s)G_n(s)}{C(s)G_n(s)} - F_r(s)e^{-\theta_m s}\right]\Bigg|_{s=a} = 0 \tag{4.24}$$

and for the integrating case ($a = 0$),

$$\left[\frac{1+C(s)G_n(s)}{C(s)G_n(s)} - F_r(s)e^{-\theta_m s}\right]\Bigg|_{s=0} = 0, \tag{4.25}$$

$$\frac{d}{ds}\left[\frac{1+C(s)G_n(s)}{C(s)G_n(s)} - F_r(s)e^{-\theta_m s}\right]\Bigg|_{s=0} = 0. \tag{4.26}$$

Note that (4.23) and (4.24) or (4.25) and (4.26) may be arranged as a linear system of size two whose variables of interest are b_1 and b_2, leading to obtain $b_2 = k_r$ and, for the stable case,

$$b_1 = -\frac{(\tau_m - \alpha)^2}{\tau_m e^{\theta_m/\tau_m}} + b_2\tau_m, \tag{4.27}$$

for the unstable case,

$$b_1 = \frac{(\tau_m + \alpha)^2 e^{\theta_m/\tau_m}}{\tau_m} - b_2\tau_m \tag{4.28}$$

and for integrating processes

$$b_1 = 2\alpha + \theta_m + \frac{1}{k_c\mu_m}. \tag{4.29}$$

4.2 Estimation of model parameters

4.2.1 Stable processes

4.2.1.1 Set-point step change

After a set-point step change and applying the FVT to the signal $e_f(t)$, it is obtained

$$IE_f = \int_0^\infty e_f(t)dt = \lim_{s\to 0} E_f(s) = \lim_{s\to 0} \frac{F_{eq}(s)}{1 + C_{eq}(s)P(s)}R(s). \tag{4.30}$$

Substituting (2.1), (2.5), (4.6) and (4.7) in (4.30) and applying the l'Hôpital's rule results

$$IE_f = \frac{\phi A_r}{\mu}, \tag{4.31}$$

where

$$\phi = \frac{2\alpha + \tau_m + k_c\mu_m(2\alpha - b_1 + b_2\theta_m)}{b_2 k_c}. \tag{4.32}$$

After some algebraic manipulations this expression results

$$\phi = \mu_m(2\alpha - b + \theta_m + \tau_c), \tag{4.33}$$

with $b = b_1/b_2$. It is important to highlight that the constant ϕ appears in many of the following derived relations for stable and unstable processes.

The process gain then results

$$\mu = \frac{\phi A_r}{IE_f}. \tag{4.34}$$

By applying the FVT to the integral of $e_{su}(t)$ (2.7) one gets

$$IE_{su} = \int_0^\infty e_{su}(t)dt = \lim_{s\to 0} E_{su}(s) = \lim_{s\to 0}[\mu - P(s)]U(s) = \lim_{s\to 0}[\mu - P(s)]C_{eq}(s)\lim_{s\to 0} E_f(s). \tag{4.35}$$

Substituting in the expression above (2.1), (4.6) and (4.31), and applying the l'Hôpital's rule to the first limit, results

$$IE_{su} = T_0 A_r. \tag{4.36}$$

Therefore,

$$T_0 = \frac{IE_{su}}{A_r}, \tag{4.37}$$

leading to the time constant

$$\tau = T_0 - \theta. \tag{4.38}$$

4.2.1.2 Step load disturbance

At first, an estimation of the magnitude A_d of the step load disturbance is needed. By applying the FVT to integral of the output of the system, it is obtained

$$IY = \int_0^\infty y(t)dt = \lim_{s\to 0} Y(s) = \lim_{s\to 0} \frac{P(s)}{1 + C_{eq}(s)P(s)} D(s) \tag{4.39}$$

Substituting (2.1), (2.14) and (4.6) in the expression above and applying the l'Hôpital's rule one gets

$$IY = \phi A_d. \tag{4.40}$$

Therefore,

$$A_d = \frac{IY}{\phi}. \tag{4.41}$$

By applying the FVT to the integral of $j(t)$ (2.12) it is obtained

$$IJ = \int_0^\infty j(t)dt = \lim_{s\to 0} J(s) = \lim_{s\to 0} \frac{1}{1 + C_{eq}(s)P(s)} D(s) \tag{4.42}$$

Substituting (2.1), (2.14) and (4.6) in (4.42) and applying the l'Hôpital's rule:

$$IJ = \frac{\phi A_d}{\mu}. \tag{4.43}$$

Therefore, the process gain is

$$\mu = \frac{\phi A_d}{IJ}. \tag{4.44}$$

By applying the FVT to the double integral of $e_{sj}(t)$ (2.16) results

$$DIE_{sj} = \int_0^\infty \int_0^t e_{sj}(\nu) d\nu dt = \lim_{s\to 0} \frac{E_{sj}(s)}{s} = \lim_{s\to 0} \frac{[\mu - P(s)]}{s} \lim_{s\to 0} J(s). \tag{4.45}$$

Substituting (2.1) and (4.43) in the expression above and applying the l'Hôpital's rule, it is obtained

$$DIE_{sj} = T_0 \phi A_d \tag{4.46}$$

and

$$T_0 = \frac{DIE_{sj}}{\phi A_d}. \tag{4.47}$$

Therefore, the time constant is

$$\tau = T_0 - \theta. \tag{4.48}$$

4.2.2 Unstable processes

4.2.2.1 Set-point step change

Applying the FVT to the integral of the signal $e_f(t)$ after a set-point step change, (4.30) can be obtained. Substituting (2.1), (2.5), (4.6) and (4.7) in (4.30) and applying the l'Hôpital's rule results

$$IE_f = \frac{\phi A_r}{\mu}. \tag{4.49}$$

where

$$\phi = \frac{\tau_m - 2\alpha + k_c \mu_m (2\alpha - b_1 + b_2 \theta_m)}{b_2 k_c}. \tag{4.50}$$

And after some algebraic manipulations this constant results, as in the stable processes case, in (4.33):

$$\phi = \mu_m (2\alpha - b + \theta_m + \tau_c). \tag{4.51}$$

Then the process gain can be given by

$$\mu = \frac{\phi A_r}{IE_f}. \tag{4.52}$$

Applying the FVT to the integral of $e_{uu}(t)$ (2.9), it can be obtained

$$IE_{uu} = \int_0^\infty e_{uu}(t)dt = \lim_{s\to 0} E_{uu}(s) = \lim_{s\to 0} -[\mu + P(s)]U(s) = \lim_{s\to 0} -[\mu + P(s)]C_{eq}(s) \lim_{s\to 0} E_f(s). \tag{4.53}$$

Substituting in expression (4.53) the expressions (2.2), (4.6) and (4.49), and applying the l'Hôpital's rule to the first limit, one gets

$$IE_{uu} = T_0' A_r \tag{4.54}$$

and

$$T_0' = \frac{IE_{uu}}{A_r}. \tag{4.55}$$

Therefore, from (2.35), the time constant is

$$\tau = \theta - T_0'. \tag{4.56}$$

4.2.2.2 *Step load disturbance*

Applying the FVT to the integral of the output variable $y(t)$ results in (4.39). Substituting (2.1), (2.14) and (4.6) in that expression and applying the l'Hôpital's rule one gets

$$IY = -\phi A_d. \tag{4.57}$$

Therefore, the magnitude of the step load disturbance is

$$A_d = -\frac{IY}{\phi}. \tag{4.58}$$

By applying the FVT to the integral of $j(t)$ (2.12), (4.42) can be obtained. Substituting (2.1), (2.14) and (4.6) in that expression and applying the l'Hôpital's rule one gets

$$IJ = \frac{\phi A_d}{\mu}. \tag{4.59}$$

Therefore, the process gain results

$$\mu = \frac{\phi A_d}{IJ}. \tag{4.60}$$

By applying the FVT to the double integral of $e_{uj}(t)$ (2.18) results

$$DIE_{uj} = \int_0^\infty \int_0^t e_{uj}(\nu)d\nu dt = \lim_{s\to 0} \frac{E_{uj}(s)}{s} = \lim_{s\to 0} \frac{-[\mu + P(s)]}{s} \lim_{s\to 0} J(s). \tag{4.61}$$

Substituting (2.2) and (4.59) in expression (4.61) and applying the l'Hôpital's rule, one gets

$$DIE_{uj} = -T_0' \phi A_d, \tag{4.62}$$

then

$$T_0' = -\frac{DIE_{uj}}{\phi A_d}. \tag{4.63}$$

Therefore, the time constant is

$$\tau = \theta - T_0'. \tag{4.64}$$

4.2.3 Integrating processes

4.2.3.1 Set-point step change

By applying the FVT to the control variable $u(t)$ of a process described by (2.3) it is obtained

$$IU = \int_0^\infty u(t)dt = \lim_{s\to 0} U(s) = \lim_{s\to 0} \frac{C_{eq}(s)F_{eq}(s)}{1 + C_{eq}(s)P(s)} R(s). \tag{4.65}$$

Substituting (2.3), (2.5), (4.6) and (4.7) in the expression above, results

$$IU = \frac{A_r}{\mu}, \tag{4.66}$$

leading to the process gain

$$\mu = \frac{A_r}{IU}. \tag{4.67}$$

Applying the FVT to the integral of $e_{iu}(t)$ (2.11) one gets

$$IE_{iu} = \int_0^\infty e_{iu}(t)dt = \lim_{s\to 0} E_{iu}(s) = \lim_{s\to 0} \left[\frac{\mu}{s} - P(s)\right] \lim_{s\to 0} U(s). \tag{4.68}$$

Substituting (2.3) and (4.66) in the expression above and solving the first limit expression by applying the l'Hôpital's rule, results

$$IE_{iu} = \theta A_r. \tag{4.69}$$

The apparent dead time then results

$$\theta = \frac{IE_{iu}}{A_r}. \tag{4.70}$$

4.2.3.2 Step load disturbance

By applying the FVT to the integral of the output variable $y(t)$:

$$IY = \int_0^\infty y(t)dt = \lim_{s\to 0} Y(s) = \frac{P(s)}{1+C_{eq}(s)P(s)}D(s). \tag{4.71}$$

Substituting (2.3), (2.14) and (4.6) in the above equation and applying the l'Hôpital's rule, it is obtained

$$IY = \psi A_d, \tag{4.72}$$

where

$$\psi = \frac{4\alpha + k_c\mu_m(2\alpha^2 - \theta_m^2 + 2b_1\theta_m)}{2k_c}. \tag{4.73}$$

After algebraic manipulations this constant results

$$\psi = \mu_m(\alpha^2 + 2\alpha\tau_c - \theta_m^2/2 + b_1\theta_m). \tag{4.74}$$

That results in the magnitude of the step load disturbance as

$$A_d = \frac{IY}{\psi}. \tag{4.75}$$

Applying the FVT to the double integral of $j(t)$ results

$$DIJ = \int_0^\infty \int_0^t j(\nu)d\nu dt = \lim_{s\to 0}\frac{J(s)}{s} = \lim_{s\to 0}\frac{1}{s}\frac{1}{1+C_{eq}(s)P(s)}D(s). \tag{4.76}$$

Substituting (2.3), (2.14) and (4.6) in the above expression and applying the l'Hôpital's rule one gets

$$DIJ = \frac{\psi A_d}{\mu}, \tag{4.77}$$

resulting in the process gain as given by

$$\mu = \frac{\psi A_d}{DIJ}. \tag{4.78}$$

Applying the FVT to the double integral of $e_{ij}(t)$ (2.20) results

$$DIE_{ij} = \int_0^\infty \int_0^t e_{ij}(\nu)d\nu dt = \lim_{s\to 0}\frac{E_{ij}(s)}{s} = \lim_{s\to 0}\frac{\mu - sP(s)}{s}\lim_{s\to 0}\frac{J(s)}{s}. \tag{4.79}$$

Substituting (2.3) and (4.77) in (4.79) and using the l'Hôpital's rule in the first limit expression one gets

$$DIE_{ij} = \theta\psi A_d, \tag{4.80}$$

leading to the apparent dead time as

$$\theta = \frac{DIE_{ij}}{\psi A_d}. \tag{4.81}$$

4.3 Tuning

Once the new model (for the uncertain system) has been identified, we proceed to apply simple tuning rules to the controller. Once the controller is reset, then the performance assessment is performed based on the new parameters and the actual response of the system, in order to compute performance indexes.

The tuning rules that are defined for the SFSP were devised for the FSP in (NORMEY-RICO et al., 2014). Given the similarities of the two controllers, that tuning rules can apply to the corresponding tuning parameters of the SFSP, namely, α and τ_c.

For disturbance rejection, the tuning rules were devised through the nominal sensitivity peak M_s using an interval of $\theta_m/\tau_m \in (0,10]$, that is, covering a considerable range of lag-dominant and dead-time dominant models. The tuning can be done with $\alpha = \theta_m/2$ (for $M_s = 1.5$) for stable processes and with $\alpha = \theta_m$ (for $M_s = 2.2$) for integrating processes. For unstable processes, it can also be done $\alpha = \theta_m$ (for $M_s = 3$), since $\theta_m/\tau_m < 0.6$.

For set-point tracking, considering lag-dominant processes, the closed-loop time constant τ_c can be chosen between the interval $[\theta_m/4, \theta_m/2]$, where there is a trade-off between robustness and performance. Hence, lower values result in higher performance and higher values result in robust responses. For dead-time dominant processes, a conservative rule is to choose $\tau_c = \tau_m$ (HÄGGLUND, 1996).

After applying the tuning rules to the identified model, the new parameters of the SFSP are computed. Considering that ϕ (4.33) and ψ (4.74) were computed using the parameters obtained by the initial tuning, therefore, using the new parameters of the SFSP, respectively equivalent constants Φ and Ψ are computed.

4.4 Performance assessment

In general, the performance assessment of a control system is made by comparing the actual performance with a target performance. As the performance index used to the assessment it is chosen the integrated absolute error IAE, defined as

$$IAE = \int_0^\infty |e(t)|dt. \tag{4.82}$$

This choice is based on the characteristic that its minimization results generally in low overshoot and reduced settling time (SHINSKEY, 1994).

The actual integrated absolute error IAE_a value is computed after a set-point step change or a step load disturbance. After the identification, the target IAE can then be computed assuming that the identified model perfectly represents the plant.

4.4.1 Set-point step change

For set-point tracking, the desired closed-loop transfer function of the SFSP for stable, unstable and integrating processes is given by (4.9). For the SFSP, as for the FSP, considering this transfer function and a monotonic response of the output variable after a set-point step change, the target IAE value is computed as

$$IAE_{sp} = A_r(\tau_c + \theta_m). \tag{4.83}$$

4.4.2 Step load disturbance

For regulation tasks, the closed-loop transfer function of the SFSP for stable, unstable and integrating processes is

$$H_d(s) = \frac{Y(s)}{D(s)} = P_n(s)\left[1 - \frac{(bs+1)e^{-\theta_m s}}{(\tau_c s+1)(\alpha s+1)^2}\right]. \tag{4.84}$$

where, for stable and unstable processes, $b = b_1/b_2$ and, for integrating processes, $b = b_1$.

Based on that transfer function, the target IAE value is computed for stable and unstable processes as

$$IAE_{ld} = |\Phi A_d| \tag{4.85}$$

and for integrating processes as

$$IAE_{ld} = |\Psi A_d|. \tag{4.86}$$

4.4.3 Performance indexes

The Set-Point Performance Index (SPPI) can then be defined below as the ratio between the target and the actual IAE values:

$$SPPI = \frac{IAE_{sp}}{IAE_a}. \tag{4.87}$$

Similarly, the Load Disturbance Performance Index (LDPI) is defined as

$$LDPI = \frac{IAE_{ld}}{IAE_a}. \tag{4.88}$$

Theoretically, the SFSP has satisfactory performance when the performance index value is equal to 1. Nevertheless, in a pratical context, a FSP can be considered well tuned when that value is greater than 0.8 (NORMEY-RICO et al., 2014). Certainly, if tighter performance is required, this value must be higher.

4.5 Simulation results

The chosen examples are stable, unstable and integrating processes presented in (NORMEY-RICO; CAMACHO, 2009) and (GARCÍA; ALBERTOS, 2008), being the same as in the simulations for PID controllers. For each case, it was added model uncertainties considering that the initial model was incorrectly estimated or that the parameters of the plant changed. As the goal is to obtain initial tunings with poor performance, the uncertainties where chosen accordingly with the tuning rules. Therefore, such uncertainties have different values from the simulations for the PID controllers case. In the same simulation are performed both the auto-tunings based on the set-point (SP) step change as on the step load disturbance (LD). Its responses are then plotted in the same figure with the initial tuning response for comparison. Furthermore, the tuning rules of Section 4.3 were used for each controllers.

4.5.1 Stable process

The model for temperature control in a heat exchanger (NORMEY-RICO; CAMACHO, 2009) is presented below.

$$P_1(s) = \frac{0.12e^{-3s}}{6s+1}. \tag{4.89}$$

The uncertainties of the model were of $+10\%$ in the process gain, -10% in the time constant and $+20\%$ in the dead time. The tuning rules are $\alpha = \theta_m/2$ and $\tau_c = \theta_m/4$. At $t = 80$, a step load disturbance of amplitude -8 is applied and it is estimated as $A_d = -8$. The output and control signals responses are shown in Fig. 13 and the estimated parameters and performance indexes are presented in 5.

Table 5 – Parameters and indexes for process $P_1(s)$

	μ	T_0	τ	θ	SPPI	LDPI
Initial tuning	0.13	9.00	5.40	3.60	0.71	0.66
SP auto-tuning	0.12	9.00	5.96	3.04	0.99	1.00
LD auto-tuning	0.12	9.01	5.87	3.14	0.94	0.99

From Fig. 13 and Table 5, it can be seen that both auto-tunings improved the responses of the system with high performance. Furthermore, the parameters estimated analytically (μ and T_0) presented correct values.

4.5.2 Unstable process

The second example is a model of concentration control in an unstable reactor (NORMEY-RICO; CAMACHO, 2009).

$$P_2(s) = \frac{3.433e^{-20s}}{103.1s-1}. \tag{4.90}$$

Figure 13 – Set-point and load disturbance step responses for process $P_1(s)$ with the initial tuning and with the auto-tunings.

Source: The author.

The uncertainties were $+10\%$ for the process gain, -5% for the time constant and $+10\%$ for the dead time. The chosen tuning rules are $\alpha = \theta_m$ and $\tau_c = \theta_m/4$. After a step load disturbance of magnitude 0.2 at $t = 600$, its estimated value was $A_d = 0.2$. The output and control signal responses are shown in Fig. 14 and estimated parameters and performance indexes are shown in Table 6.

Table 6 – Parameters and indexes for process $P_2(s)$

	μ	T_0	τ	θ	SPPI	LDPI
Initial tuning	3.78	119.95	97.95	22	0.64	0.79
SP auto-tuning	3.46	120.63	100.32	20.30	0.91	1.00
LD auto-tuning	3.49	128.71	106.51	22.2	0.85	1.00

It can be seen from Fig. 14 that the auto-tunings reduced or eliminated the oscillations from the initial tuning and even with faster responses. From Table 6 one sees that the analytically estimated values of μ and T_0 are consistent as well as the estimated values of the apparent dead time. The performance indexes were improved to acceptable or high values.

Figure 14 – Set-point and load disturbance step responses for process $P_2(s)$ with the initial tuning and with the auto-tunings.

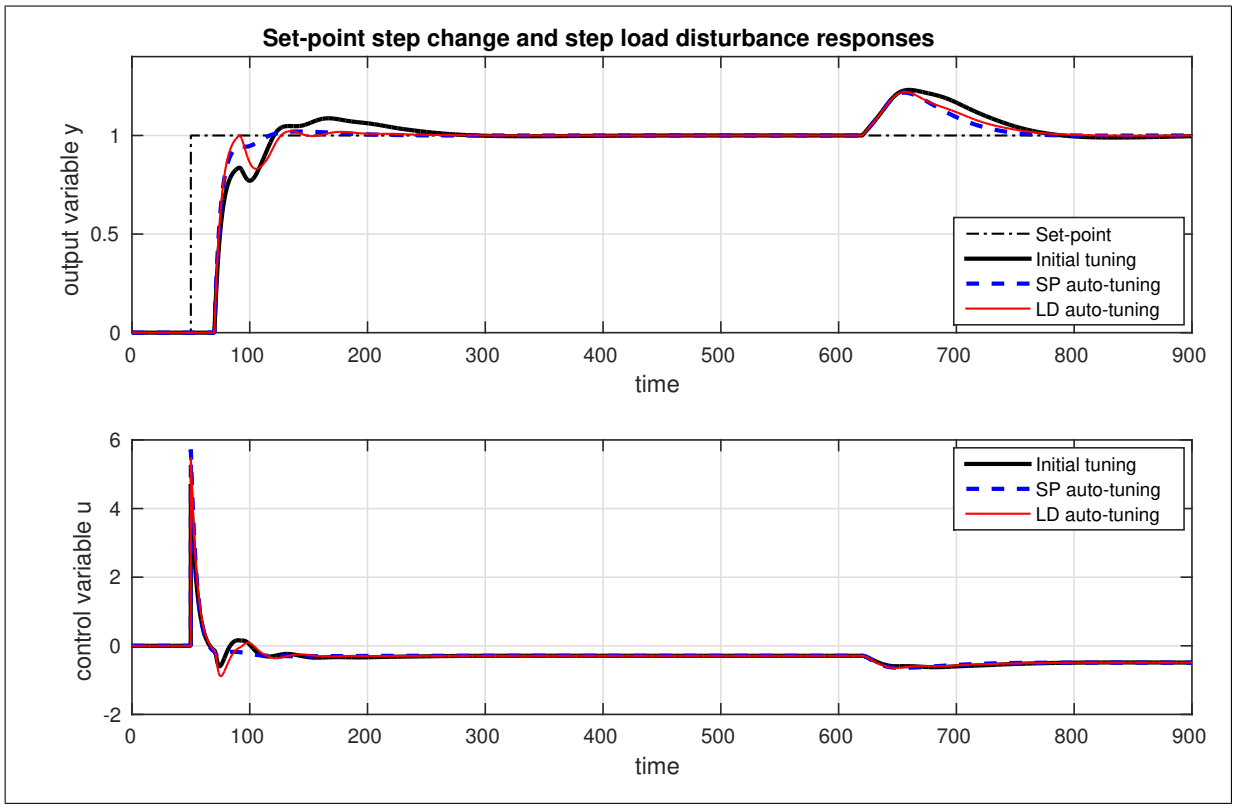

Source: The author.

4.5.3 *Integrating process*

The integrating process below is presented in (GARCÍA; ALBERTOS, 2008).

$$P_3(s) = \frac{0.1e^{-8s}}{s(s+1)(0.5s+1)(0.1s+1)}. \tag{4.91}$$

A IPDT model for this process is

$$P_n(s) = \frac{0.1e^{-9.6s}}{s}. \tag{4.92}$$

The uncertainties were -20% for the process gain and $+30\%$ for the dead time. The tuning rules are $\alpha = \theta_m$ and $\tau_c = \theta_m/4$. By applying a step load disturbance of magnitude -0.3 at $t = 450$ its estimated value was $A_d = -0.3$. The output and control signal responses are seen in Fig. 15 and in Table 7 are seen the estimated parameters and performance indexes.

For this case, where the apparent dead time is estimated analytically, the time responses of the auto-tunings were faster than that of the initial tuning and the performance indexes were considerably improved. From Table 7, it can be seen that the model parameters were correctly estimated.

Figure 15 – Set-point and load disturbance step responses for process $P_3(s)$ with the initial tuning and with the auto-tunings.

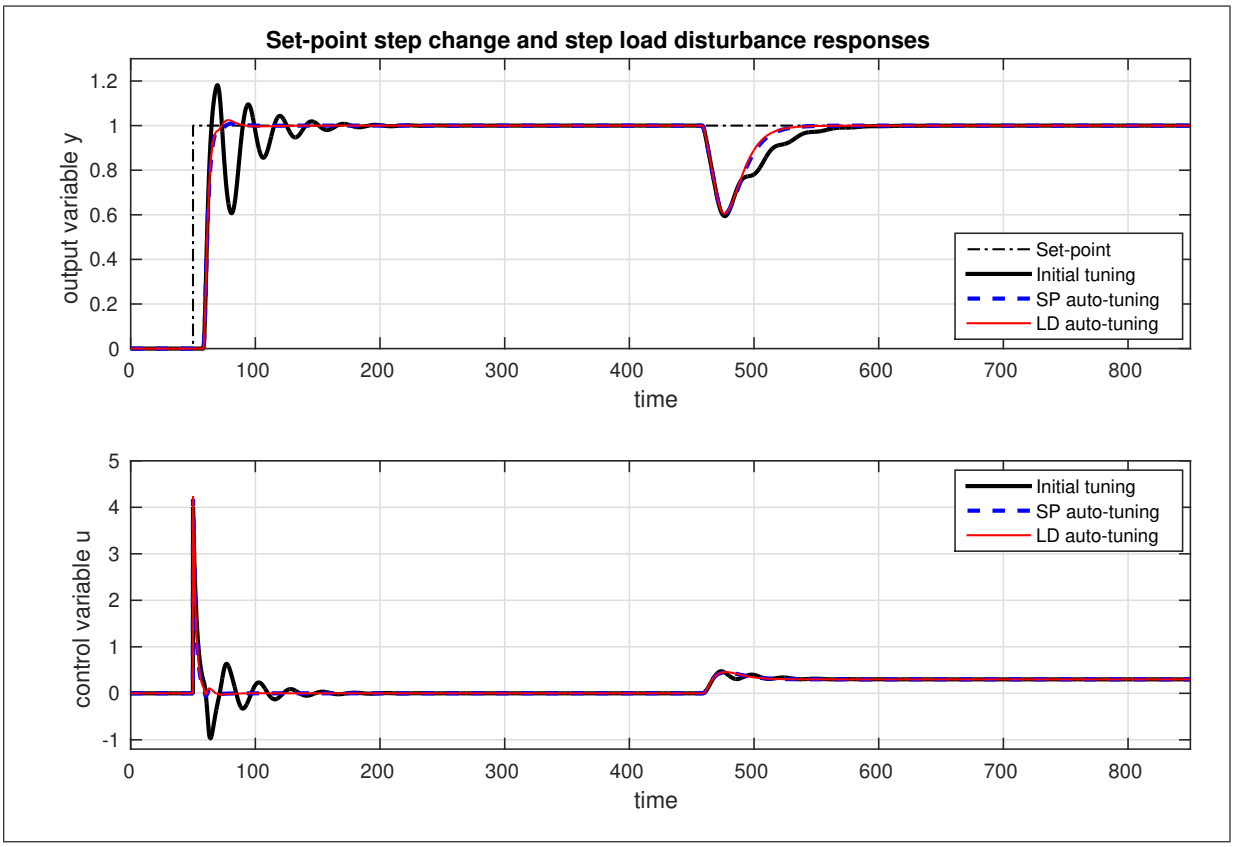

Source: The author.

Table 7 – Parameters and indexes for process $P_3(s)$

	μ	θ	SPPI	LDPI
Initial tuning	0.08	12.48	0.61	0.72
SP auto-tuning	0.10	9.60	0.99	0.97
LD auto-tuning	0.10	9.45	0.98	1.00

4.6 Experimental results

As in the previous chapter, the proposed auto-tuning technique is applied in the control of relative humidity of the neonatal incubator.

The initial tuning of the SFSP was made based on the model in (4.93):

$$P(s) = \frac{0.85e^{-1.2s}}{5.59s+1}. \tag{4.93}$$

For the tuning, it was chosen $\alpha = \theta_m/2$ and, to avoid a high value of the control signal peak in the set-point step change, it was chosen $\tau_c = 3\theta_m$. The others parameters of the SFSP

can then be obtained using the given previous ones.

The sampling time was $T_s = 0.2$ min. Initially, the relative humidity was controlled in 52% and at $t = 0$ a set-point step change of $A_r = 15\%$ was applied and at $t = 60$ min a step load disturbance of $A_d = -20\%$ was applied.

Obtaining the dead times as in Section 2.3 and by applying (4.34), (4.37) and (4.38) to the set-point step change data and by applying (4.41), (4.44), (4.47) and (4.48) to the step load disturbance data, the estimated model parameters are as in Table 8. The step load disturbance was estimated as $A_d = -14.96$.

Table 8 – Estimated parameters of the experiment with the SFSP.

	μ	T_0	τ	θ
Initial tuning	0.85	6.79	5.59	1.2
SP auto-tuning	0.61	13.84	13.04	0.8
LD auto-tuning	-0.12	-40.27	-40.47	0.2

From Table 8, it can be seen that the estimated parameters based on the step load disturbance presented not feasible values. Therefore, hereafter, it is considered just the results obtained by the auto-tuning based on the set-point step change.

The performance indexes were then computed as

$$\begin{aligned} SPPI &= 0.43, \\ IAE_a &= 47.31, \end{aligned} \tag{4.94}$$

where the index IAE_a is the IAE of the step load disturbance response. Note that the SPPI index is less than 0.8, meaning that the SFSP needs to be re-tuned.

As model validation, Fig. 16 shows a comparison between the experimental and simulation results using the initial tuning of the SFSP. The simulation used the model identified by the set-point step change case, as in Table 8.

In Fig. 17 are shown simulations using the model identified by the set-point step change case with the initial tuning and with the tuning obtained by the auto-tuning. It can be seen that with the auto-tuning the responses were much faster than the responses with the initial tuning.

Fig. 10 shows a comparison of the experiments with the initial tuning and with the auto-tuning. It can be seen that the responses with the auto-tuning were improved both for the set-point step change and for the step-load disturbance.

The performance indexes for the auto-tuning were computed as

$$\begin{aligned} SPPI &= 0.74, \\ IAE_a &= 17.74. \end{aligned} \tag{4.95}$$

Figure 16 – Relative humidity responses and control signals of the experiment and of the validation simulation with the SFSP with the initial tuning.

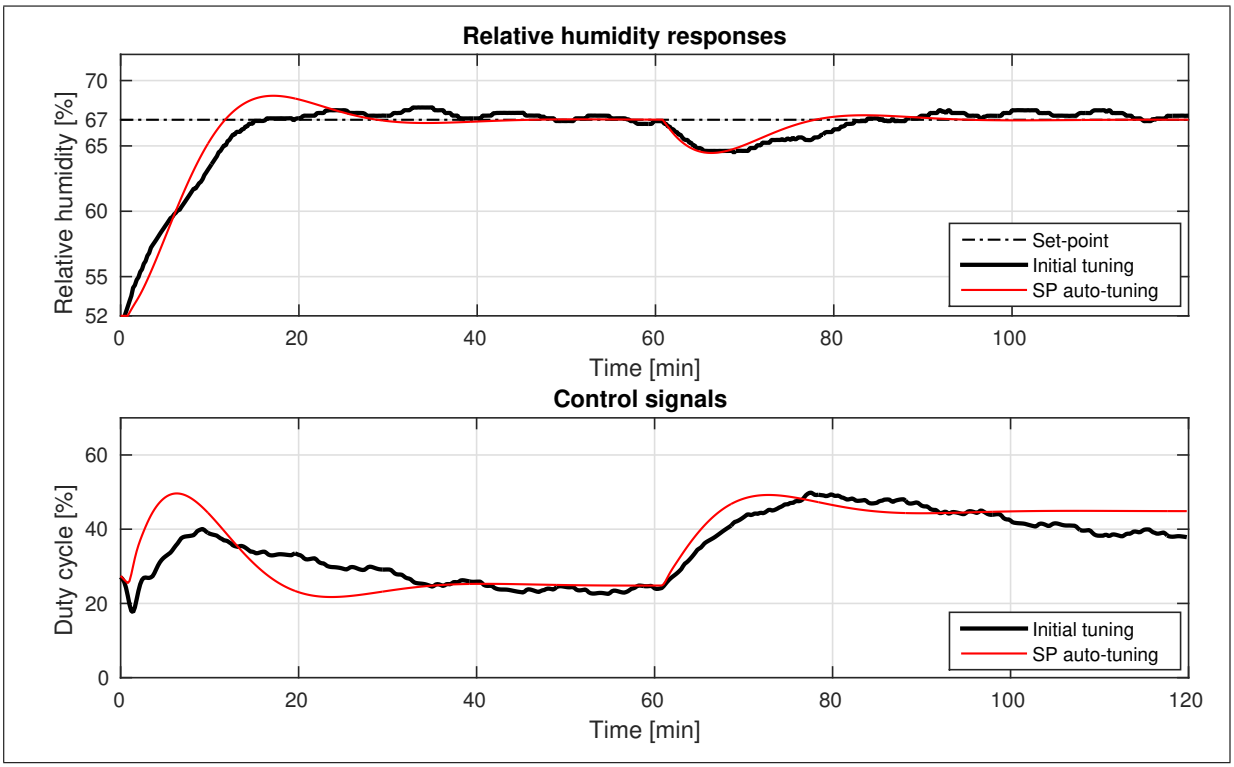

Source: The author.

The SPPI is less than 0.8, nevertheless, it can be seen that this index was much higher than with the initial tuning. And, as can be seen from Fig. 18 at the instant of the set-point step change, the control signal of the auto-tuning response was in the control limit, meaning that a more aggressive response might result in saturation of the control signal. In addition, the IAE_a presented a reduction of -62.5%.

4.7 Discussion

From the simulation results, one can notice that, for all three kind of processes, the proposed strategy was capable of improve the performance of the time responses when compared with the initial tuning.

Analyzing the experimental results, it can be seen that, as in the PID controller case, the auto-tuning based in set-point step changes had better results than the based in step load disturbances, where the identified parameters of the model do not had feasible values. It is possible that such problem occurred due to the high signal-to-noise ratio or, perhaps, because the response needed a bigger time to attain the steady-state. The former problem could be solved by applying a step load disturbance with bigger magnitude.

Figure 17 – Relative humidity responses and control signals of the simulations with the SFSP with the initial controller tuning and with the auto-tuning considering the identified model.

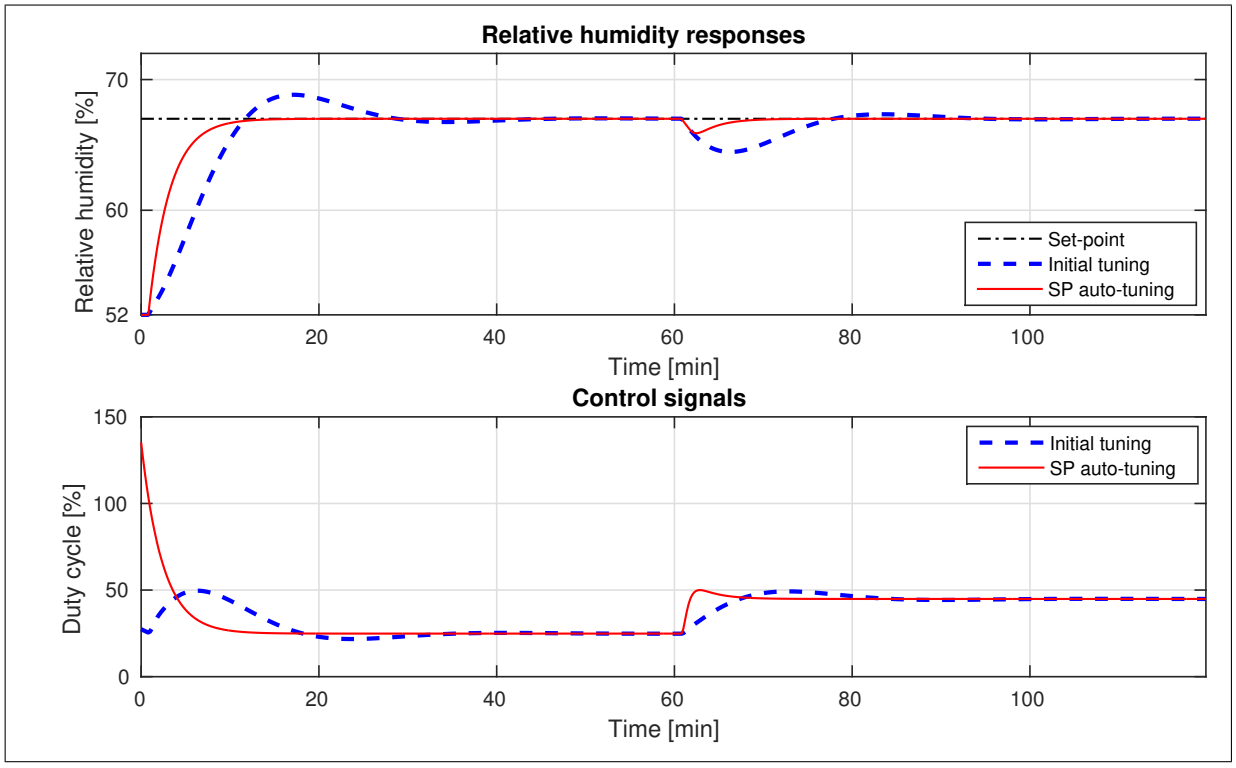

Source: The author.

Figure 18 – Relative humidity responses and control signals of the experiments with the SFSP with the initial tuning and with the auto-tuning.

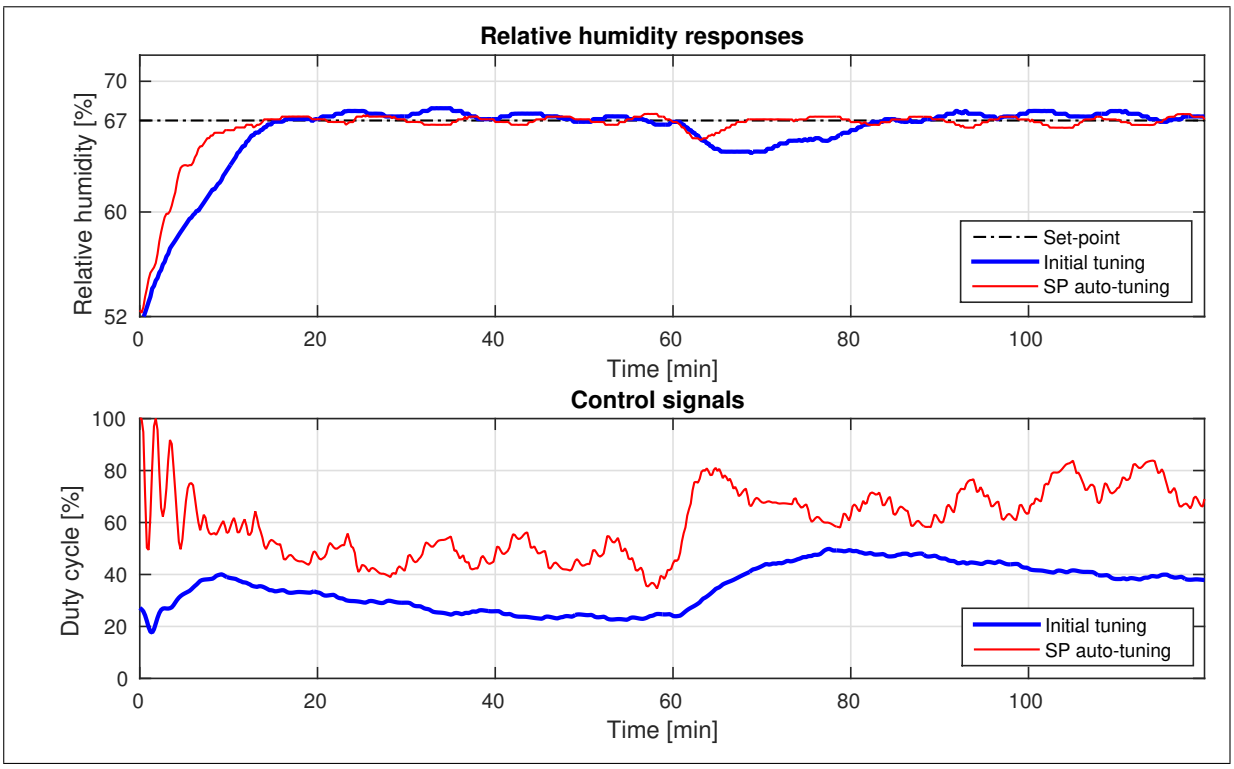

Source: The author.

5 AUTO-TUNING OF PID CONTROLLERS FOR TITO PROCESSES

The chapter is organised as follows. In Section 5.1 the problem is formulated. The method for estimating the process parameters by using the closed-loop set-point step responses is explained in Section 5.2, while the employed tuning rules is reviewed in Section 5.3. Simulation examples (where the proposed method is compared to another one) are given in Section 5.4. In Section 5.5 the experimental results are shown. Some comments are drawn in Section 5.6.

5.1 Problem formulation

We consider a linear, time-invariant, continuous-time TITO system whose matrix transfer function is:

$$\mathbf{P}(s) = \left[P_{ij}(s)\right], \quad i,j = 1,2 \tag{5.1}$$

where $(i,j = 1,2)$

$$P_{ij}(s) = \frac{\mu_{ij} e^{-s\theta_{ij}}}{q_{ij}(s)} \tag{5.2}$$

and

$$q_{ij}(s) = \prod_{k=1}^{n_{ij}} (1 + s\tau_{ij,k}) = s^{n_{ij}} \prod_{k=1} \tau_{ij,k} + \ldots + s \sum_{k=1}^{n_{ij}} \tau_{ij,k} + 1. \tag{5.3}$$

It is assumed that (5.1) is a non-singular matrix transfer function, meaning that it is not singular for any positive finite frequency on the real axis. Also, the open-loop step responses of $P_{ij}(s)$, $i,j = 1,2$ are assumed to be monotonic.

Define as

$$T_{ij}^{0} := \sum_{k=1}^{n_{ij}} \tau_{ij,k} + \theta_{ij} \tag{5.4}$$

the sum of the dead time and of the time constant of the single transfer function $P_{ij}(s)$. We consider a decentralised control law (where the input-output pairings have been previously selected), where the PID controller is in ideal form, namely,

$$\mathbf{C}(s) \quad = \begin{bmatrix} C_1(s) & 0 \\ 0 & C_2(s) \end{bmatrix}. \tag{5.5}$$

where

$$C_j(s) = K_{Pj}\left(1 + \frac{1}{T_{Ij}s} + T_{Dj}s\right) \quad j = 1,2 \tag{5.6}$$

and K_{Pj}, T_{Ij}, T_{Dj}, $j = 1,2$ are, respectively, the proportional gain, the integral time constant and the derivative time constant of the PID controller that handles loop j. Note that, in order to make the controller proper, a low-pass filter has also to be implemented. Its cut-off frequency should be selected in order for the filter to be negligible for the PID relevant dynamics and to filter the high frequency noise at the same time (ANG; CHONG; LI, 2005; VISIOLI, 2006). Hereafter we will neglect the presence of the filter in the autotuning procedure, but we will include it in the simulation results (see Section 5.4). For the analysis made in the following sections, it is convenient to write the PID controller transfer function as

$$C_j(s) = \frac{K_{Pj} c_j(s)}{sT_{Ij}}, \quad j = 1,2 \tag{5.7}$$

where

$$c_j(s) = T_{Dj} T_{Ij} s^2 + T_{Ij} s + 1, \quad j = 1,2. \tag{5.8}$$

The control scheme is shown in Fig. 19.

The aim of the methodology proposed in this work is to estimate the process parameters by evaluating closed-loop set-point step responses. In particular, given already (roughly) tuned PI(D) controllers, a step signal is applied to the first set-point and then, after the steady-state has been attained, to the second set-point. After the process parameters have been estimated, any tuning rule can be employed for re-tuning the PI(D) controllers. Among those presented in the literature, in this work we have chosen that proposed in (LEE et al., 2004) because of the high performance it has been shown to provide despite its simplicity and because of the presence of a parameters which handles the trade-off between aggressiveness and robustness (see Section 5.3).

Figure 19 – The considered TITO control scheme.

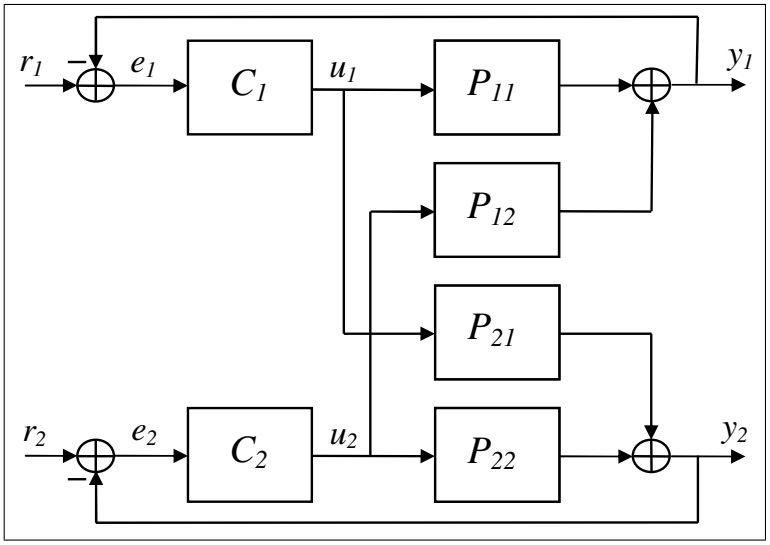

Source: The author.

5.2 Estimation of model parameters

The estimation of the process parameters can be performed by evaluating the response of the system to a sequence of step signals applied to each of the set-points starting from steady-state conditions. This means that the transient response caused by a set-point step has to be terminated before applying another set-point step and should not be perturbed by external disturbances.

By considering a set-point step change in the loop 1 (i.e. to r_1), the following relations can be easily derived:

$$\begin{aligned} U_1(s) &= C_1(s)(R_1(s) - (P_{11}(s)U_1(s) + P_{12}(s)U_2(s))), \\ U_2(s) &= C_2(s)(-(P_{22}(s)U_2(s) + P_{21}(s)U_1(s))), \end{aligned} \tag{5.9}$$

from which it can be derived that

$$\begin{aligned} U_1(s) &= \frac{-C_1(s)(1 + C_2(s)P_{22}(s))R_1(s)}{d(s)}, \\ U_2(s) &= \frac{C_1(s)C_2(s)P_{21}(s)R_1(s)}{d(s)}. \end{aligned} \tag{5.10}$$

where

$$d(s) = 1 + C_2(s)P_{22}(s) + C_1(s)P_{11}(s) + C_1(s)C_2(s)P_{11}(s)P_{22}(s) - C_1(s)C_2(s)P_{12}(s)P_{21}(s). \tag{5.11}$$

Further, the two control errors are:

$$\begin{aligned} E_{1,1}(s) &= R_1(s) - P_{11}(s)U_1(s) - P_{12}(s)U_2(s), \\ E_{2,1}(s) &= -P_{21}(s)U_1(s) - P_{22}(s)U_2(s). \end{aligned} \tag{5.12}$$

$E_{1,1}(s)$ and $E_{2,1}(s)$ are respectively, the error variable in loops 1 and 2 after the set-point change applied in loop 1. By replacing the output of the controllers in (5.12) with their expressions (5.10) and by considering (5.2) and (5.7), after some calculations the transfer functions between the set-point of the first loop (R_1) and the two control errors can be written as:

$$\begin{aligned} \frac{E_{1,1}(s)}{R_1(s)} &= \frac{sa_1(s)e^{-s(\theta_{11}+\theta_{12}+\theta_{21})}}{b_1(s)s^2 + b_2(s)b_3(s)s + b_4(s)b_5(s)}, \\ \frac{E_{2,1}(s)}{R_1(s)} &= \frac{-sa_2(s)e^{-s(\theta_{11}+\theta_{12}+\theta_{22})}}{b_1(s)s^2 + b_2(s)b_3(s)s + b_4(s)b_5(s)}, \end{aligned} \tag{5.13}$$

where

$$
\begin{aligned}
a_1(s) &= (sT_{I2}q_{22}(s)e^{-s\theta_{22}} + K_{P2}\mu_{22}c_2(s))T_{I1}q_{11}(s)q_{12}(s)q_{21}(s),\\
a_2(s) &= K_{P1}\mu_{21}T_{I2}c_1(s)q_{11}(s)q_{12}(s)q_{22}(s),\\
b_1(s) &= T_{I1}T_{I2}q_{11}(s)q_{12}(s)q_{21}(s)e^{-s(\theta_{11}+\theta_{12}+\theta_{21}+\theta_{22})},\\
b_2(s) &= q_{12}(s) + q_{21}(s)e^{-s(\theta_{12}+\theta_{21})},\\
b_3(s) &= T_{I1}K_{P2}\mu_{22}q_{11}(s)c_2(s)e^{-s\theta_{11}} + T_{I2}K_{P1}\mu_{11}q_{22}(s)c_1(s)e^{-s\theta_{22}},\\
b_4(s) &= K_{P1}K_{P2}c_1(s)c_2(s),\\
b_5(s) &= \mu_{11}\mu_{22}q_{12}(s)q_{21}(s)e^{-s(\theta_{12}+\theta_{21})} - \mu_{12}\mu_{21}q_{11}(s)q_{22}(s)e^{-s(\theta_{12}+\theta_{22})}.
\end{aligned}
\tag{5.14}
$$

By applying the final value theorem we eventually obtain the following expressions of the integrated errors:

$$
\begin{aligned}
IE_{1,1} &:= \int e_{1,1}(t)dt = \frac{\mu_{22}T_{I1}}{K_{P1}(\mu_{11}\mu_{22}-\mu_{12}\mu_{21})}A_{s1}\\
IE_{2,1} &:= \int e_{2,1}(t)dt = -\frac{\mu_{21}T_{I2}}{K_{P2}(\mu_{11}\mu_{22}-\mu_{12}\mu_{21})}A_{s1}
\end{aligned}
\tag{5.15}
$$

where A_{s1} denotes the amplitude of the set-point step change applied to the first loop.

Denote now as A_{u1} and A_{u2} the steady-state values of the output of the controllers C_1 and C_2 respectively. By considering that, at the steady state, after a step change in the set-point r_1, it has to be:

$$
\begin{aligned}
\mu_{11}A_{u1} + \mu_{12}A_{u2} &= A_{s1}\\
\mu_{21}A_{u1} + \mu_{22}A_{u2} &= 0
\end{aligned}
\tag{5.16}
$$

we can express A_{u1} and A_{u2} in terms of the process gains as follows:

$$
\begin{aligned}
A_{u1} &= \frac{\mu_{22}}{\mu_{11}\mu_{22}-\mu_{12}\mu_{21}}A_{s1},\\
A_{u2} &= -\frac{\mu_{21}}{\mu_{11}\mu_{22}-\mu_{12}\mu_{21}}A_{s1}.
\end{aligned}
\tag{5.17}
$$

Define now the two following variables:

$$
\begin{aligned}
v(t) &:= \mu_{11}u_1(t) + \mu_{12}u_2(t) - y_1(t),\\
w(t) &:= \mu_{21}u_1(t) + \mu_{22}u_2(t) - y_2(t).
\end{aligned}
\tag{5.18}
$$

By using (5.2), (5.3), and (5.18) we can derive:

$$
\begin{aligned}
V(s) &= \frac{\mu_{11}}{q_{11}(s)}(q_{11}(s) - e^{-s\theta_{11}})U_1(s) + \frac{\mu_{12}}{q_{12}(s)}(q_{12}(s) - e^{-s\theta_{12}})U_2(s),\\
W(s) &= \frac{\mu_{21}}{q_{21}(s)}(q_{21}(s) - e^{-s\theta_{21}})U_1(s) + \frac{\mu_{22}}{q_{22}(s)}(q_{22}(s) - e^{-s\theta_{22}})U_2(s).
\end{aligned}
\tag{5.19}
$$

Hence, by applying the final value theorem, we obtain

$$\begin{aligned}
\lim_{s\to 0}\frac{V(s)}{s} &= \mu_{11}\lim_{s\to 0}\left(\frac{q_{11}(s)-1}{s}+\frac{1+e^{-s\theta_{11}}}{s}\right)A_{u1} \\
&\quad +\mu_{12}\lim_{s\to 0}\left(\frac{q_{12}(s)-1}{s}+\frac{1+e^{-s\theta_{12}}}{s}\right)A_{u2} \\
&= \mu_{11}T_{11}^0A_{u1}+\mu_{12}T_{12}^0A_{u2}, \\
\lim_{s\to 0}\frac{W(s)}{s} &= \mu_{21}\lim_{s\to 0}\left(\frac{q_{21}(s)-1}{s}+\frac{1+e^{-s\theta_{21}}}{s}\right)A_{u1} \\
&\quad +\mu_{22}\lim_{s\to 0}\left(\frac{q_{22}(s)-1}{s}+\frac{1+e^{-s\theta_{22}}}{s}\right)A_{u2} \\
&= \mu_{21}T_{21}^0A_{u1}+\mu_{22}T_{22}^0A_{u2},
\end{aligned} \tag{5.20}$$

that is, by taking into account (5.17), (5.3), and (5.4), we have

$$\begin{aligned}
IV_1 &:= \int v(t)dt = \frac{\mu_{11}\mu_{22}T_{11}^0}{\mu_{11}\mu_{22}-\mu_{12}\mu_{21}}A_{s1}-\frac{\mu_{12}\mu_{21}T_{12}^0}{\mu_{11}\mu_{22}-\mu_{12}\mu_{21}}A_{s1} \\
IW_1 &:= \int w(t)dt = \frac{\mu_{21}\mu_{22}T_{21}^0}{\mu_{11}\mu_{22}-\mu_{12}\mu_{21}}A_{s1}-\frac{\mu_{21}\mu_{22}T_{22}^0}{\mu_{11}\mu_{22}-\mu_{12}\mu_{21}}A_{s1}
\end{aligned} \tag{5.21}$$

which can be rewritten as

$$\begin{aligned}
IV_1 &= \frac{\mu_{11}\mu_{22}T_{11}^0-\mu_{12}\mu_{21}T_{12}^0}{\mu_{11}\mu_{22}-\mu_{12}\mu_{21}}A_{s1}, \\
IW_1 &= \frac{\mu_{21}\mu_{22}(T_{21}^0-T_{22}^0)}{\mu_{11}\mu_{22}-\mu_{12}\mu_{21}}A_{s1}.
\end{aligned} \tag{5.22}$$

A similar reasoning can be applied when a step change is applied to the set-point of the other loop (i.e. to r_2). Hence, using symmetry of the system structure $IE_{1,2}, IE_{2,2}, IV_2, IW_2$ are obtained. Thus, by applying a step change to the set-point of the first loop and then, at the end of the transient, a step change to the set-point of the second loop, the four process gains and the values of the four sums of the lags and dead times T_{ij}^0 $(i,j=1,2)$ can be computed using:

$$\begin{aligned}
\mu_{11} &= \frac{T_{I1}IE_{2,2}}{K_{P1}(IE_{1,1}IE_{2,2}-IE_{1,2}IE_{2,1})}A_{s1}, \\
\mu_{12} &= \frac{T_{I2}IE_{1,2}}{K_{P2}(IE_{1,2}IE_{2,1}-IE_{1,1}IE_{2,2})}A_{s1}, \\
\mu_{21} &= \frac{T_{I1}IE_{2,1}}{K_{P1}(IE_{1,2}IE_{2,1}-IE_{1,1}IE_{2,2})}A_{s2}, \\
\mu_{22} &= \frac{T_{I2}IE_{1,1}}{K_{P2}(IE_{1,1}IE_{2,2}-IE_{1,2}IE_{2,1})}A_{s2}.
\end{aligned} \tag{5.23}$$

$$
\begin{aligned}
T_{11}^0 &= \frac{\mu_{21} IV_2}{\mu_{11} A_{s2}} + \frac{IV_1}{A_{s1}}, \\
T_{12}^0 &= \frac{\mu_{22} IV_2}{\mu_{12} A_{s2}} + \frac{IV_1}{A_{s1}}, \\
T_{21}^0 &= \frac{\mu_{11} IW_1}{\mu_{21} A_{s1}} + \frac{IW_2}{A_{s2}}, \\
T_{22}^0 &= \frac{\mu_{12} IW_1}{\mu_{22} A_{s1}} + \frac{IW_2}{A_{s2}}.
\end{aligned}
\tag{5.24}
$$

Summarising, the identification procedure initially consists of evaluating $IE_{1,1}$, $IE_{2,1}$, $IE_{1,2}$, $IE_{2,2}$, IV_1, IW_1, IV_2, IW_2, and then by determining μ_{ij} and T_{ij}^0 $(i, j = 1, 2)$ by applying (5.23) and (5.24). Note that the values of the parameters of the PID controllers employed (those that need to be re-tuned) are obviously known.

Once μ_{ij} and T_{ij}^0 $(i, j = 1, 2)$ have been determined, each transfer function $P_{ij}(s)$ can be approximated as a FOPDT transfer functon, namely:

$$
\tilde{P}_{ij}(s) = \frac{\mu_{ij} e^{-s\tilde{\theta}_{ij}}}{\tilde{\tau}_{ij} s + 1}. \tag{5.25}
$$

In this context it is worth considering the so-called "half-rule" (SKOGESTAD, 2003) which states that the largest neglected (denominator) time constant is distributed evenly to the effective dead time and the smallest retained time constant. This means that an appropriate approximation of the possibily high-order system (5.2) is obtained by setting

$$
\tilde{\tau}_{ij} = \tau_{ij,1} + \frac{\tau_{ij,2}}{2}, \qquad \tilde{\theta}_{ij} = \theta_{ij} + \frac{\tau_{ij,2}}{2} + \sum_{k=3}^{n_{ij}} \tau_{ij,k}. \tag{5.26}
$$

It is worth stressing that we have

$$
T_{ij}^0 := \sum_{k=1}^{n_{ij}} \tau_{ij,k} + \theta_{ij} = \tilde{\tau}_{ij} + \tilde{\theta}_{ij}, \tag{5.27}
$$

namely, the sum of the dead time and of the time constants of the process (5.2) is unchanged in the reduced model. Thus, T_{ij}^0 is a relevant process parameter that is worth estimating for the purpose of the re-tuning of the PID controllers.

Finally, the apparent dead time $\tilde{\theta}_{ij}$ of each transfer function $\tilde{P}_{ij}(s)$ can be evaluated by considering respectively the time interval from the application of the step signal to the set-point r_j and the time instant when the output y_i attains a certain percentage of the steady-state value corresponding to the new set-point value A_{sj} (using several simulation studies, 2% was considered suitable for this method). Actually, from a practical point of view, in order to cope with the measurement noise, a simple sensible solution is to define a noise band *NB* (ÅSTRÖM

et al., 1993) (whose amplitude should be equal to the amplitude of the measurement noise) and to rewrite the condition as $y_i > NB$.

It is important to note that in this set-point test the process output y_1 (or y_2) will change before its open-loop delay when the coupling delay ($\tilde{\theta}_{12} + \tilde{\theta}_{21}$) is smaller than $\tilde{\theta}_{11}$ (or $\tilde{\theta}_{22}$). This can be easily confirmed computing the closed-loop transfer function between r_1 and y_1 (the same is valid for r_2 and y_2):

$$\frac{Y_1(s)}{R_1(s)} = \frac{(1+C_2(s)P_{22}(s))C_1(s)P_{11}(s) - C_1(s)C_2(s)P_{12}(s)P_{21}(s)}{(1+C_1(s)P_{11}(s))(1+C_2(s)P_{22}(s)) - C_1(s)C_2(s)P_{12}(s)P_{21}(s)}$$

and noting that the delay of this transfer function is the minimal value between $\tilde{\theta}_{11}$ and $\tilde{\theta}_{12} + \tilde{\theta}_{21}$.

Thus, in these cases, the proposed procedure will give a wrong estimation of the delays. Therefore, the proposed method only works for systems that have diagonal delays smaller than the coupling delay. However, this condition is not very restrictive, because, in general, if the pairs manipulated-controlled variables are correctly defined, the delays in the diagonal elements should be smaller than the non-diagonal ones (NORMEY-RICO, 2007). This condition is adequate to have the possibility of effective rejecting disturbances caused by the other channel.

It is clear at this point that the time constants of each transfer function can be trivially obtained as

$$\tilde{\tau}_{ij} = T_{ij}^0 - \tilde{\theta}_{ij}, \quad i,j = 1,2. \tag{5.28}$$

Remark 1. The values of process parameters are determined by considering the integral of signals and therefore the method is inherently effective even in the presence of measurement noise (VERONESI; VISIOLI, 2009). Further, the use of the final value theorem implies that the process parameters are obtained independently from the values of the initial PID parameters (obviously, provided that the stability is guaranteed). This is an advantage with respect to the use of other methods for the identification of the process transfer function (for example, the least squares approach), whose result depends on the control variable and process variable signals. However, it has to be stressed that the steady-state of the step responses have to be attained for a correct model estimation and this implies that the initial PID parameters have an influence of the duration of the overall identification experiment.

Remark 2. Note that all the proposed computations can be done on line. Note that even the integrals of the virtual signals $v(t)$ and $w(t)$ are obtained using (5.18) and the integrals IY_1, IY_2, IU_1 and IU_2, which can be separately incrementally integrated and are known values at the end of the transient. Thus, the final values of T_{ij}^0 can be computed using the estimated gains. Note that, if the system can be described by a non-singular matrix transfer function, meaning that the gain matrix is not singular, then the differences in the denominators of (5.23) and the sums in (5.24) will never be equal to zero. That can be seen from (5.15) and (5.22), where, for a

non-singular gain matrix, the difference in the denominators of these integrals is always different from zero, assuring their convergence to finite values. In that case, the computed values of $IE_{1,1}$, $IE_{2,1}$, $IE_{1,2}$, $IE_{2,2}$, IV_1, IW_1, IV_2 and IW_2 lead to obtain feasible values of μ_{ij} and T_{ij}^0.

Remark 3. It is worth noting that the method can be applied with any initial (possibly wrong) input-output pairing. However, the estimation of the process parameters and, in particular, of the gain matrix (5.23), can be exploited in order to evaluate the pairings of the input-output signals by means of methodologies already proposed in the literature such as the well-known relative gain array (RGA) technique (see, for example, (SEBORG; EDGAR; MELLICHAMP, 2004)). Further, the knowledge of the model allows the user to decide if use of a decoupler is advisable or a decentralised controller is sufficient for the given control requirements in the considered application.

5.2.1 PV-derivative PID formulation

As it happens for the SISO loop, the presented formulae are still true even if the derivative actions are applied to the process variables (instead of to the deviation from the set-point). In fact, being

$$\begin{aligned} U_1(s) &= C_1(s)E_1(s) - K_{P1}T_{D1}sY_1(s), \\ U_2(s) &= C_2(s)E_2(s) - K_{P2}T_{D2}sY_2(s), \end{aligned} \tag{5.29}$$

with

$$\begin{aligned} C_1(s) &= \frac{K_{P1}c_1(s)}{sT_{I1}}, \quad c_1(s) = (1+sT_{I1}), \\ C_2(s) &= \frac{K_{P2}c_2(s)}{sT_{I2}}, \quad c_2(s) = (1+sT_{I2}), \end{aligned} \tag{5.30}$$

after a step change to set-point 1, in this case we would have

$$\begin{aligned} E_{1,1}(s) &= sT_{I1}\frac{s^3G_1(s)+s^2G_2(s)+sG_3(s)+G_4(s)}{s^4G_5(s)+s^3G_6(s)+s^2G_7(s)+sG_8(s)+G_9(s)}R_1(s), \\ E_{1,2}(s) &= -\frac{sK_{P1}T_{I2}c_1(s)P_{21}}{s^4G_5(s)+s^3G_6(s)+s^2G_7(s)+sG_8(s)+G_9(s)}R_1(s), \end{aligned} \tag{5.31}$$

where

$$
\begin{aligned}
G_1(s) &= K_{P1}T_{D1}K_{P2}T_{D2}\left(P_{11}(s)P_{22}(s)-P_{12}(s)P_{21}(s)\right),\\
G_2(s) &= -T_{I2}\left(K_{P1}T_{D1}P_{11}(s)+K_{P2}T_{D2}P_{22}(s)\right),\\
G_3(s) &= K_{P1}T_{D1}K_{P2}c_2(s)\left(P_{12}(s)P_{21}(s)-P_{11}(s)P_{22}(s)\right),\\
G_4(s) &= K_{P2}c_2(s)P_{22}(s),\\
G_5(s) &= K_{P1}T_{I1}T_{D1}K_{P2}T_{I2}T_{D2}\left(P_{11}(s)P_{22}(s)-P_{12}(s)P_{21}(s)\right),\\
G_6(s) &= -T_{I1}T_{I2}\left(K_{P1}T_{D1}P_{11}(s)+K_{P2}T_{D2}P_{22}(s)\right),\\
G_7(s) &= \left(K_{P1}K_{P2}T_{I2}T_{D2}c_1(s)+K_{P1}K_{P2}T_{I1}T_{D1}c_2(s)\right)\left(P_{12}(s)P_{21}(s)-P_{11}(s)P_{22}(s)\right),\\
G_8(s) &= K_{P1}T_{I2}c_1(s)P_{11}(s)+K_{P2}T_{I1}c_2(s)P_{22}(s),\\
G_9(s) &= K_{P1}K_{P2}c_1(s)c_2(s)\left(P_{11}(s)P_{22}(s)-P_{12}(s)P_{21}(s)\right),
\end{aligned}
\tag{5.32}
$$

from which

$$
\begin{aligned}
IE_{1,1} &= \frac{\mu_{22}T_{I1}}{K_{P1}\left(\mu_{11}\mu_{22}-\mu_{12}\mu_{21}\right)}A_{s1},\\
IE_{2,1} &= -\frac{\mu_{21}T_{I2}}{K_{P2}\left(\mu_{11}\mu_{22}-\mu_{12}\mu_{21}\right)}A_{s1},
\end{aligned}
\tag{5.33}
$$

exactly as it happens when the derivative action is applied to the deviation (see the gains as in (5.15)). Therefore, we can obtain again the gains as in (5.23).

On the other hand, being the derivative action null at steady state, it is clear that nothing changes in (5.16) and (5.17) and, therefore, (5.18) still leads to (5.19), then to (5.20) and finally to (5.21) and (5.22); therefore, at the end, T_{ij}^0 can still be obtained as in (5.24).

5.3 Tuning

Once the process parameters have been obtained, any of the tuning rules proposed in the literature for MIMO processes can be applied and the choice can be driven by the particular application (for example, by mainly considering the set-point following task rather than the rejection of disturbances, or viceversa).

Hereafter, for the purpose of evaluating the overall auto-tuning methodology, the method proposed in (LEE et al., 2004) is considered. It extends the generalised IMC-PID method for SISO systems (LEE et al., 1998) to MIMO systems and consists of determining the multiloop PID controller in order to obtain a desired closed-loop response for the ith loop, which is specified as

$$
\frac{Y_i(s)}{R_i(s)} = \frac{e^{-s\tilde{\theta}_{ii}}}{1+\lambda_i s} \quad i=1,2
\tag{5.34}
$$

The result of the design method proposed in (LEE et al., 2004), based on the expansion

of the process model in a Maclaurin series, is the following set of tuning formulae ($j = 1,2$):

$$\begin{aligned} K_{Pj} &= \frac{\mu_{jj}((\lambda_j + \tilde{\theta}_{jj})\tilde{\tau}_{jj} + \frac{\tilde{\theta}_{jj}^2}{2})}{(\mu_{jj}(\lambda_j + \tilde{\theta}_{jj}))^2}, \\ T_{Dj} &= \frac{1}{2K_{Pj}} \left(\frac{\tilde{\theta}_{jj}^2 \left(6\tilde{\tau}_{jj}\tilde{\theta}_{jj} + \tilde{\theta}_{jj}^2 - 2\lambda_j\tilde{\theta}_{jj} + 6\tilde{\tau}_{jj}\lambda_j \right)}{6\mu_{jj}(\lambda_j + \tilde{\theta}_{jj})^3} \right), \\ T_{Ij} &= \frac{K_{Pj}(\tilde{\theta}_{jj} + \lambda_j)}{\tilde{\mathbf{P}}^{-1}(0)_{jj}}, \end{aligned} \tag{5.35}$$

where $\tilde{\mathbf{P}}^{-1}(0)_{jj}$ is the jth element of the diagonal of the inverse of the matrix $\tilde{\mathbf{P}}(s) = \left[\tilde{P}_{ij}(s)\right]$ for $s = 0$. In this way the integral action of the PID can take into account even the off-diagonal terms of $\tilde{P}(s)$. This is reasonable because both the integral action and the loop interactions are more significant at low frequencies.

The choice of the desired closed-loop time constant λ_j can be done, for example, as suggested in (SKOGESTAD, 2003), as

$$\lambda_j = \tilde{\theta}_{jj}. \tag{5.36}$$

In this way the tuning formulae can be rewritten simply as:

$$\begin{aligned} K_{Pj} &= \frac{1}{8\mu_{jj}} \frac{4\tilde{\tau}_{jj} + \tilde{\theta}_{jj}}{\tilde{\theta}_{jj}}, \\ T_{Dj} &= \frac{1}{12} \frac{\left(12\tilde{\tau}_{jj} - \tilde{\theta}_{jj}\right)\tilde{\theta}_{jj}}{4\tilde{\tau}_{jj} + \tilde{\theta}_{jj}}, \\ T_{Ij} &= \frac{4\tilde{\tau}_{jj} + \tilde{\theta}_{jj}}{4} \frac{\mu_{11}\mu_{22} - \mu_{12}\mu_{21}}{\mu_{11}\mu_{22}}. \end{aligned} \tag{5.37}$$

Remark 4. As it is well-known in the IMC design, parameter λ_j handles effectively the trade-off between aggressiveness and robustness (and control effort) and represents therefore a very desirable feature from the user viewpoint. Actually, the rule (5.36) has been selected as in (SKOGESTAD, 2003) but the user can modify the value of λ_j in order to meet specific requirements (for example, the value of λ_j can be increased in order to reduce the overshoot in the set-point step response).

5.4 Simulation results

In this section two examples are presented in order to compare the proposed new method by means of simulations with another TITO process identification from closed-loop step responses proposed in (LI et al., 2005). In addition, results in the presence of additive noise are presented.

The PID controllers that have been considered are those described by the PV-derivative PID formulation (see (5.29)) where, as already mentioned in Section 5.1, an additional first-order filter has been applied to the derivative term in order to make the controller proper. The filter time constant has been selected so that the corresponding pole frequency is one decade higher than the highest frequency associated with the zeros of the controller. For each example, the tuning rules that are applied are the same for the two compared methods.

The noise bands of the examples are approximately ± 0.04 and ± 0.08. The noise signal is generated so that, for each band, the signal is the same for all examples. The step magnitudes, for all simulations, are $A_{s1} = A_{s2} = 1$ and the set-point step changes occur at the same time for simulations of the same example, with additive noise and noise free. It is important to note that the levels of additive noise do not try to simulate industrial levels of measurement noise. The presence of additive noise is used only to illustrate the effectiveness of the proposed method and to compare it with (LI et al., 2005) in possible unfavourable conditions.

5.4.1 *Example 1*

As a first example, the well-known distillation column model reported in (WOOD; BERRY, 1973) is considered:

$$\mathbf{P}(s) = \begin{bmatrix} \dfrac{12.8e^{-s}}{16.7s+1} & \dfrac{-18.9e^{-3s}}{21s+1} \\ \dfrac{6.6e^{-7s}}{10.9s+1} & \dfrac{-19.4e^{-3s}}{14.4s+1} \end{bmatrix}. \tag{5.38}$$

By applying the identification procedure presented in Section 5.2 and the identification procedure described in (LI et al., 2005) (namely, by evaluating the two step responses), the estimated models by the two methods are presented in Table 9 and their respective Bode plots are presented in Fig. 20. The initial controller parameters were obtained by applying the "biggest log modulus tuning" (BLT) technique proposed in (LUYBEN, 1986), as shown in Table 10.

Table 9 – Estimated models by the method proposed in (LI et al., 2005) and by the new method in Example 1

	$P_{11}(s)$	$P_{12}(s)$	$P_{21}(s)$	$P_{22}(s)$
Model	$\frac{12.8e^{-s}}{16.7s+1}$	$\frac{-18.9e^{-3s}}{21s+1}$	$\frac{6.6e^{-7s}}{10.9s+1}$	$\frac{-19.4e^{-3s}}{14.4s+1}$
Li et al. method	$\frac{12.8e^{-1.001s}}{16.702s+1}$	$\frac{-18.9e^{-3.001s}}{21.003s+1}$	$\frac{6.601e^{-6.421s}}{11.511s+1}$	$\frac{-19.4e^{-2.995s}}{14.402s+1}$
New method	$\frac{12.801e^{-1.071s}}{16.633s+1}$	$\frac{-18.908e^{-3.298s}}{20.774s+1}$	$\frac{6.604e^{-7.089s}}{10.823s+1}$	$\frac{-19.424e^{-3.197s}}{14.395s+1}$

Analysing the frequency responses in Fig. 20, it can be observed that the frequency responses of the estimated models by the two methods can reproduce the frequency responses of the nominal model even at high frequencies.

Figure 20 – Example 1: Bode plots of the nominal model (black line) and of the estimated models by the method proposed in (LI et al., 2005) (blue dash-doted line) and by the new method (red dashed line).

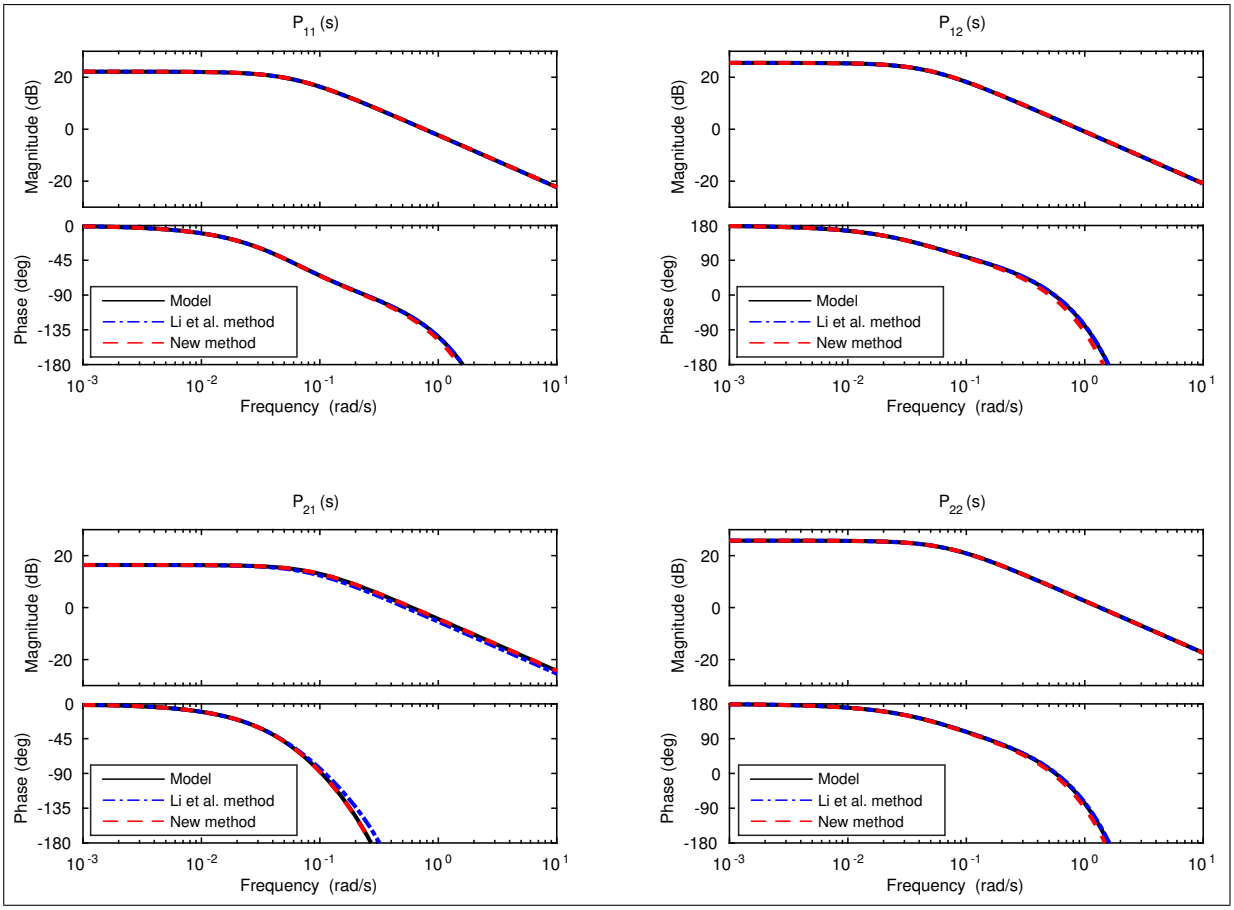

Source: The author.

Hence, by applying the tuning formulae (5.37) and using first order filters with time constants T_{cj}, the PID parameters shown in Table 10 are obtained by the two methods for re-tuning of the controllers.

Table 10 – PID parameters for the initial controller tuning, the tuning obtained by the method proposed in (LI et al., 2005) and for the tuning obtained by applying the new method in Example 1 (note that $j = 1, 2$ correspond to the first and second row of each tuning, respectively)

PID Parameters	K_{Pj}	T_{Ij}	T_{Dj}	T_{cj}
Initial tuning	0.375	8.29	0	NA
	-0.075	23.6	0	NA
Li et al. method	0.663	8.433	0.245	0.0245
	-0.133	7.563	0.69	0.069
New method	0.616	8.413	0.262	0.0262
	-0.122	7.564	0.743	0.0743

The simulated step responses are shown in Fig. 21, where the effectiveness of the auto-

tuning methodology can be evaluated. The set-point step changes occur at times $t = 50$ sec and $t = 400$ sec. It can be observed that the responses with the re-tuned controllers are more aggressive than those with the initial tuning controller. In practice, if more conservative responses and control actions are desired, using an IMC tuning method, the trade-off between robustness and aggressiveness can be adjusted accordingly to *Remark 4*.

Figure 21 – Example 1: responses of process variables y_1 and y_2 and control signals u_1 and u_2 with the initial (BLT) controller tuning (black thick solid line), with the tuning obtained by applying the method proposed in (LI et al., 2005) (blue thick dashed line) and with the tuning obtained by applying the new method (red solid line). The set-point step changes (black dash-dotted line) occur at times $t = 50$ sec and $t = 400$ sec.

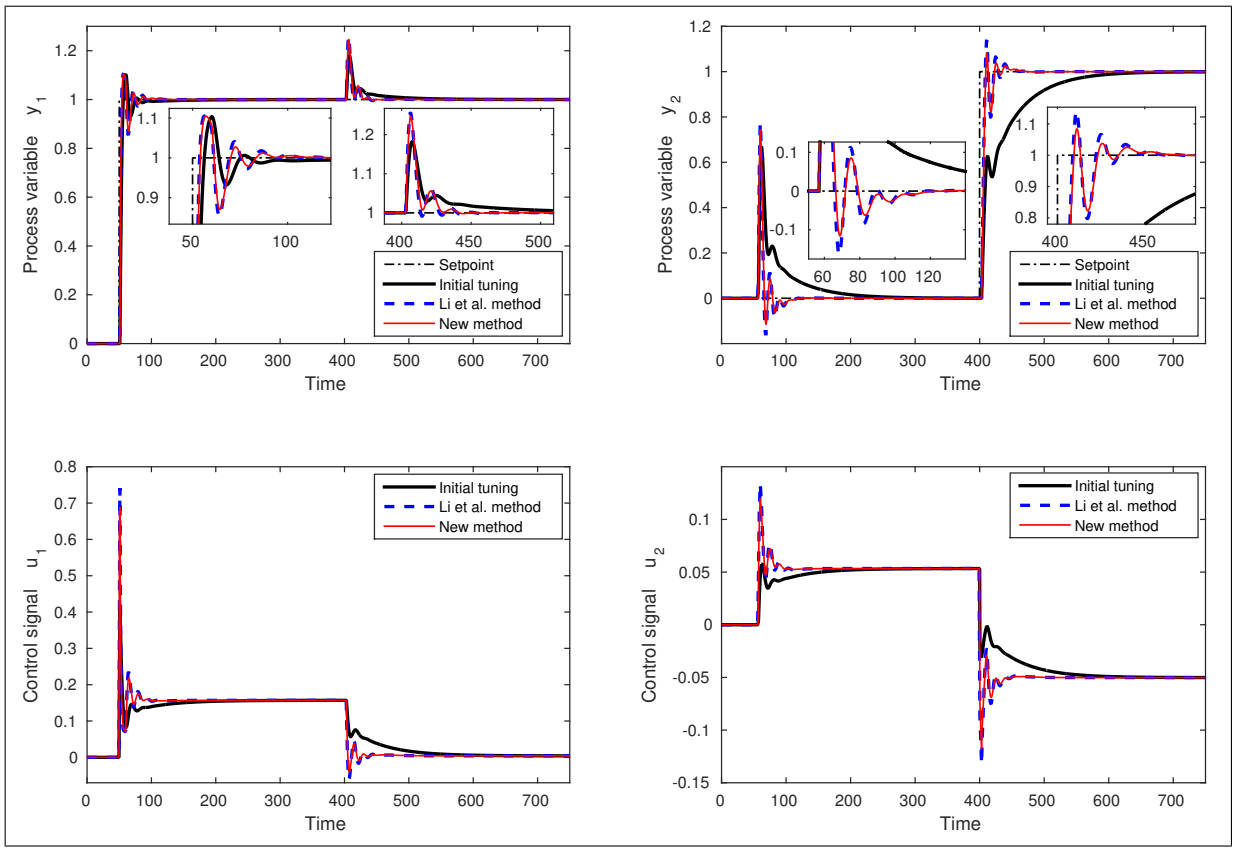

Source: The author.

Hereafter, new simulations are presented with the purpose of investigating and comparing the efficacy of the two methods in the presence of additive noise.

5.4.1.1 *Additive noise with a* ± 0.04 *band*

The simulations with additive noise were performed adding band-limited white noise to the process variables. For this case, the noise signal was generated with noise power of 1.4×10^{-7}, sampling time of 10^{-3} and starting seed equals 1.

The different approach of the new method is to define a noise band *NB* to estimate the dead times of the model, as mentioned in Section 5.2. In practice, the value of *NB* is defined as the level of measurement noise. In the following simulations, as a rule of thumb, the noise band *NB* was chosen as 75% of the maximum peak absolute value of the additive noise. Therefore, for this case $NB = 0.043$.

The models identified by the method proposed in (LI et al., 2005) and by the new method are shown in Table 11 and their respective Bode plots are shown in Fig. 22.

Table 11 – Estimated models by the method proposed in (LI et al., 2005) and by the new method with additive noise band of approximately ± 0.04 in Example 1

	$P_{11}(s)$	$P_{12}(s)$	$P_{21}(s)$	$P_{22}(s)$
Model	$\frac{12.8e^{-s}}{16.7s+1}$	$\frac{-18.9e^{-3s}}{21s+1}$	$\frac{6.6e^{-7s}}{10.9s+1}$	$\frac{-19.4e^{-3s}}{14.4s+1}$
Li et al. method	$\frac{13.303e^{-1.118s}}{17.233s+1}$	$\frac{-20.38e^{-3.0516s}}{20.557s+1}$	$\frac{6.943e^{-6.084s}}{12.585s+1}$	$\frac{-20.407e^{-3.155s}}{14.209s+1}$
New method	$\frac{12.804e^{-1.069s}}{16.81s+1}$	$\frac{-18.906e^{-3.282s}}{20.964s+1}$	$\frac{6.605e^{-7.082s}}{10.988s+1}$	$\frac{-19.422e^{-3.246s}}{14.419s+1}$

From Table 11, it can be seen that, for most of the model parameters, the new method obtained better identification results than the method proposed in (LI et al., 2005). Furthermore, concerning the dead times, the noise band approach has produced consistent results, with a maximum error of $+9.4\%$ of the nominal value for $P_{12}(s)$.

From the Bode plots in Fig. 22, one can see that, even with that additive noise level, the identified models by the two methods still reproduce well the frequency responses of the nominal model.

5.4.1.2 Additive noise with a ± 0.08 band

The additive noise signal for this case was generated with noise power of 5×10^{-7}, sampling time of 10^{-3} and starting seed equals 1. The noise band for this case was defined as in the previous section and its value is $NB = 0.0812$.

The models identified by the two methods are presented in Table 12 and their respective frequency responses can be seen in Fig. 23.

Table 12 – Estimated models by the method proposed in (LI et al., 2005) and by the new method with additive noise band of approximately ± 0.08 in Example 1

	$P_{11}(s)$	$P_{12}(s)$	$P_{21}(s)$	$P_{22}(s)$
Model	$\frac{12.8e^{-s}}{16.7s+1}$	$\frac{-18.9e^{-3s}}{21s+1}$	$\frac{6.6e^{-7s}}{10.9s+1}$	$\frac{-19.4e^{-3s}}{14.4s+1}$
Li et al. method	$\frac{13.788e^{-1.223s}}{17.744s+1}$	$\frac{-21.806e^{-3.0916s}}{20.256s+1}$	$\frac{7.273e^{-5.977s}}{13.358s+1}$	$\frac{-21.378e^{-3.254s}}{14.12s+1}$
New method	$\frac{12.807e^{-1.08s}}{16.955s+1}$	$\frac{-18.904e^{-3.306s}}{21.0953s+1}$	$\frac{6.606e^{-7.169s}}{11.0409s+1}$	$\frac{-19.42e^{-3.306s}}{14.425s+1}$

Figure 22 – Example 1 with additive noise band of approximately ±0.04: Bode plots of the nominal model (black line) and of the estimated models by the method proposed in (LI et al., 2005) (blue dash-doted line) and by the new method (red dashed line).

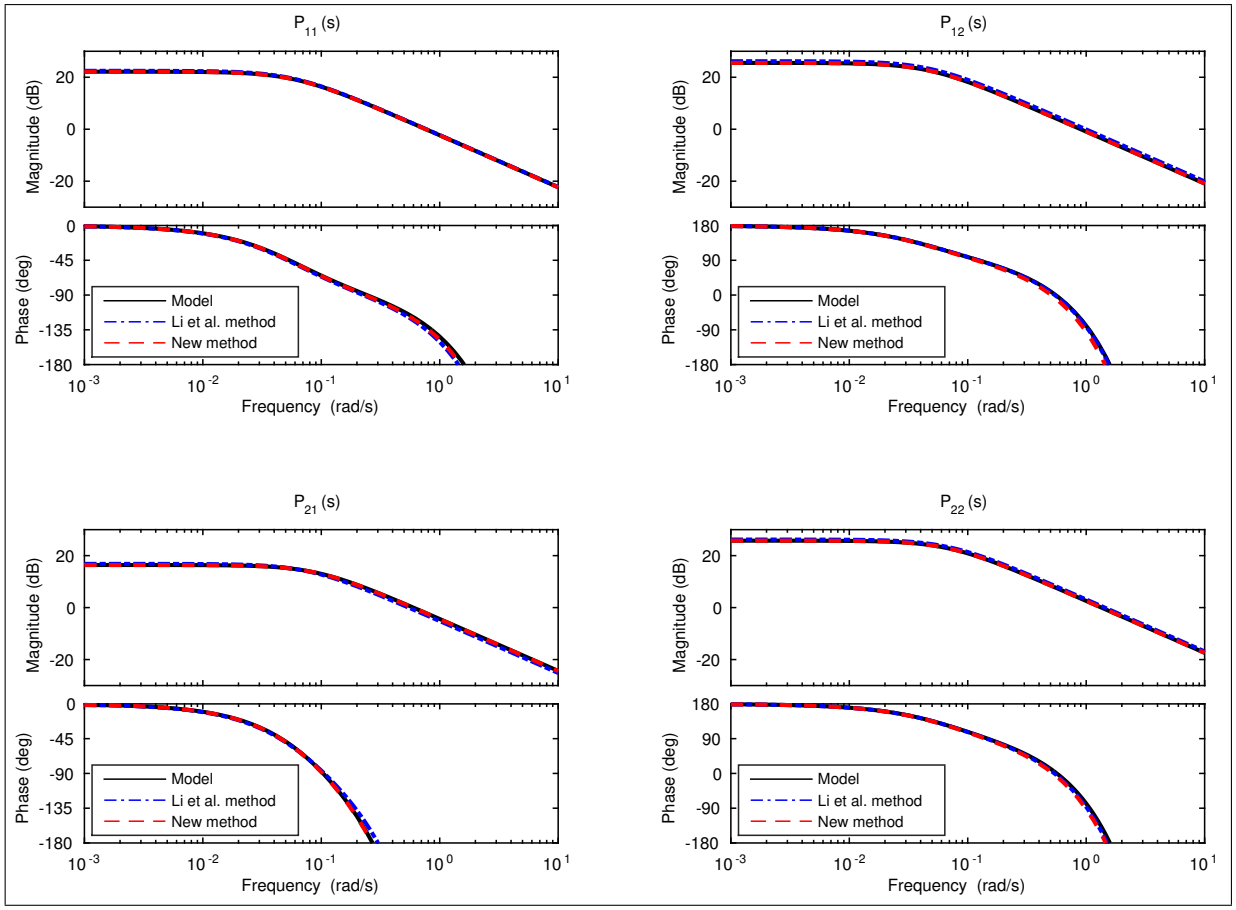

Source: The author.

It can be seen from Table 12 that, concerning the process gains and time constants, the new method estimated, for all cases, better parameters values. For the dead times, the noise band approach still showed consistent results, with a maximum error of 10.2% for $P_{12}(s)$ and $P_{22}(s)$.

It can be seen from the Bode plots in Fig. 23 that, despite the additive noise, the two identified models still can reproduce well the frequency responses of the nominal model.

5.4.2 *Example 2*

In order to verify the robustness of the methodology to modelling uncertainties, as a second example, the following high-order process model (LI et al., 2005) is considered:

$$\mathbf{P}(s) = \begin{bmatrix} \dfrac{0.5}{(0.1s+1)^2(0.2s+1)^2} & \dfrac{-1}{(0.1s+1)(0.2s+1)^2} \\ \dfrac{1}{(0.1s+1)(0.2s+1)^2} & \dfrac{2.4}{(0.1s+1)(0.2s+1)^2(0.5s+1)} \end{bmatrix} \tag{5.39}$$

By applying the (LI et al., 2005) procedure and the proposed identification procedure, the models in Table 13 are determined and their respective Bode plots are presented in Fig. 24.

Figure 23 – Example 1 with additive noise band of approximately ±0.08: Bode plots of the nominal model (black line) and of the estimated models by the method proposed in (LI et al., 2005) (blue dash-doted line) and by the new method (red dashed line).

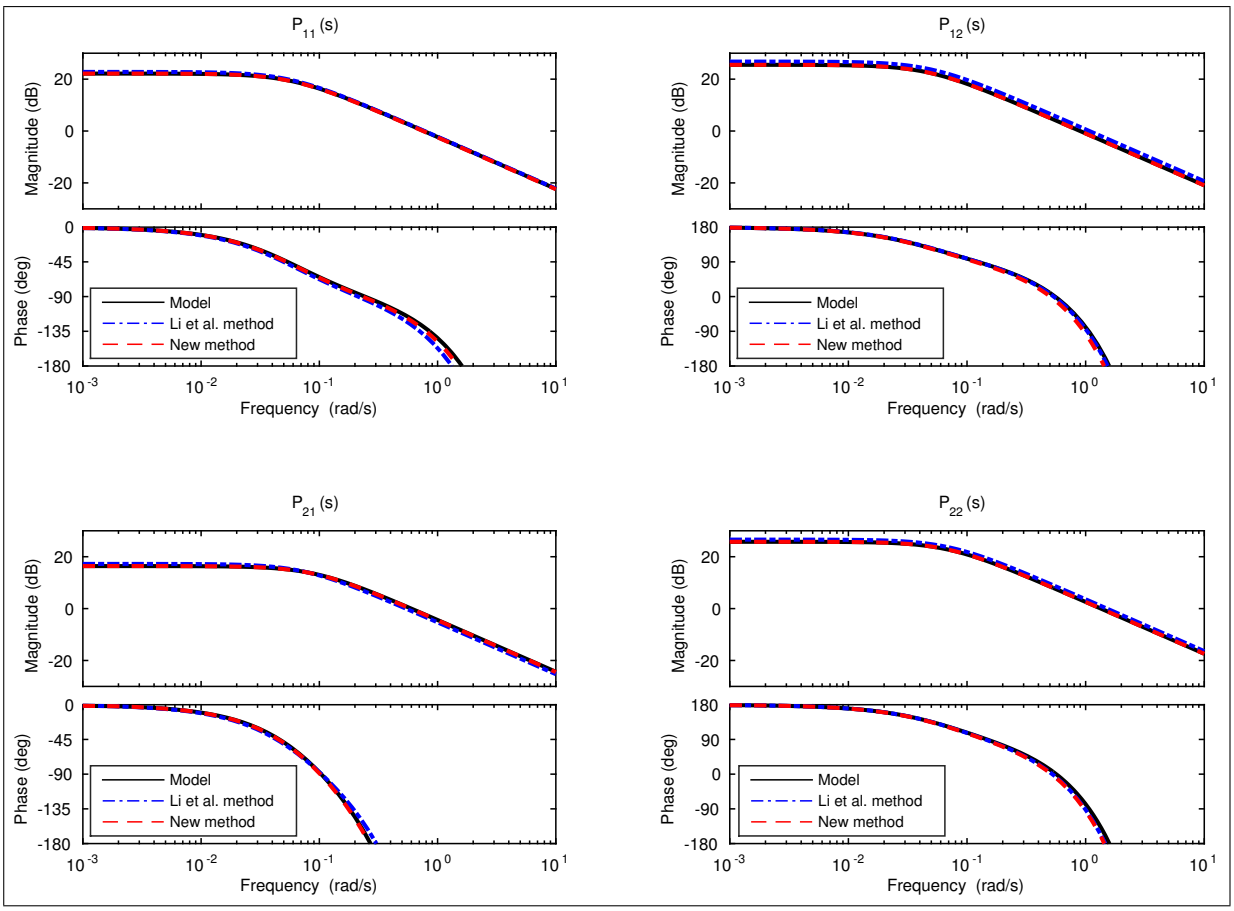

Source: The author.

Before the estimation, the initial PID parameters have been tuned as indicated in Table 14 and the process variables responses are shown in Fig. 25 as black thick solid lines.

Table 13 – Estimated models by the method proposed in (LI et al., 2005) and by the new method in Example 2

	$P_{11}(s)$	$P_{12}(s)$	$P_{21}(s)$	$P_{22}(s)$
Li et al. method	$\frac{0.5e^{-0.304s}}{0.296s+1}$	$\frac{-1e^{-0.226s}}{0.275s+1}$	$\frac{1e^{-0.225s}}{0.276s+1}$	$\frac{2.4e^{-0.43s}}{0.57s+1}$
New method	$\frac{0.5e^{-0.202s}}{0.355s+1}$	$\frac{-0.999e^{-0.15s}}{0.332s+1}$	$\frac{1e^{-0.106s}}{0.377s+1}$	$\frac{2.398e^{-0.239s}}{0.72s+1}$

From Fig. 24, as expected for FOPDT models, the identified models reproduced the frequency responses of the nominal model only at low frequencies. Nevertheless, the frequency responses of the model identified by the new method reproduce the frequency responses of the nominal model at middle and high frequencies better than the model identified by the method proposed in (LI et al., 2005).

Figure 24 – Example 2: Bode plots of the nominal model (black line) and of the estimated models by the method proposed in (LI et al., 2005) (blue dash-doted line) and by the new method (red dashed line).

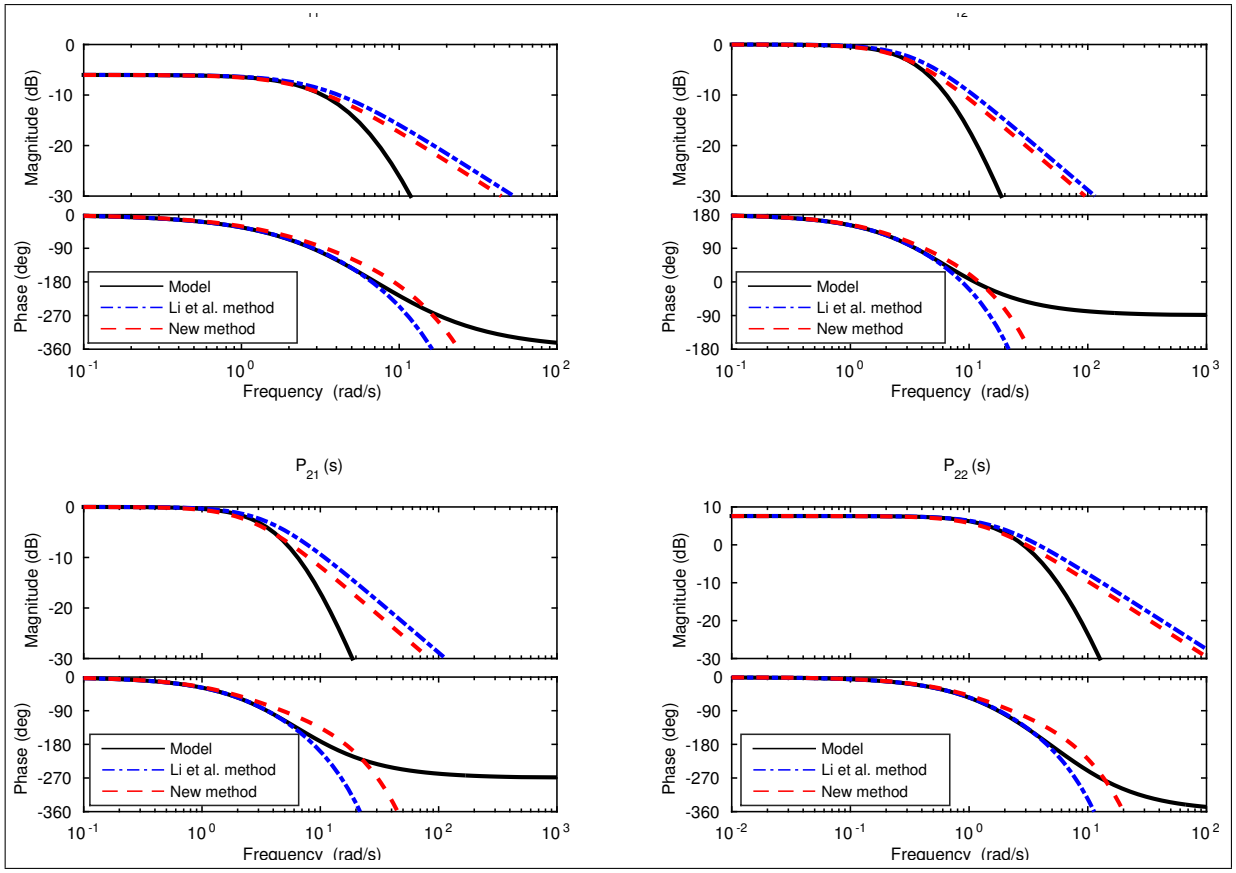

Source: The author.

Hence, by applying the tuning formulae (5.35) and choosing a robust tuning to define $\lambda_1 = 3\theta_{11}$ and $\lambda_2 = 3\theta_{22}$, the PID parameters obtained for re-tuning the two controllers are shown in Table 14.

Table 14 – PID parameters for the initial controller tuning, the tuning obtained by the method proposed in (LI et al., 2005) and for the tuning obtained by applying the new method in Example 2 (note that $j = 1, 2$ correspond to the first and second row of each tuning, respectively)

PID Parameters	K_{Pj}	T_{Ij}	T_{Dj}	T_{cj}
Initial tuning	0.7	3	0.1	0.01
	0.3	5	0.1	0.01
Li et al. method	0.55	0.613	0.0265	0.00265
	0.151	1.144	0.0414	0.00414
New method	0.942	0.697	0.0208	0.00208
	0.327	1.375	0.0267	0.00267

The step responses obtained with the re-tuned controllers obtained by the two methods are shown in Fig. 25. The set-point step changes occur at times $t = 10$ sec and $t = 85$ sec. As in

Example 1, it appears that the initial PID controller could have been tuned more aggressively.

These results confirm the effectiveness of the methodology also in the presence of modelling uncertainties.

Figure 25 – Example 2: responses of process variables y_1 and y_2 and control signals u_1 and u_2 with the initial controller tuning (black thick solid line), with the tuning obtained by applying the method proposed in (LI et al., 2005) (blue thick dashed line) and with the tuning obtained by applying the new method (red solid line). The set-point step changes (black dash-dotted line) occur at times $t = 10$ sec and $t = 85$ sec.

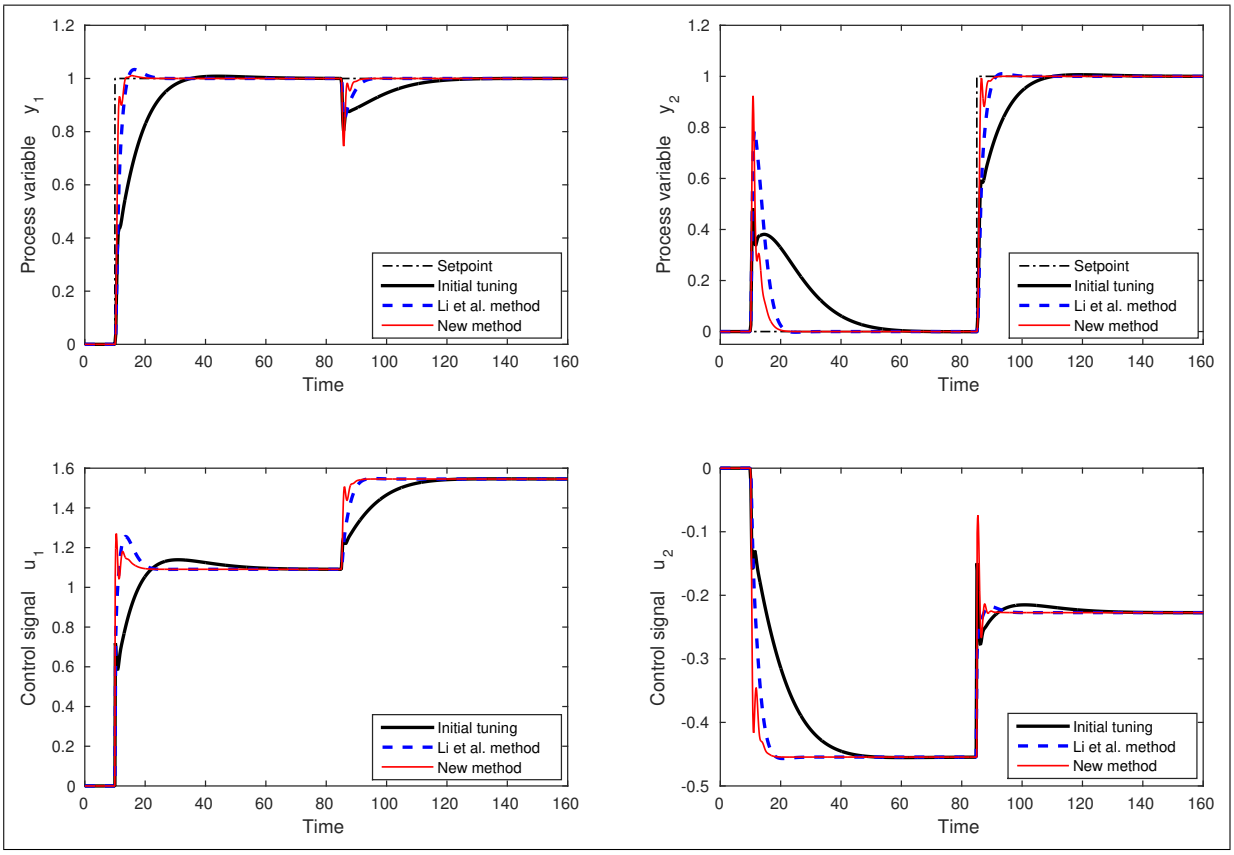

Source: The author.

Hereafter, noise effect is studied for this example.

5.4.2.1 *Additive noise with a* ± 0.04 *band*

The additive noise signal is the same as in Example 1. Therefore, the noise band defined for the new method is also $NB = 0.043$.

The models identified by the procedure in (LI et al., 2005) and by the new method are shown in Table 15.

Table 15 – Estimated models by the method proposed in (LI et al., 2005) and by the new method with additive noise band of approximately ±0.04 in Example 2 (note that the model shown in the first row of the table for each method corresponds to the noise free case and it is presented for comparison purposes)

	$P_{11}(s)$	$P_{12}(s)$	$P_{21}(s)$	$P_{22}(s)$
Li et al. method	$\frac{0.5e^{-0.304s}}{0.296s+1}$	$\frac{-1e^{-0.226s}}{0.275s+1}$	$\frac{1e^{-0.225s}}{0.276s+1}$	$\frac{2.4e^{-0.43s}}{0.57s+1}$
	$\frac{0.595e^{-3.723s}}{-3.455s+1}$	$\frac{-0.773e^{-(-0.208)s}}{3.28s+1}$	$\frac{1.9e^{-(-82.534)s}}{78.124s+1}$	$\frac{4.684e^{-(-9.68)s}}{6.112s+1}$
New method	$\frac{0.5e^{-0.202s}}{0.355s+1}$	$\frac{-0.999e^{-0.15s}}{0.332s+1}$	$\frac{1e^{-0.106s}}{0.377s+1}$	$\frac{2.398e^{-0.239s}}{0.72s+1}$
	$\frac{0.5e^{-0.191s}}{0.363s+1}$	$\frac{-0.999e^{-0.186s}}{0.285s+1}$	$\frac{1e^{-0.122s}}{0.372s+1}$	$\frac{2.398e^{-0.257s}}{0.715s+1}$

It can be observed from Table 15 that the method proposed in (LI et al., 2005) estimated most of the parameters with inconsistent or not feasible values. Particularly, one time constant and most of the dead times have negative values. Nevertheless, the proposed method still estimated a consistent model with parameters values near to the values of the noise free case.

The frequency responses of the nominal model, of the model estimated by the new method in the noise free case and of the model estimated by the new method are presented in Fig. 26 for comparison.

It can be seen from Fig. 26 that, with that additive noise level, the frequency responses of the model identified by the proposed method and the respective noise free case frequency responses are still alike.

5.4.2.2 *Additive noise with a* ±0.08 *band*

The additive noise signal for this case was generated in the same way as in Example 1. The noise band was defined as mentioned in Section 5.4.1.1 and its value is $NB = 0.0812$.

The models identified by the two methods are presented below in Table 16.

Table 16 – Estimated models by the method proposed in (LI et al., 2005) and by the new method with additive noise band of approximately ±0.08 in Example 2 (note that the model shown in the first row of the table for each method corresponds to the noise free case and it is presented for comparison purposes)

	$P_{11}(s)$	$P_{12}(s)$	$P_{21}(s)$	$P_{22}(s)$
Li et al. method	$\frac{0.5e^{-0.304s}}{0.296s+1}$	$\frac{-1e^{-0.226s}}{0.275s+1}$	$\frac{1e^{-0.225s}}{0.276s+1}$	$\frac{2.4e^{-0.43s}}{0.57s+1}$
	$\frac{1.377e^{-2.774s}}{-17.177s+1}$	$\frac{1.127e^{-(-38.225)s}}{-17.086s+1}$	$\frac{9.978e^{-(-2.919)s}}{-17.063s+1}$	$\frac{23.853e^{-(-8.77)s}}{-17.103s+1}$
New method	$\frac{0.5e^{-0.202s}}{0.355s+1}$	$\frac{-0.999e^{-0.15s}}{0.332s+1}$	$\frac{1e^{-0.106s}}{0.377s+1}$	$\frac{2.398e^{-0.239s}}{0.72s+1}$
	$\frac{0.5e^{-0.27s}}{0.281s+1}$	$\frac{-0.999e^{-0.228s}}{0.233s+1}$	$\frac{1e^{-0.153s}}{0.35s+1}$	$\frac{2.399e^{-0.276s}}{0.707s+1}$

Figure 26 – Example 2 with additive noise band of approximately ± 0.04: Bode plots of the nominal model (black line), of the model estimated by the new method in the noise free case (black doted line) and of the estimated model by the new method (red dashed line).

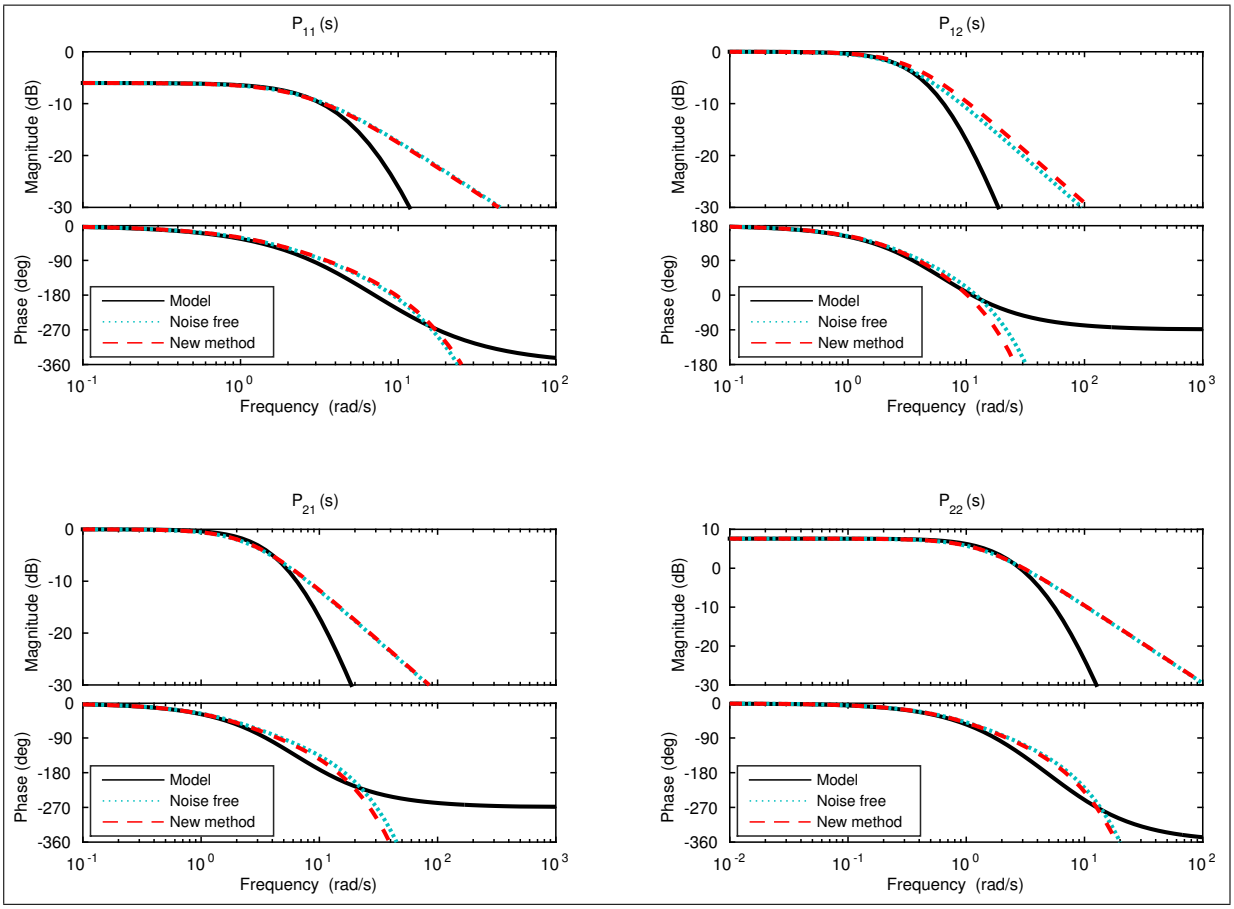

Source: The author.

What can be seen from Table 16 is that, by applying the other identification method, the model estimated have almost all the parameters values inconsistent or not feasible. On the other hand, the new method estimated a model where still most of the parameters values are near the values of the free noise case. Furthermore, the noise band approach has produced satisfactory results for the dead times.

The Bode plots of the nominal model, of the model estimated by the new method in the noise free case and of the model estimated by the new method are presented in Fig. 27. As can be seen, for that additive noise level, the frequency responses of the identified model still reproduce well the frequency responses of the nominal model at low frequencies, but presented a lower performance at higher frequencies. Nevertheless, the high noise levels presented in this example are not common in real applications.

Figure 27 – Example 2 with additive noise band of approximately ±0.08: Bode plots of the nominal model (black line), of the model estimated by the new method in the noise free case (black doted line) and of the estimated model by the new method (red dashed line).

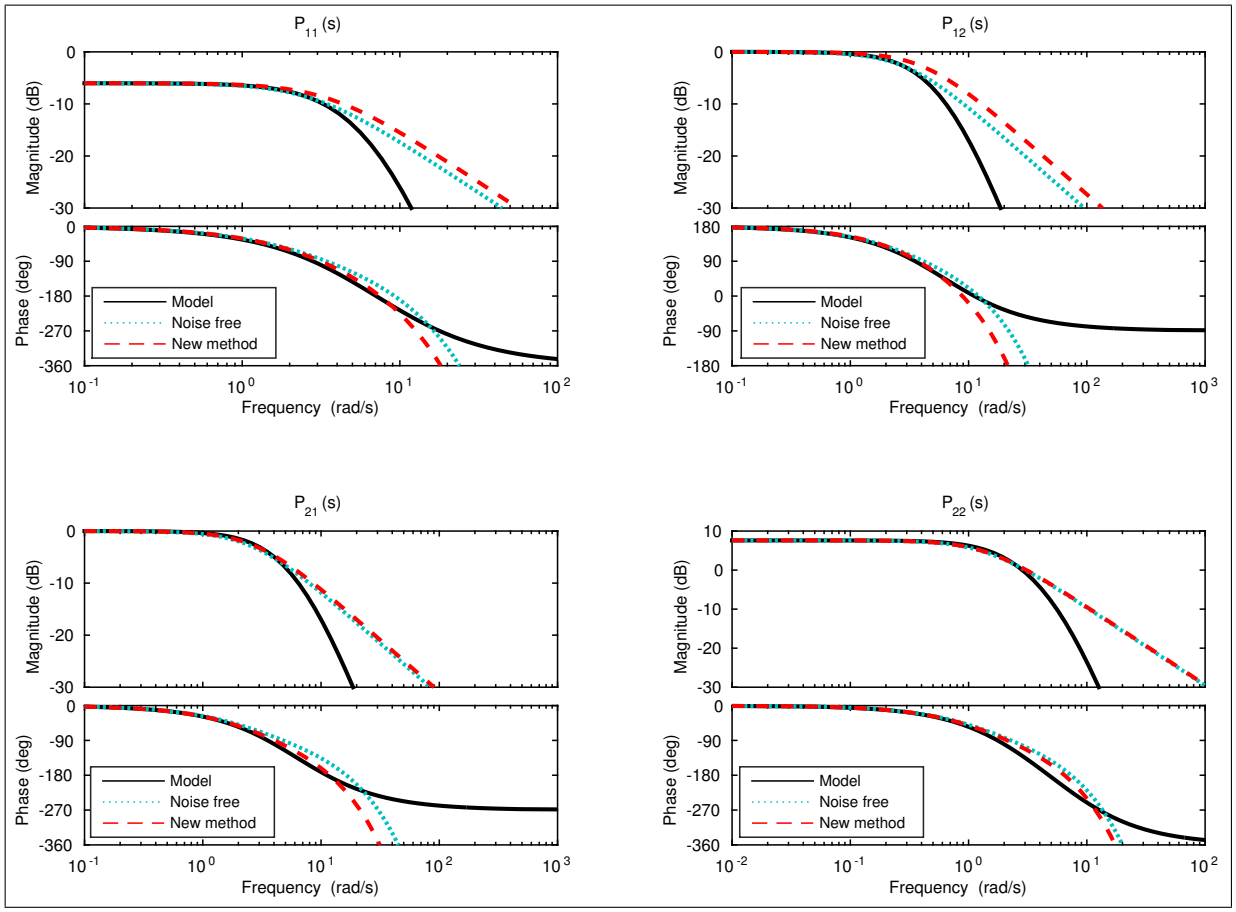

Source: The author.

5.5 Experimental results

The experiments with the neonatal incubator were performed using PI controllers. The derivative action was set to zero in order to facilitate the avoidance of saturation of the control signals and in order to minimize the effects of the measurement noise.

In order to identify the process model, an experiment using a roughly tuned PI was performed. Starting from steady-state values of 50% for the humidity and of 29°C for the temperature, step changes of A_{s1} = 15% and A_{s2} = 4°C were applied to the relative humidity and temperature set-points at times $t = 0$ and $t = 100$ min, respectively. The parameters of the initial PI controllers were:

$$\begin{aligned} K_{P1} &= 1.5, \quad T_{I1} = 5, \\ K_{P2} &= 2, \quad\;\; T_{I2} = 10. \end{aligned} \tag{5.40}$$

In practice, the controllers were implemented in a discrete form, thus, they were discretised using Tustin method with sampling time $T_s = 0.4$ min. Using the experimental data and (5.23), (5.24) and (5.28), the model parameters were identified as:

$$\begin{array}{llll} T_{11}^0 = 3.81, & T_{12}^0 = 2.19, & T_{21}^0 = 36.13, & T_{22}^0 = 11.45, \\ \tilde{\theta}_{11} = 0.4, & \tilde{\theta}_{12} = 2, & \tilde{\theta}_{21} = 2, & \tilde{\theta}_{22} = 2.8, \\ \mu_{11} = 0.41, & \mu_{12} = -0.4, & \mu_{21} = -0.016, & \mu_{22} = 0.19, \\ \tilde{\tau}_{11} = 3.41, & \tilde{\tau}_{12} = 0.19, & \tilde{\tau}_{21} = 34.13, & \tilde{\tau}_{22} = 8.65. \end{array} \tag{5.41}$$

From the process gains of (5.41), it can be observed that the humidity is strongly coupled and the temperature coupling is lower, as expected for the system of the neonatal incubator. This shows that the proposed identification method also works with TITO processes close to the triangular structure.

Fig. 28 shows a comparison between experimental and simulation results using the PI defined in (5.40). The simulation was performed using the identified model (5.41). It can be seen that despite the real process output is noisy, the model has captured the dynamic behaviour of the process.

In order to improve the closed loop behaviour, the PI was re-tuned applying the method proposed in (LEE et al., 2004), which is expressed in (5.35). As robustness is of major concern for this kind of system, the tuning constants were chosen as $\lambda_1 = 3\theta_{11}$ for the relative humidity and $\lambda_2 = 3\theta_{22}$ for the temperature. Therefore, by applying the new method, the following PI parameters were obtained:

$$\begin{array}{ll} K_{P1} = 5.29, & T_{I1} = 3.18, \\ K_{P2} = 4.23, & T_{I2} = 8.27. \end{array} \tag{5.42}$$

Fig. 29 shows a simulation comparison between the first roughly tuned PI controller (5.40) and the re-tuned PI used in the proposed approach (5.42). As can be seen the set-point tracking was improved and the interaction between loops were attenuated.

Finally, an experiment was performed using the re-tuned PI. Fig. 30 shows the comparison of the experiments using the roughly tuned PI and the re-tuned PI. As expected from simulations the re-tuned PI improved the set-point tracking. In addition, in order to quantify the improvement, the following three indexes are used: the settling time t_s (based on a 5% criterion), the undershoot (US) due to interactions from a set-point change on the other loop, and the integrated absolute error IAE defined as

$$IAE_i = \int_0^\infty |e_i(t)|dt \qquad i = 1, 2. \tag{5.43}$$

The resulting values are presented in Table 17.

Figure 28 – Relative humidity and temperature responses and control signals in the experiment with the initial controller tuning (thick line) and in the simulation with the model identified and the initial controller tuning (dashed line). The set-point step changes (dash-dotted line) occur at times $t = 0$ and $t = 100$ min.

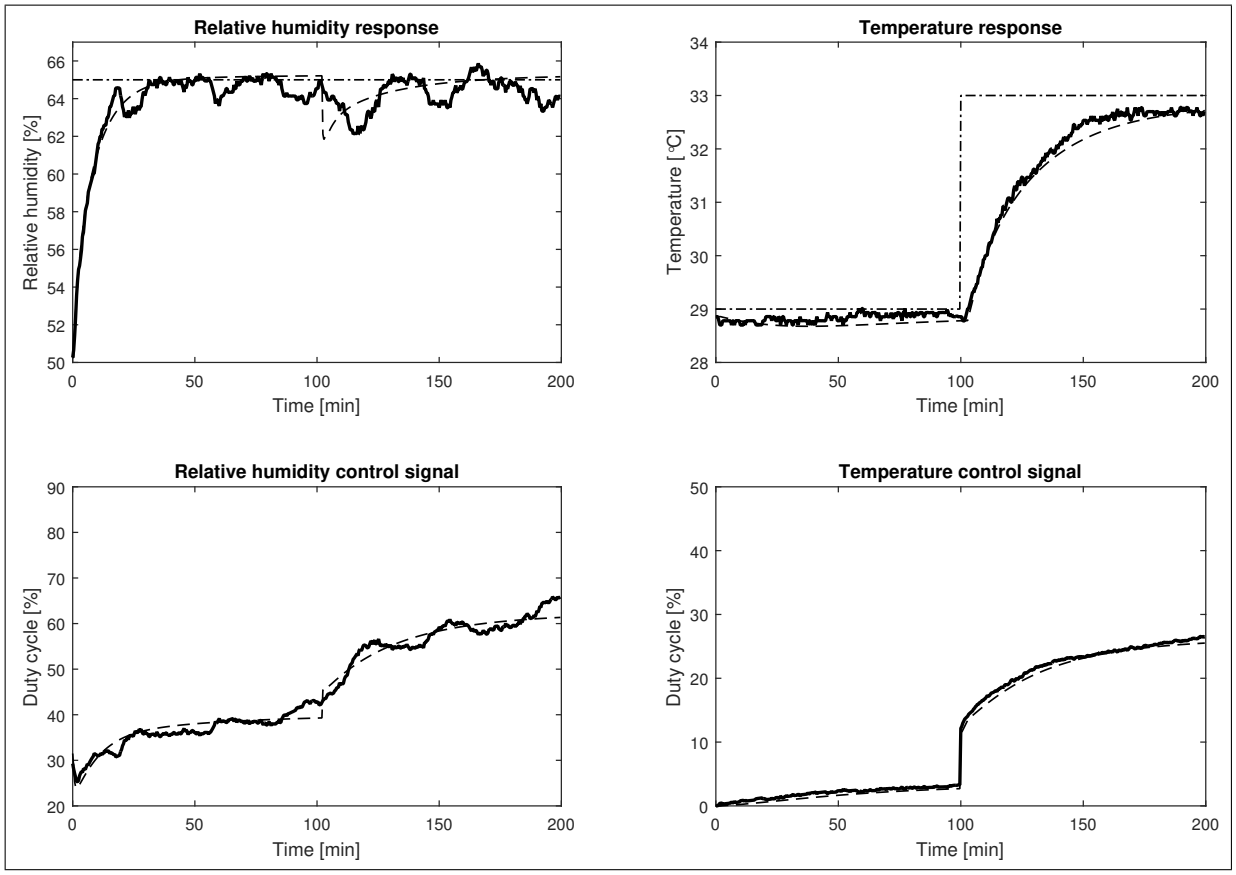

Source: The author.

Table 17 – Performance indexes of the steps responses for the initial controller tuning and for the tuning obtained by applying the new method (note that with the initial controller tuning the temperature does not attain the set-point desired value within the experiment interval)

Responses		Relative Humidity		Temperature	
Steps		$A_{s1} = 15\%$	$A_{s2} = 4°C$	$A_{s1} = 15\%$	$A_{s2} = 4°C$
Initial tuning	t_s[min]	28.8	–	–	N/A
	US	–	2.5[%]	0.3[°C]	–
	IAE	140.27	85.17	16.35	114.42
Autotuning	t_s[min]	3.6	–	–	64.4
	US	–	1.62[%]	0.58[°C]	–
	IAE	37.73	31.8	10.7	75.48

Analysing Table 17, it can be seen that the new auto-tuning method: (a) reduced of 87.5% the humidity settling time; in the case of temperature, the initial controller did not reached the steady-state within the 5% criterion in a reasonable time, (b) kept the US for both temperature

Figure 29 – Relative humidity and temperature responses and control signals of the system with the model identified with the initial controller tuning (dashed line) and with the tuning obtained by applying the new method (solid line). The set-point step changes (dash-dotted line) occur at times $t = 0$ and $t = 100$ min.

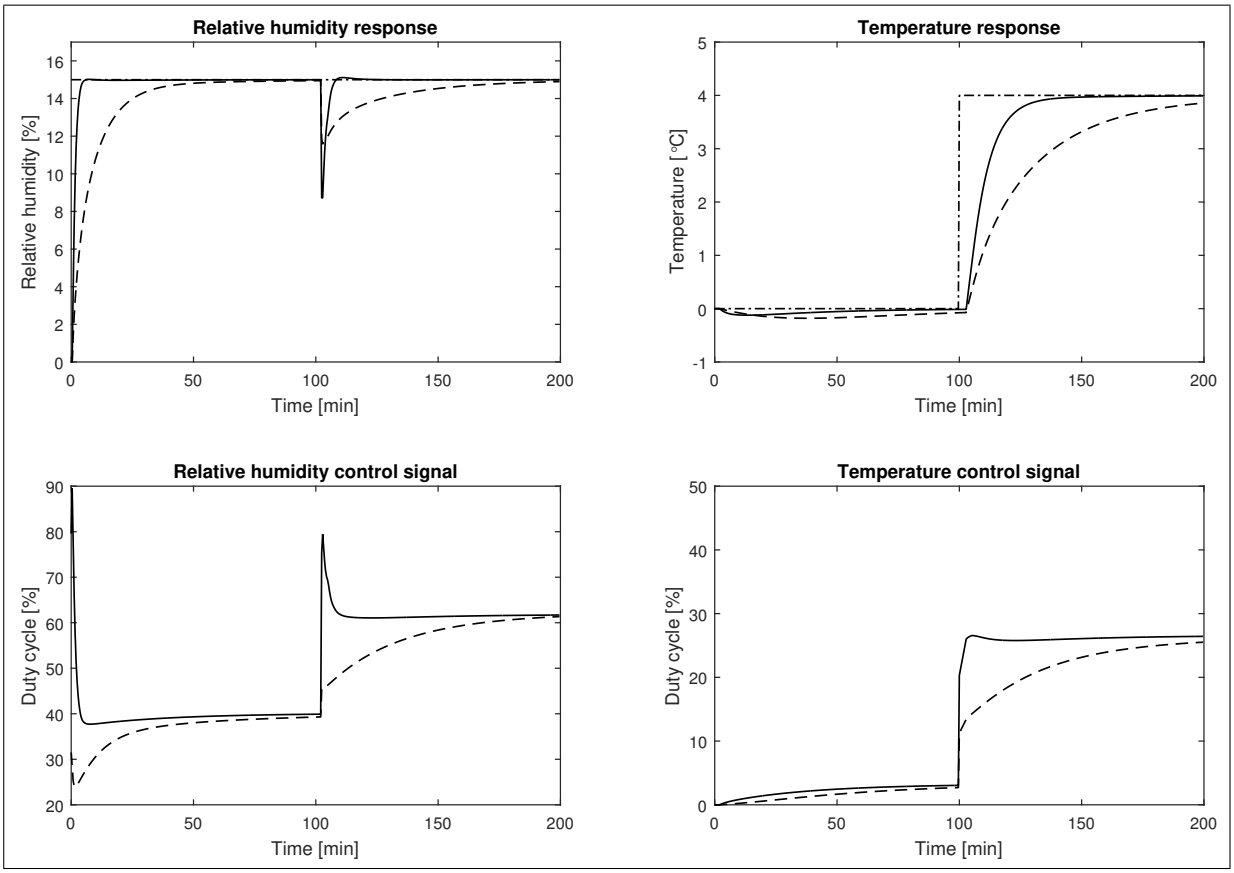

Source: The author.

and relative humidity at acceptable values, and (c) reduced considerably all *IAE* indexes.

5.6 Discussion

This chapter presents the studied auto-tuning methodology applied to multivariable TITO systems. It was addressed topics like noise robustness, on-line computations, independence from input and output values to identify model parameters, parameters feasibility, input-output paring and use of decouplers.

The simulations compared the proposed method to another method in the literature and presented results without and with additive noise. The proposed method obtained similar or better results in the noise free case. In the presence of additive noise the proposed method kept the identified parameters feasibility while the other method estimated not feasible parameters in some cases. Therefore, the simulation results with additive noise proved the robustness of the new method to certain levels of noise.

The application of the auto-tuning method in the neonatal incubator prototype improved

Figure 30 – Relative humidity and temperature responses and control signals in the experiments with the initial controller tuning (thin dashed line) and with the tuning obtained by applying the new method (thick line). The set-point step changes (dash-dotted line) occur at times $t = 0$ and $t = 100$ min.

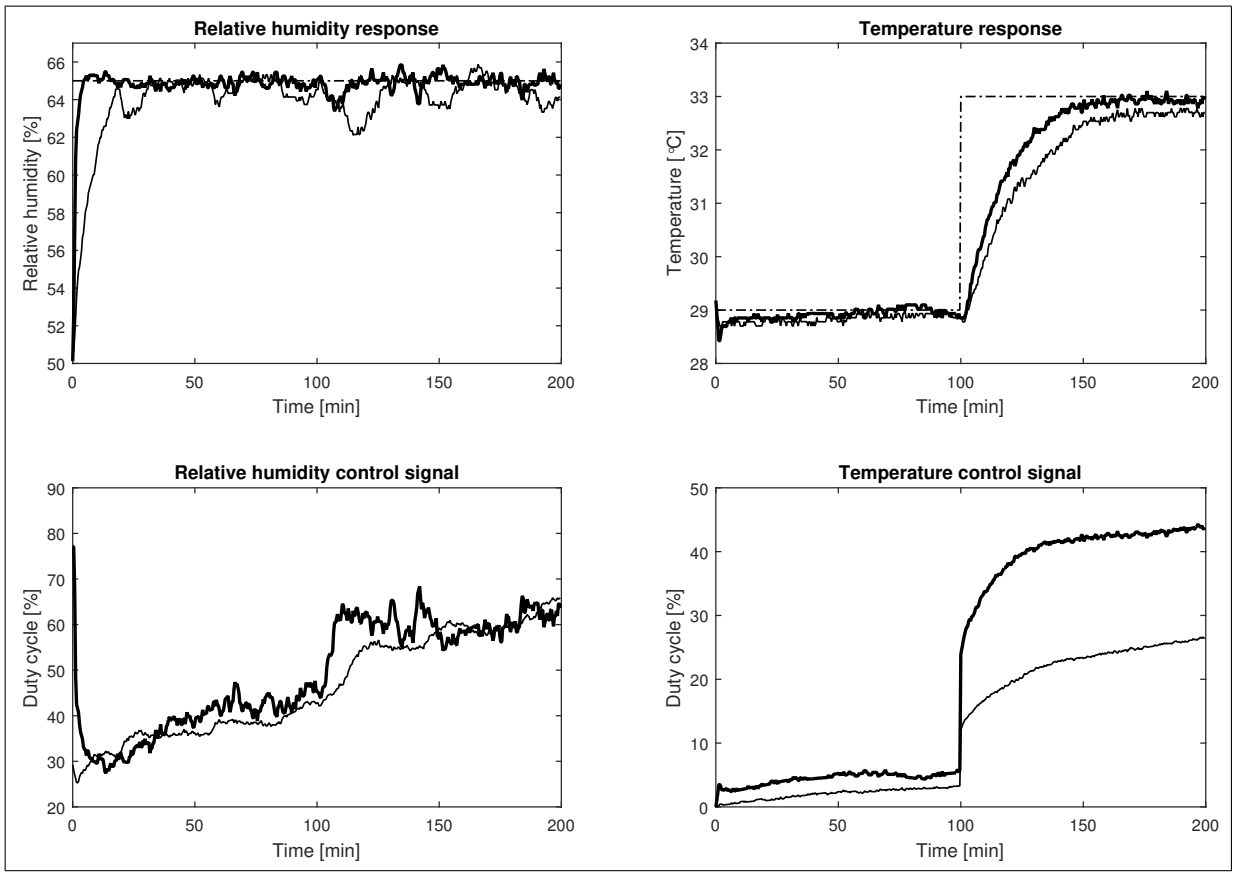

Source: The author.

the performance of the PID controller, as could be seen by the performance indexes. Therefore, the experiment proved the method practical effectiveness and robustness to real measurement noise.

6 ANTI-WINDUP DEAD-TIME COMPENSATOR BASED ON GENERALIZED PREDICTIVE CONTROL

This chapter is organized as follows. In Section 6.1, the DTC is formulated and are presented the predictions and optimal control input computations. In Section 6.2, a simplification of the control structure is proposed and the tunings for set-point tracking and for disturbance rejection are presented. In Section 6.3, are presented simulation results for stable, integrative and unstable processes. In Section 6.4 the experimental results are presented. In Section 6.5, important observations and comments about the proposed DTC are made.

6.1 Generalized predictive control

The GPC strategy for dead-time processes can be represented as the control sequence that minimizes the following cost function:

$$J = \sum_{k=d+1}^{d+N} (y(t+k|t) - \omega(t+k))^2 + \sum_{j=1}^{N_u} \lambda(j)(\Delta u(t-1+j|t))^2, \tag{6.1}$$

where $y(t+k|t)$ is the k-step ahead prediction of the process output on data up to time t, $\Delta u(t-1+j|t)$ is the future control increment, $\omega(t+k)$ is the future reference, λ_j is the control weight, d is the input dead time, N is the prediction horizon window and N_u is the control horizon window. Eq. (6.1) can be written in a compact form as:

$$J = (\mathbf{Y} - \mathbf{W})^T(\mathbf{Y} - \mathbf{W}) + \Delta\mathbf{U}^T\mathbf{Q}\Delta\mathbf{U}, \tag{6.2}$$

where

$$\mathbf{Y} = \begin{bmatrix} y(t+d+1|t) \\ y(t+d+2|t) \\ \vdots \\ y(t+N|t) \end{bmatrix}, \Delta\mathbf{U} = \begin{bmatrix} \Delta u(t|t) \\ \Delta u(t+1|t) \\ \vdots \\ \Delta u(t+N_u-1|t) \end{bmatrix},$$

$$\mathbf{W} = \begin{bmatrix} \omega(t+d+1) \\ \omega(t+d+2) \\ \vdots \\ \omega(t+d+N) \end{bmatrix}, \mathbf{Q} = \begin{bmatrix} \lambda_1 & 0 & \dots & 0 \\ 0 & \lambda_2 & \dots & 0 \\ \vdots & \vdots & \ddots & \vdots \\ 0 & 0 & \dots & \lambda_{N_u} \end{bmatrix}.$$

In the proposed approach the control input is used as a decision variable, instead of the control increment. Therefore, (6.2) can be written as:

$$J = (\mathbf{Y} - \mathbf{W})^T(\mathbf{Y} - \mathbf{W}) + (\mathbf{MU} - \bar{\mathbf{U}})^T\mathbf{Q}(\mathbf{MU} - \bar{\mathbf{U}}), \tag{6.3}$$

where $\mathbf{U} = [u(t|t), u(t+1|t), \ldots, u(t+N_u-1|t)]$ and $\mathbf{M}$ and $\bar{\mathbf{U}}$ are matrices with size $N_u \times N_u$ and $N_u \times 1$, respectively. They are given by:

$$\mathbf{M} = \begin{bmatrix} 1 & 0 & \ldots & 0 & 0 \\ -1 & 1 & \ldots & 0 & 0 \\ \vdots & \vdots & \ddots & \vdots & \vdots \\ 0 & 0 & \ldots & -1 & 1 \end{bmatrix}, \bar{\mathbf{U}} = \begin{bmatrix} u(t-1) \\ 0 \\ \vdots \\ 0 \end{bmatrix}. \tag{6.4}$$

Note that, in order to minimize the cost function (6.3), first, the output prediction must be computed.

6.1.1 Computing the Predictions

The GPC strategy uses the CARIMA model to compute the predictions. In case of dead-time processes, the following CARIMA model with dead time d can be used:

$$A(q)y(t) = B(q)u(t-1-d) + \frac{C(q)}{\Delta}e(t), \tag{6.5}$$

which can be written as follows:

$$y(t) = x(t) + n(t), \tag{6.6}$$

$$x(t) = \frac{B(q)u(t-1-d)}{A(q)}, \tag{6.7}$$

$$n(t) = \frac{C(q)}{\tilde{A}(q)}e(t), \tag{6.8}$$

where $\tilde{A}(q) = \Delta A(q)$, $\Delta = 1 - q^{-1}$,

$$\begin{aligned} A(q) &= 1 + a_1 q^{-1} + \ldots + a_{n_a} q^{-n_a}, \\ B(q) &= b_0 + b_1 q^{-1} 1 + \ldots + b_{n_b} q^{-n_b}, \\ C(q) &= 1 + c_1 q^{-1} 1 + \ldots + a_{n_c} q^{-n_c}. \end{aligned} \tag{6.9}$$

Without loss of generality it is assumed that $n_c = n_a + 1$ (however, in practice, it can be used $n_c \leq n_a + 1$).

Two Diophantine equations are defined as follows:

$$1 = A(q)E_j(q) + q^{-j}F_j(q), \tag{6.10}$$

$$C(q) = \tilde{A}(q)\tilde{E}_k(q) + q^{-k}\tilde{F}_k(q), \tag{6.11}$$

where:

$$\begin{aligned} F_j(q) &= f_{j,0} + f_{j,1}q^{-1} + \ldots + f_{j,n_a}q^{-n_a}, \\ \tilde{F}_k(q) &= \tilde{f}_{k,0} + \tilde{f}_{k,1}q^{-1} + \ldots + \tilde{f}_{k,n_a}q^{-n_a}, \\ E_j(q) &= e_0 + e_1q^{-1} + \ldots + e_{j-1}q^{-j+1}, \\ \tilde{E}_k(q) &= \tilde{e}_0 + \tilde{e}_1q^{-1} + \ldots + \tilde{e}_{k-1}q^{-k+1}. \end{aligned} \tag{6.12}$$

Eq. (6.7) at the time $t+k$ can be written as:

$$x(t+k|t) = \frac{B(q)u(t-1-d+k|t)}{A(q)}. \tag{6.13}$$

Making $k = d+j$, (6.13) becomes:

$$x(t+d+j|t) = \frac{B(q)u(t-1+j|t)}{A(q)}. \tag{6.14}$$

Using (6.10), (6.14) can be written as:

$$x(t+d+j|t) = B(q)E_j(q)u(t-1+j|t) + F_j(q)x(t+d). \tag{6.15}$$

In addition, making $B(q)E_j(q) = G(q) + \tilde{G}(q)q^{-j}$, (6.15) can be written as:

$$x(t+d+j|t) = G(q)u(t-1+j|t) + \tilde{G}(q)u(t-1) + F_j(q)x(t+d), \tag{6.16}$$

where:

$$\begin{aligned} G_j(q) &= h_1 + h_2\,q^{-1} + \ldots + h_j\,q^{-j+1}, \\ \tilde{G}_j(q) &= \tilde{g}_{j,0} + \tilde{g}_{j,1}\,q^{-1} + \ldots + \tilde{g}_{j,n_b-1}\,q^{-n_b+1}. \end{aligned} \tag{6.17}$$

On the other hand, considering (6.11), (6.8) can be written as:

$$n(t+k) = \frac{\tilde{F}_k(q)n(t)}{C(q)} + \tilde{E}_k(q)e(t+k). \tag{6.18}$$

Making $k = d+j$, (6.18) becomes:

$$n(t+d+j) = \frac{\tilde{F}_{d+j}(q)n(t)}{C(q)} + \tilde{E}_{d+j}(q)e(t+d+j). \tag{6.19}$$

Since all terms of $\tilde{E}_{d+j}(q)e(t+d+j)$ are in the future, its expected value is zero. Therefore, the disturbance prediction is given by:

$$n(t+d+j|t) = \frac{\tilde{F}_{d+j}(q)n(t)}{C(q)}. \tag{6.20}$$

Using (6.16) and (6.20), the output prediction can be written as:

$$y(t+d+j|t) = G_j(q)u(t-1+j|t) + f_j, \tag{6.21}$$

where f_j (also called free response) is given by

$$f_j = \tilde{G}_j(q)u(t-1) + F_j(q)x(t+d) + \frac{\tilde{F}_{d+j}(q)n(t)}{C(q)}. \tag{6.22}$$

For $j = 1, \ldots, N$, the predicted output can be represented in the matrix form:

$$\mathbf{Y} = \mathbf{G}\mathbf{U} + \mathbf{f}, \tag{6.23}$$

where:

$$\mathbf{G} = \begin{bmatrix} h_1 & 0 & \ldots & 0 \\ h_2 & h_1 & \ldots & 0 \\ \vdots & \vdots & \ddots & 0 \\ h_{N_u} & h_{N_u-1} & \ldots & g_1 \\ \vdots & \vdots & \ddots & \vdots \\ h_N & h_{N-1} & \ldots & g_{N-N_u+1} \end{bmatrix}, \tag{6.24}$$

$$g_i = h_1 + \ldots + h_i, \tag{6.25}$$

$$\mathbf{f} = \tilde{\mathbf{G}}(q)u(t-1) + \mathbf{F}(q)x(t+d) + \frac{\tilde{\mathbf{F}}(q)n(t)}{C(q)}, \tag{6.26}$$

$$\tilde{\mathbf{G}}(q) = \begin{bmatrix} \tilde{G}_1(q) \\ \tilde{G}_2(q) \\ \vdots \\ \tilde{G}_N(q) \end{bmatrix}, \mathbf{F}(q) = \begin{bmatrix} F_1(q) \\ F_2(q) \\ \vdots \\ F_N(q) \end{bmatrix} \text{ and } \tilde{\mathbf{F}}(q) = \begin{bmatrix} \tilde{F}_{d+1}(q) \\ \tilde{F}_{d+2}(q) \\ \vdots \\ \tilde{F}_{d+N}(q) \end{bmatrix}.$$

6.1.2 Computing the Optimal Control Input

In order to compute the optimal control input, the cost function (6.3) is written as:

$$J = \frac{1}{2}\mathbf{U}^T\mathbf{H}\mathbf{U} + \mathbf{b}^T\mathbf{U} + \mathbf{K}_0, \tag{6.27}$$

where

$$\begin{aligned} \mathbf{H} &= 2(\mathbf{G}^T\mathbf{G} + \mathbf{M}^T\mathbf{Q}\mathbf{M}), \\ \mathbf{b}^T &= 2\left[(\mathbf{f}-\mathbf{W})^T\mathbf{G} - \bar{\mathbf{U}}^T\mathbf{Q}\mathbf{M}\right] \end{aligned} \tag{6.28}$$

and $\mathbf{K}_0$ is a constant.

The unconstrained optimal control can be found making the gradient of J equal to zero. Therefore,

$$\mathbf{U} = -\mathbf{H}^{-1}\mathbf{b} = (\mathbf{G}^T\mathbf{G} + \mathbf{M}^T\mathbf{Q}\mathbf{M})^{-1}(\mathbf{G}^T(\mathbf{W}-\mathbf{f}) + \mathbf{M}^T\mathbf{Q}\bar{\mathbf{U}}). \tag{6.29}$$

Due to the receding control strategy, only the first element of $\mathbf{U}$ will be applied to the process, which is:

$$u(t) = k_r r(t) - \mathbf{k}_1 \mathbf{f} + k_0 u(t-1), \tag{6.30}$$

where $r(t)$ is the set-point, $\mathbf{k}_1$ is the first row of $(\mathbf{G}^T\mathbf{G} + \mathbf{M}^T\mathbf{Q}\mathbf{M})^{-1}\mathbf{G}^T$, k_r is the sum of the elements of $\mathbf{k}_1$ and k_0 the element of the first row and first column of $(\mathbf{G}^T\mathbf{G} + \mathbf{M}^T\mathbf{Q}\mathbf{M})^{-1}\mathbf{M}^T\mathbf{Q}$. Using (6.26), the term $\mathbf{k}_1\mathbf{f}$ can be written as:

$$\mathbf{k}_1\mathbf{f} = P_0(q)u(t-1) + P_1(q)x(t+d) + \frac{P_2(q)n(t)}{C(q)}, \tag{6.31}$$

where $P_0(q) = \mathbf{k}_1\tilde{\mathbf{G}}(q)$, $P_1(q) = \mathbf{k}_1\mathbf{F}(q)$ and $P_2(q) = \mathbf{k}_1\tilde{\mathbf{F}}(q)$. Using (6.31), the control input from (6.30) can be written as:

$$u(t) = k_r r(t) - P_1(q)x(t+d) - \frac{P_2(q)n(t)}{C(q)} - P_3(q)u(t-1), \tag{6.32}$$

where $P_3(q) = P_0(q) - k_0$. The control structure is illustrated in Fig. 31, where $\mathrm{T}(z) = P_2(z)/C(z)$.

Figure 31 – Block-diagram of the proposed GPC.

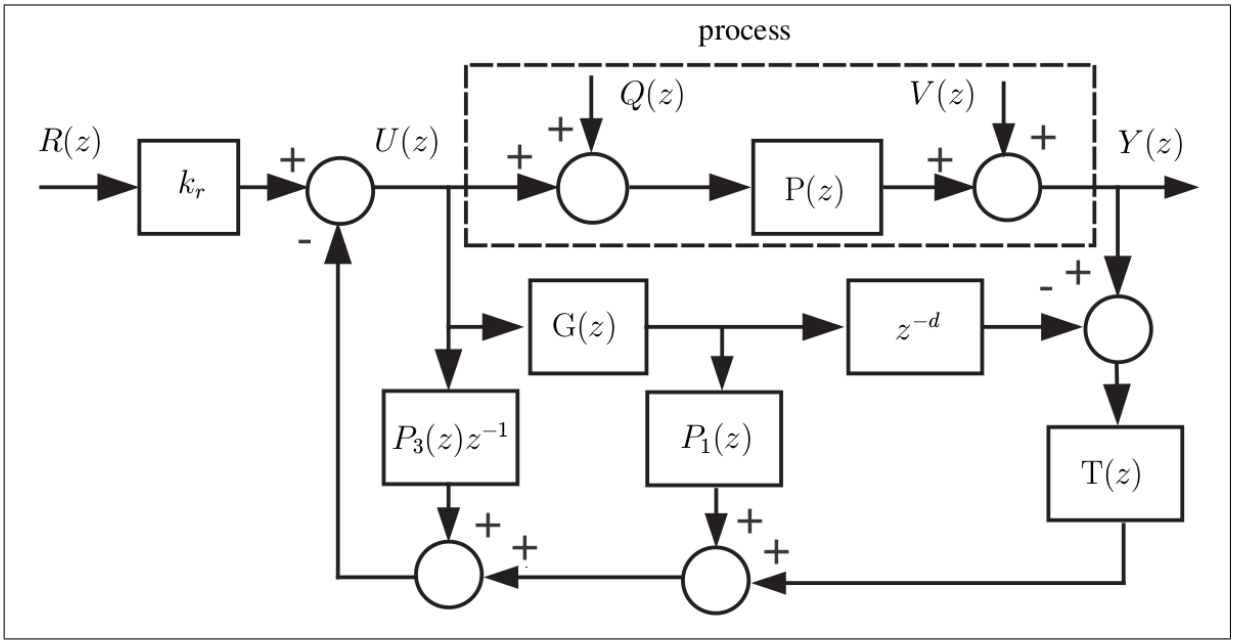

Source: The author.

It is important to note that the order of the polynomials $P_1(q)$, $P_2(q)$, and $P_3(q)$ are $n_a - 1$, n_a and $n_b - 1$, respectively. This simplicity is important from practical implementation point of view. In order to show some properties of this controller, some input-output relationships in the nominal case (which is the process Z-transfer function $\mathrm{P}(z) = \mathrm{G}(z)z^{-d}$, where $\mathrm{G}(z) = B(z)z^{-1}/A(z)$) are computed:

$$\frac{Y(z)}{R(z)} = \mathrm{H}_{\mathrm{yr}}(z) = \frac{k_r \mathrm{P}(z)}{1 + P_3(z)z^{-1} + P_1(z)\mathrm{G}(z)}, \tag{6.33}$$

$$\frac{Y(z)}{Q(z)} = \mathrm{H_{yq}}(z) = \mathrm{P}(z)\left(1 - \frac{P_2(z)}{C(z)}\frac{\mathrm{H_{yr}}(z)}{k_r}\right) \text{ and} \tag{6.34}$$

$$\frac{U(z)}{V(z)} = \mathrm{H_{uv}}(z) = -\frac{P_2(q)}{C(q)}\frac{\mathrm{H_{yr}}(z)}{k_r\,\mathrm{P}(z)}. \tag{6.35}$$

In addition, a condition of robustness is given by (MORARI; ZAFIRIOU, 1989)

$$\Delta P(z) \leq I_r(z) = \frac{|C(z)|}{|P_2(z)|}\frac{|kr|}{|\mathrm{H_{yr}}(z)|}, \tag{6.36}$$

where $z = e^{j\omega}$, $0 < \omega < \pi$, and I_r is defined as a robustness index.

It is important to note that the controller parameters N, N_u, and $\lambda(j)$ affect the polynomials $P_1(q)$ and $P_3(q)$. On the other hand, the disturbance polynomial $C(q)$ affects only the polynomial $P_2(q)$. Therefore, it can be stated that:

- The set-point tracking can be tuned using N, N_u, and $\lambda(j)$, since (6.33) depends on $P_1(q)$ and $P_3(q)$. In practice, it is common to fix N and N_u and use only $\lambda(j)$ as a tuning parameter;
- The polynomial $C(q)$ affects the disturbance rejection, acts as a low pass filter in the noise attenuation and appears in the numerator of the robustness index. Therefore, $C(q)$ can be tuned with a trade off between the disturbance rejection and both robustness index and noise attenuation.

6.2 Proposed control structure

The control structure shown in Fig. 31 is internally unstable in case of open-loop integrating or unstable processes and the windup problem was not addressed. In order to overcome these problems, this work proposes the use of an equivalent control structure that includes the saturation model (as illustrated in Fig. 32), where:

$$S(q) = \frac{B(q)}{A(q)}q^{-1}\left(P_1(q) - \frac{P_2(q)}{C(q)}q^{-d}\right). \tag{6.37}$$

Note that $S(q)$ from (6.37) can present internal stability problems if the roots of $A(q)$ are outside the unit circle. Futhermore, it is common in real processes the control action to attain the lower $u_{\min}$ or the upper $u_{\max}$ limits of the process. In which case, if the controller was not properly designed, windup problems can arise. Meaning that some unstable modes can appear, making the system oscillatory or even unstable. Therefore, in the proposed control structure illustrated in Fig. 32, it was included the saturation model, which constraints the control action $u(t)$ to $u_{\min}$ or $u_{\max}$ when the computed control action is less or greater than these limits, respectively.

Figure 32 – Block-diagram of the proposed anti-windup GPC.

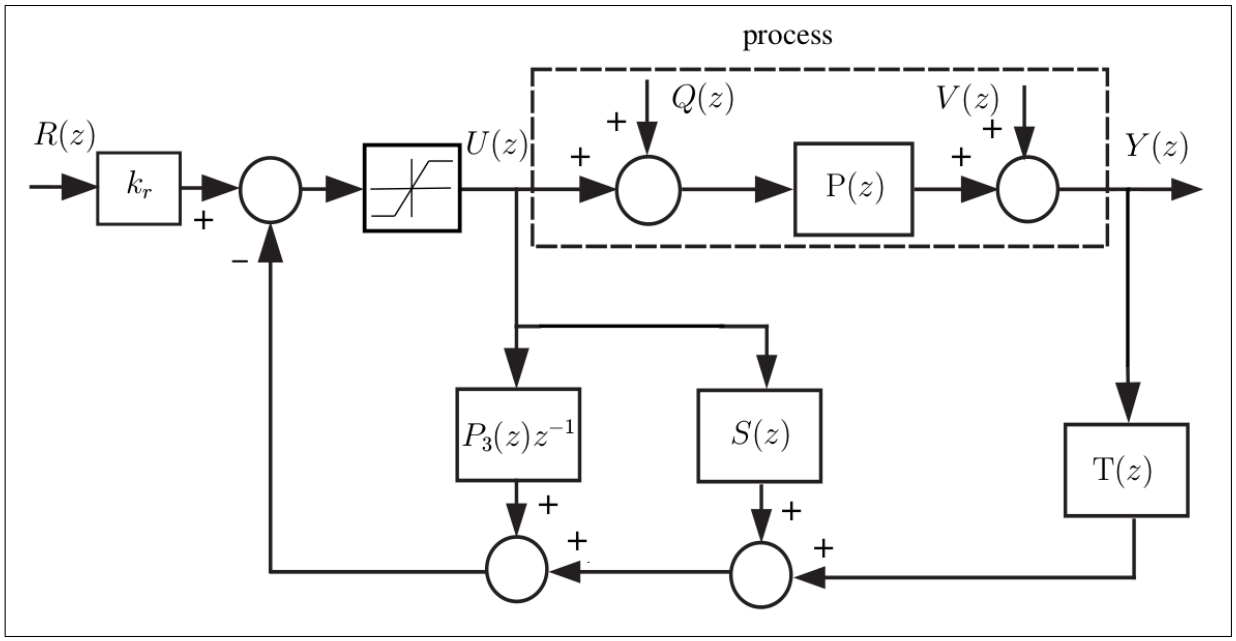

Source: The author.

The next two lemmas show how $S(q)$ can be implemented in order to guarantee internal stability and why there is not unstable modes when the process is under saturation.

Lemma 1. *In GPC strategy, the polynomial $A(q)$ can be explicitly eliminated from the denominator of $S(q)$ (see (6.37)), so that the controller becomes internally stable in case of unstable open-loop models. As a result of this cancellation, $S(q)$ can be written as:*

$$S(q) = \frac{q^{-1}P_4(q)}{C(q)}, \tag{6.38}$$

where $P_4(q)$ is a $d+n_b$ order polynomial. Observe that the only term in the denominator of $S(q)$ is $C(q)$. Since $C(q)$ is designed so that all its roots are inside the unit circle, $S(q)$ will be internally stable.

Proof. Eq. (6.37) can be written as:

$$S(q) = \frac{B(q)P_5(q)q^{-1}}{A(q)C(q)}, \tag{6.39}$$

where $P_5 = C(q)P_1(q) - P_2(q)q^{-d}$. Then, using (6.10) and (6.11), $P_5(q)$ can be written as:

$$P_5(q) = \mathbf{k}_1 \begin{bmatrix} A(q)\left(\Delta\tilde{E}_{d+1} - E_1(q)C(q)\right)q \\ A(q)\left(\Delta\tilde{E}_{d+2} - E_2(q)C(q)\right)q^2 \\ \vdots \\ A(q)\left(\Delta\tilde{E}_{d+N} - E_N(q)C(q)\right)q^N \end{bmatrix}. \tag{6.40}$$

Using (6.10) and (6.11), the terms in brackets of (6.40) can be written as:

$$A(q)\left(\Delta\tilde{E}_{d+j} - E_j(q)C(q)\right)q^j = (\tilde{F}_{d+j}(q)q^{-d} - F_j(q)), \tag{6.41}$$

that is, (6.41) is a polynomial in the backward shift operator q^{-1} of order $n_a + d$. Eq. (6.40) can also be written as:

$$P_5(q) = A(q)P_6(q), \tag{6.42}$$

where $P_6(q)$ is a d-order polynomial given by:

$$P_6(q) = \mathbf{k}_1 \begin{bmatrix} \left(\Delta\tilde{E}_{d+1} - E_1(q)C(q)\right)q \\ \left(\Delta\tilde{E}_{d+2} - E_2(q)C(q)\right)q^2 \\ \vdots \\ \left(\Delta\tilde{E}_{d+N} - E_N(q)C(q)\right)q^N \end{bmatrix}. \tag{6.43}$$

Using (6.42), (6.39) can be written as:

$$S(q) = \frac{B(q)P_6(q)q^{-1}}{C(q)} = \frac{q^{-1}P_4(q)}{C(q)}, \tag{6.44}$$

where $P_4(q) = B(q)P_6(q)$. As can be seen in (6.44), $A(q)$ has been eliminated from the denominator of $S(q)$, completing the proof. □

Lemma 2. *If the proposed controller is under saturation, therefore there is no integral action, avoiding windup problems.*

Proof. Note that, in case the control signal is saturated (u_{sat}), therefore the computed control is given by:

$$U(z) = (z^{-1}P_3(z) + S(z))U_{sat}(z) + T(z)Y(z), \tag{6.45}$$

where $P_3(z)$ is a FIR filter and the poles of $S(z)$ and $T(z)$ are the roots of $C(z)$, which are inside the unit circle. Consequently the controller does not present an integrating mode, completing the proof. □

6.2.1 Tuning of the Set-Point Tracking

The set-point tracking can be tuned using the parameters N, N_u and λ_j. In practice it is common to use the following two approaches. At first, N and N_u are fixed as larger as the transient region, and then, λ_j is used to obtain the desired set-point response. Lower and bigger values of λ_j causes faster and slower responses, respectively. The second approach intends to reduce the computational cost and, for this reason, $N_u = 1$ and $\lambda_j = 0$ are fixed so that the only tuning parameter is N. Lower values of N are used to obtain faster responses and bigger values of N to obtain slower responses (see (IONESCU et al., 2008)). Additionally, if $N_u > 1$, to obtain a more aggressive response, the element λ_1 of the diagonal matrix $\mathbf{Q}$ can be made equal to zero.

6.2.2 *Tuning of* $C(q)$

First, lets define the following filter:

$$\mathrm{T}(z) = \frac{P_2(z)}{C(z)}, \tag{6.46}$$

where $P_2(z)$ is the only polynomial of the control action (see (6.32)) that depends on $C(z)$. Furthermore, as shown in previous sections, the order of $P_2(z)$ and $C(z)$ are n_a and n_a+1, respectively. Therefore, $\mathrm{T}(z)$ is a low pass filter. Using (6.46), Eqs. (6.34), (6.35) and (6.36) can be written as:

$$\mathrm{H_{yq}}(z) = \mathrm{P}(z)\left(1 - \mathrm{T}(z)\frac{\mathrm{H_{yr}}(z)}{k_r}\right), \tag{6.47}$$

$$\mathrm{H_{uv}}(z) = -\mathrm{T}(z)\frac{\mathrm{H_{yr}}(z)}{k_r\,\mathrm{P}(z)}, \tag{6.48}$$

$$I_r(z) = \frac{|kr|}{|\mathrm{T}(z)\,\mathrm{H_{yr}}(z)|}. \tag{6.49}$$

From (6.47), (6.48) and (6.49), it is possible to see that $\mathrm{T}(z)$ can be used to improve the noise attenuation $\mathrm{H_{uv}}(z)$ and robustness $I_r(z)$. However, there is a trade off between the disturbance rejection $I_r(z)$, $\mathrm{H_{yq}}(z)$ and $\mathrm{H_{uv}}(z)$.

Notwithstanding there are other options, this work makes use of only a C-polynomial for stable, integrating, and open-loop processes. For general cases of process, where the priority is more the disturbance rejection than the noise attenuation, the C-polynomial can be a Low-Pass filter with n_c real stable poles. Therefore, its discrete form results as:

$$C(z) = \left(1 - \alpha z^{-1}\right)^{n_c}, \tag{6.50}$$

where $1 \leq n_c \leq n_a + 1$. Therefore, the order of the filter n_c and the parameter α can be tuned to improve the disturbance rejection and the noise attenuation.

6.3 Simulation results

The chosen cases are stable, integrating and unstable processes present in (RIBIĆ; MATAUŠEK, 2012). The simulations compare the performance of the proposed DTC based on GPC (DTC-GPC) with the DTC-PID proposed in (RIBIĆ; MATAUŠEK, 2012) (with the same controller parameters as in that work). They were performed considering a unit step set-point and a -0.5 step disturbance. At each part of the simulation, the integral of absolute error (*IAE*)

was computed. For the unstable process case, also was performed a simulation with the addition of uncertainties.

The tuning of DTC-GPC was performed considering the following procedure. First, the DTC-PID was simulated adding uncertainties in the nominal plant until the system reached a response near the instability. Then, the DTC-GPC was tuned until its response looked alike the DTC-PID response near the instability. For all cases, the DTC-GPC tuning was performed with $N = N_u$ and $\lambda_1 = 0$.

6.3.1 Stable process

The model of a thermal plant (RIBIĆ; MATAUŠEK, 2012) is given below.

$$P(s) = \frac{1.507(3.42s+1)(1-0.816s)}{(577s+1)(18.1s+1)(0.273s+1)(104.6s^2+15s+1)}. \tag{6.51}$$

The parameters of the DTC-GPC were $N = N_u = 100$, $\lambda_j = 200$, $nc = 1$ and $\alpha = 0.925$. It can be seen the responses of the two controllers in Fig. 33 and the performance indices in Table 18.

Figure 33 – The DTC-PID and the proposed DTC-GPC responses for a stable process.

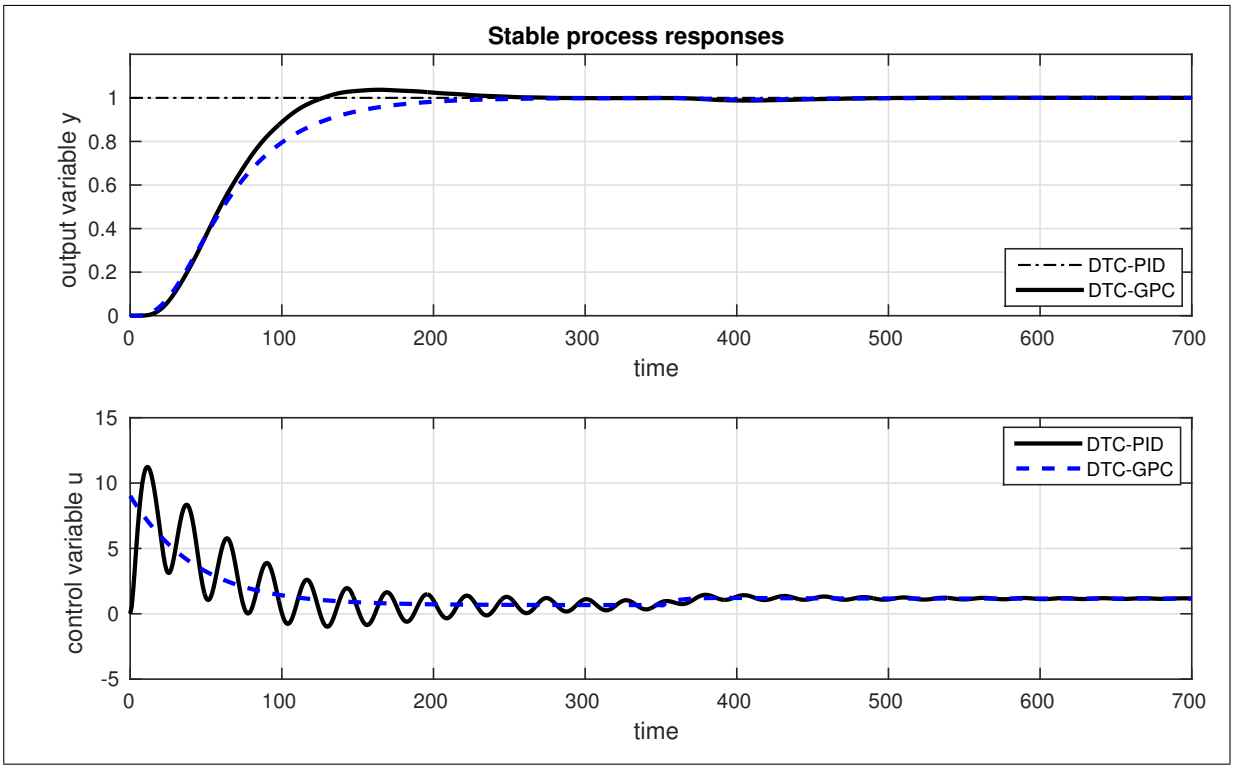

Source: The author.

Table 18 – Performance indices of the DTC-PID and the proposed DTC-GPC responses for a stable process.

Controller	IAE_1	IAE_2
DTC-PID	65.42	0.98
DTC-GPC	72.21	0.7

What can be observed from Fig. 33 and Table 18 is that the DTC-GPC has a more smooth and robust response, with the tuning priority in the input disturbance rejection.

6.3.2 *Integrating process*

The integrating process is the model of fluid level in a chain of evaporators (NORMEY-RICO; CAMACHO, 2009).

$$P(s) = \frac{-0.1}{s(2s+1)^5}. \tag{6.52}$$

For the DTC-GPC the parameters were $N = N_u = 40$, $\lambda_j = 100$, $nc = 1$ and $\alpha = 0.704$. The responses and the performance indices of the two controllers can be seen in Fig. 34 and Table 19, respectively.

Figure 34 – The DTC-PID and the proposed DTC-GPC responses for an integrating process.

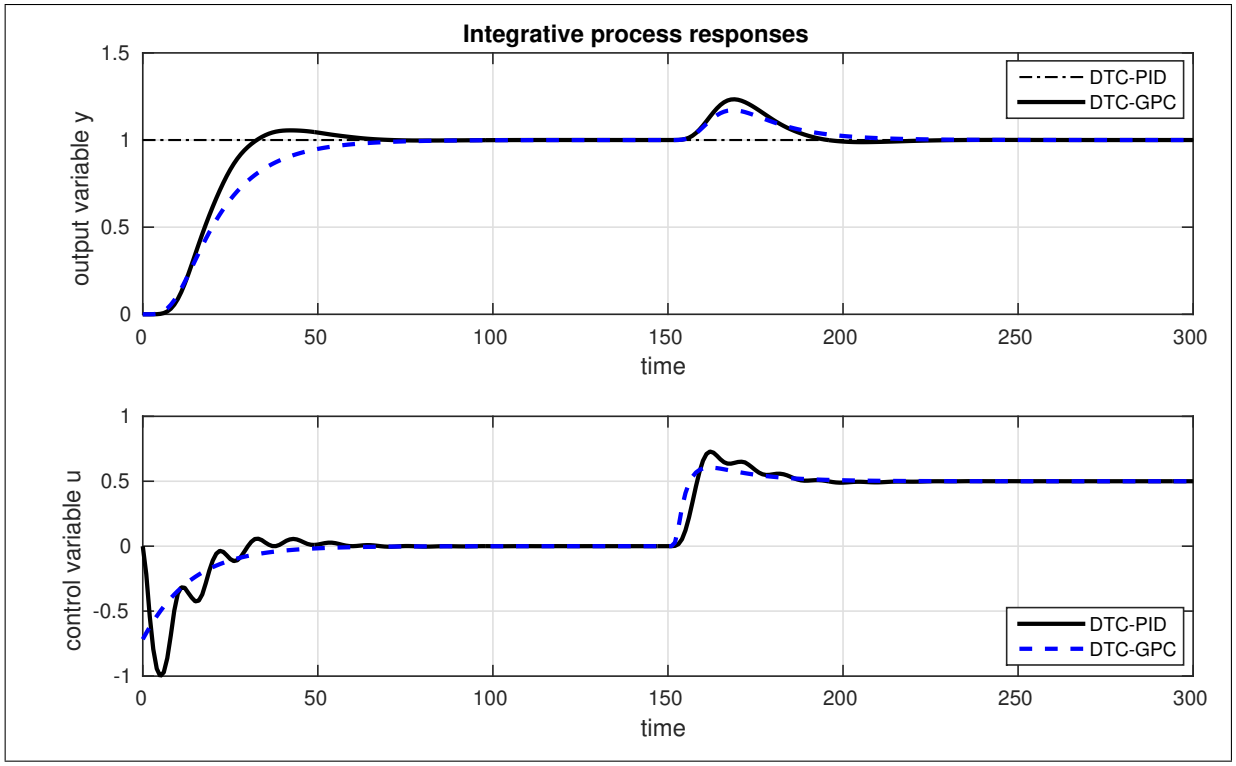

Source: The author.

Table 19 – Performance indices of the DTC-PID and the proposed DTC-GPC responses for an integrating process.

Controller	IAE_1	IAE_2
DTC-PID	19.46	4.81
DTC-GPC	23.71	4.38

The responses of the DTC-GPC were more robust and conservative, while the responses of the DTC-PID presented bigger overshoots and the control signal had oscillations.

6.3.3 Unstable process

The unstable process (MATAUŠEK; RIBIĆ, 2012) is presented in (6.53).

$$P(s) = \frac{2e^{-5s}}{(10s-1)(2s+1)}. \tag{6.53}$$

The DTC-GPC parameters were $N = N_u = 20$, $\lambda_j = 5$, $nc = 2$ and $\alpha = 0.631$. Fig. 35 and Table 20 and Fig. 36 and Table 21 present the responses and the performance indices for the nominal case and for the case with addition of uncertainties, respectively.

Figure 35 – The DTC-PID and the proposed DTC-GPC responses for an unstable process.

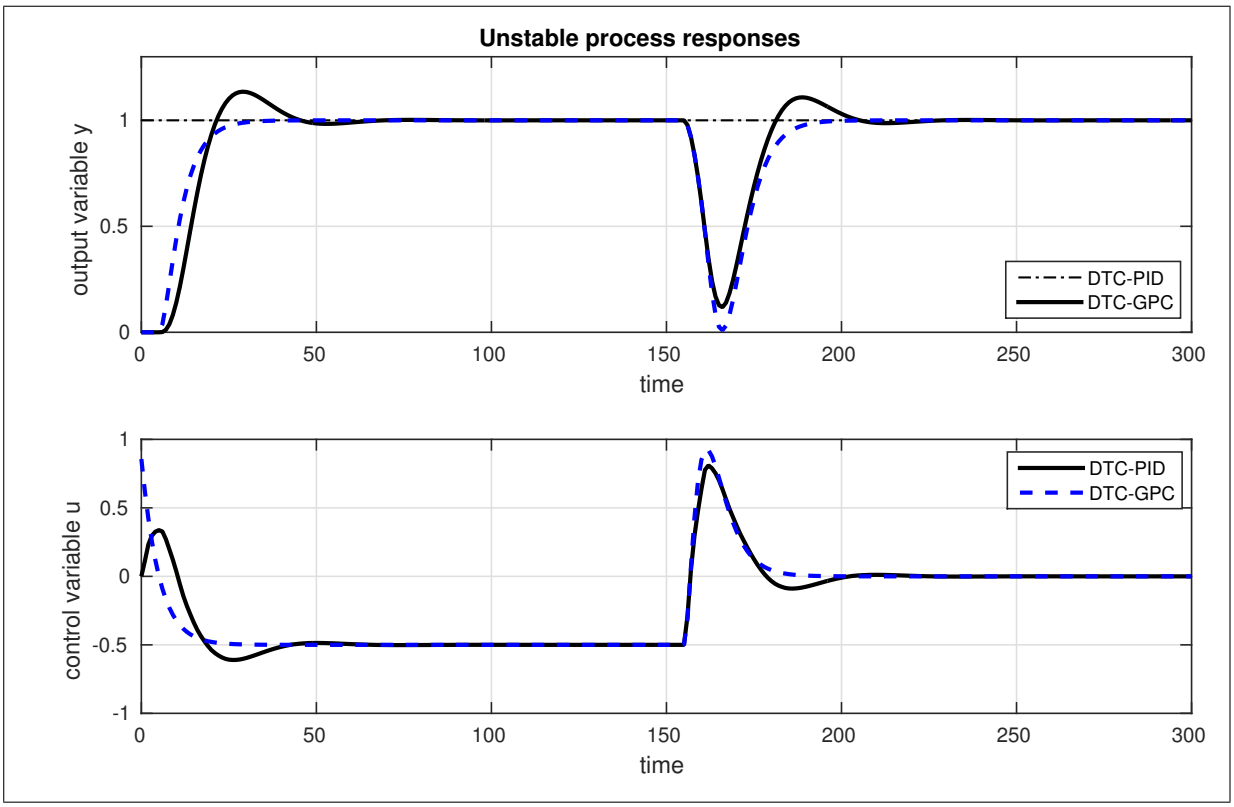

Source: The author.

Table 20 – Performance indices of the DTC-PID and the proposed DTC-GPC responses for an unstable process.

Controller	IAE_1	IAE_2
DTC-PID	16.38	13.24
DTC-GPC	12.4	13.72

Figure 36 – The DTC-PID and the proposed DTC-GPC responses for an unstable process with uncertainties.

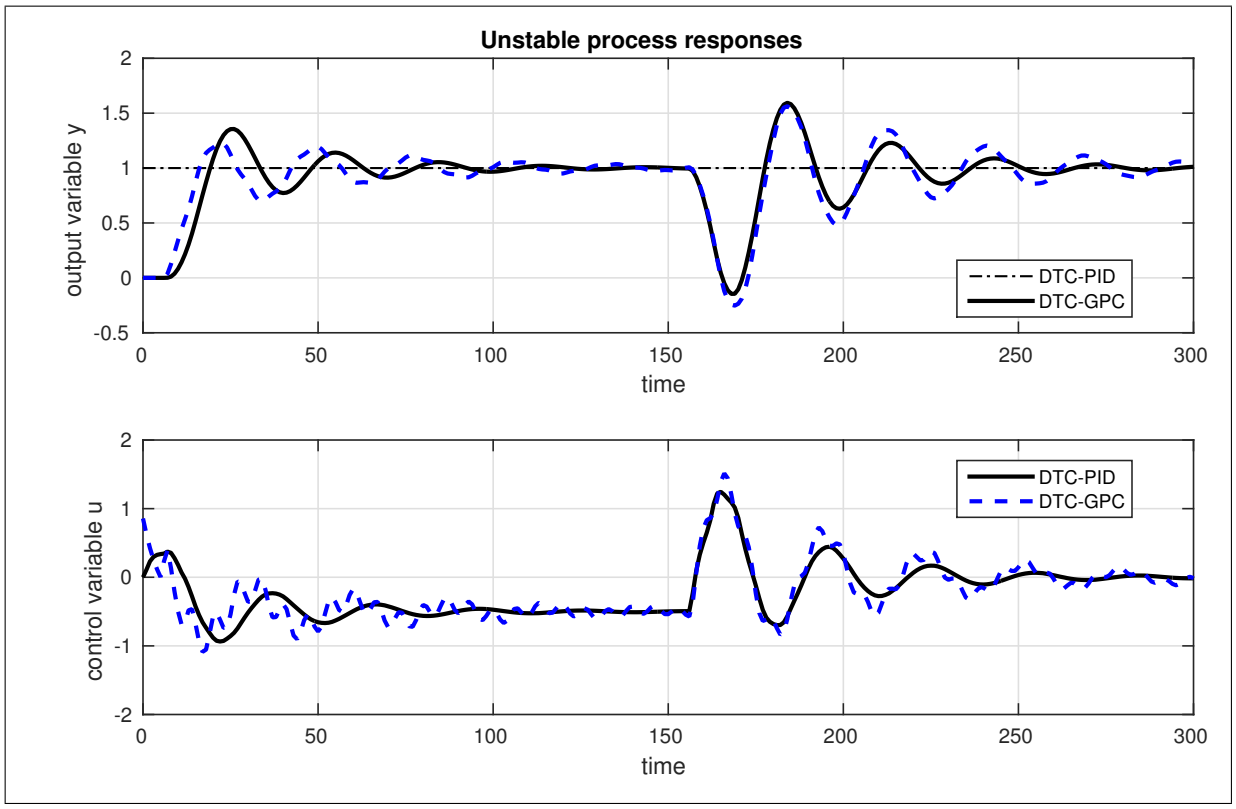

Source: The author.

Table 21 – Performance indices of the DTC-PID and the proposed DTC-GPC responses for an unstable process with uncertainties.

Controller	IAE_1	IAE_2
DTC-PID	23.24	27.9
DTC-GPC	22.32	35.53

For this case, the proposed DTC-GPC had much faster responses, but was less robust than the DTC-PID.

6.4 Experimental results

In the presented experiment it was chosen to control the relative humidity loop. The model identified for the relative humidity loop at the time that the experiment was performed

was

$$P(s) = \frac{0.41e^{-0.4s}}{3.41s+1}. \tag{6.54}$$

The parameters of the controller were: prediction horizon and control horizon windows $N = N_u = 50$, control weight $\lambda(j) = 0.1$, parameters of the $C(z)$ filter $n_c = 1$ and $\alpha = 0.1$ and the sampling time was $T_s = 0.25$ min.

The experiment was performed initially controlling the relative humidity and the temperature at 50% and 29°C, respectively. At $t = 0$ a set-point step change of $A_{s1} = 15\%$ was applied at the relative humidity loop. At $t = 60$ min a load disturbance in that loop occurs by applying a set-point step change in the temperature loop of $A_{s2} = 4$°C.

The relative humidity responses and control signals of the experiment are shown in Fig. 37 and the performance indexes, namely, settling time t_s (in minutes), percent overshoot $OS\%$, undershoot US (absolute value of relative humidity) and IAE are in Table 22.

Figure 37 – Relative humidity responses and control signals of the experiment with the GPC based DTC.

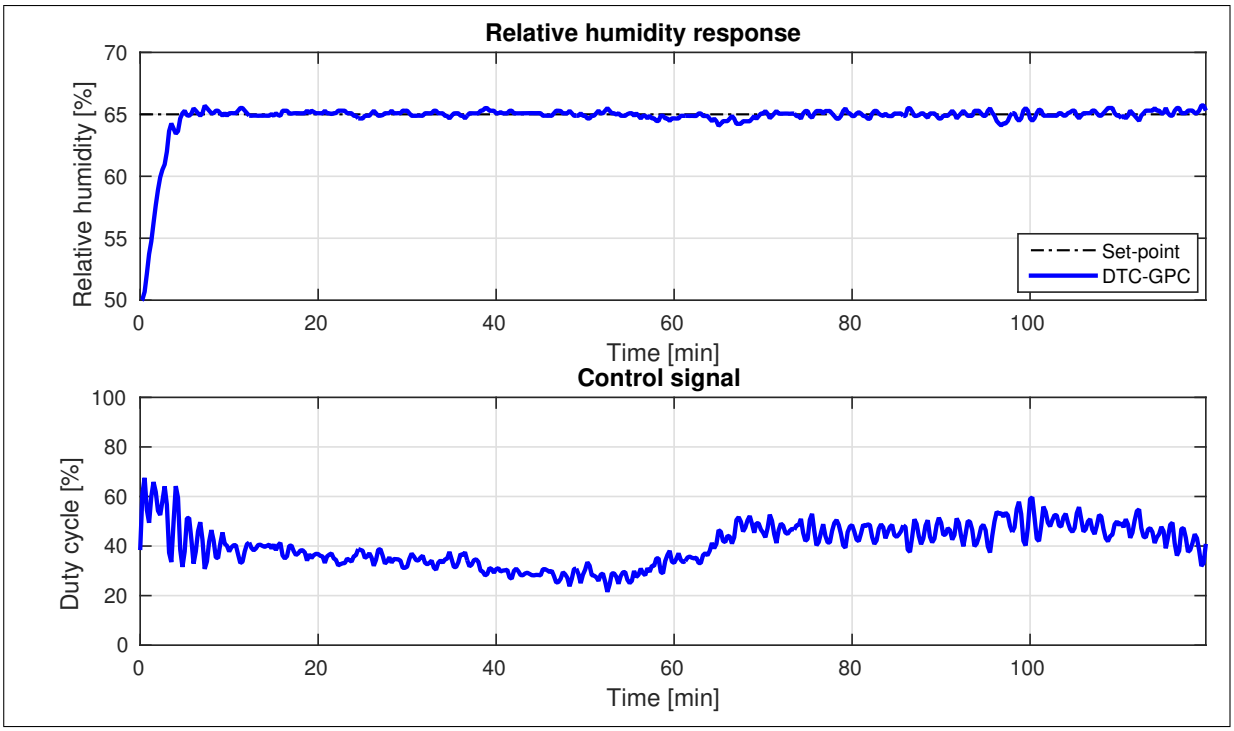

Source: The author.

From Fig. 37 it can be seen that the control signal is noisy but responsive, resulting in a much constant output signal. That response can be explained by the small value of the coefficient of the $C(z)$ filter, responsible for the noise attenuation at the output signal. From Table 22, for the neonatal incubator in question, the set-point step change response is fast and almost without overshoot and the load disturbance rejection results in just a small undershoot.

Table 22 – Performance indexes of the experiment with the GPC based DTC.

Steps	$A_{s1} = 15\%$	$A_{s2} = 4°C$
t_s[min]	4.40	–
$OS\%/US[\%]$	4.69%	0.93
IAE	38.27	14.21

6.5 Discussion

The proposed DTC based on GPC presented better results in most of the scenarios from the simulations results section when compared with the DTC-PID from (RIBIĆ; MATAUŠEK, 2012).

The experimental results also showed that the proposed strategy can cope with the presence of measurement noise. As can be seen in Fig. 37, the relative humidity response was smoother than those of experiments from previous chapters of this work.

7 CONCLUSIONS

An auto-tuning methodology for SISO PID controllers, for the SISO SFSP, for stable, unstable, and integrating processes, and for TITO PID controllers, for stable processes was presented. Without the need of special experiments, the procedure can be performed when desired by the operator or can use routine set-point changes or (abrupt) load disturbances data from the closed-loop plant operation. Based on computation of integrals, the estimation method has the advantage of being inherently robust to measurement noise. The rationale of the method relies in the "half rule" model reduction technique and the tuning rules can be freely chosen in accordance with the performance requirements of the system.

The simulation and experimental results showed that the performance assessment, by means of the derived performance indexes, is effective and that the identification method can estimate consistent and suitable models for SISO and TITO PID controllers design and for SFSP design. In the TITO PID controllers chapter, the effectiveness of the proposed method has been corroborated through simulation results where the proposed method is compared with another technique presented in literature. The proposed approach have shown better performance even in the presence of high-order processes and better robustness to high levels of additive noise.

The real applications on a neonatal incubator prototype showed that the estimated models were suitable for control purposes, since the initial controller of relative humidity and, for the TITO case, of temperature was improved. Those experiments also demonstrated that the method is robust to measurement noise in a real context. Furthermore, the experiments proved that the auto-tuning methodology can be implemented in a simple way and is suitable for practical applications. Therefore, the proposed technique has potential for industrial applications.

In future works, it is intended to implement the auto-tuning in a commercial incubator and evaluate the results using a Brazilian standard for neonatal incubators. Besides, the potential of the new method to self-tuning applications will be exploited. In addition, the auto-tuning of the SFSP will be extended to the TITO case.

An anti-windup GPC-based DTC that can cope with stable, integrating and unstable plants was also presented. The proposed controller addresses the problems of open-loop unstable processes control and windup, that are important questions concerning DTCs. Furthermore, solutions for the tuning for set-point tracking, disturbance rejection, and noise attenuation were presented.

Simulation results showed better performance of the proposed GPC-based DTC in most scenarios when compared to another proposed in literature called DTC-PID. In addition, the proposed controller presented satisfactory behaviour for dead-time uncertainties.

When applied to a neonatal incubator for relative humidity control, the proposed GPC-

based DTC was implemented in an straightforward way and presented satisfactory results and good performance. Therefore, the proposed controller has great potential in industrial applications because of its simplicity and optimal criteria.

As future works, the anti-windup action will be largely exploited, the proposed GPC-based DTC will be extended to the MIMO case and compared to MIMO GPC strategies present in the literature.

BIBLIOGRAPHY

ANG, K. H.; CHONG, G.; LI, Y. PID control systems analysis, design, and technology. *IEEE Transactions on Control Systems Technology*, v. 13, p. 559–576, 2005. Cited in page 94.

ÅSTRÖM, K. J.; HÄGGLUND, T. *Advanced PID Control*. Research Triangle Park, USA: ISA Press, 2006. Cited in page 37.

ÅSTRÖM, K. J. et al. Automatic tuning and adaptation for PID controllers - a survey. *Control Engineering Practice*, v. 1, p. 699–714, 1993. Cited 2 times in pages 49 and 99.

CAMACHO, E.; BORDONS, C. *Model Predictive Control*. Second edition. London: Springer-Verlag, 2007. 422 p. Cited in page 35.

CAVALCANTE, M. U. et al. Filtered model-based predictive control applied to the temperature and humidity control of a neonatal incubator. In: *Proceedings 9th IEEE/IAS International Conference on Industry Applications*. São Paulo: [s.n.], 2010. p. 1–6. Cited in page 67.

CONTROL ENGINEERING. *Auto-Tuning Control Using Ziegler-Nichols*. 2006. <https://www.controleng.com/articles/auto-tuning-control-using-ziegler-nichols/>. Accessed: 06-02-2017. Cited in page 35.

GARCÍA, P.; ALBERTOS, P. A new dead-time compensator to control stable and integrating processes with long dead-time. *Automatica*, Elsevier, v. 44, p. 1062–1071, 2008. Cited 4 times in pages 62, 64, 85, and 87.

GILBERT, A. F. et al. Tuning of PI controllers with one-way decoupling in 2×2 MIMO systems based on finite frequency response data. *Journal of Process Control*, v. 13, p. 553–567, 2003. Cited in page 37.

HÄGGLUND, T. An industrial dead-time compensating PI controller. *Control Engineering Practice*, Elsevier, v. 4, n. 6, p. 749–756, 1996. Cited in page 83.

HALEVI, Y.; PALMOR, Z. J.; EFRATI, T. Automatic tuning of decentralized PID for MIMO processes. *Journal of Process Control*, v. 7, p. 119–128, 1997. Cited in page 37.

IONESCU, C. et al. Robust predictive control strategy applied for propofol dosing using BIS as a controlled variable during anesthesia. *IEEE Transactions on Biomedical Engineering*, v. 55, p. 2161–2170, 2008. Cited in page 126.

KAREN, T. Thermoregulation in neonates. *Neonatal Network 13*, v. 2, p. 15–21, 1994. Cited in page 66.

KEYES, M.; KAYA, A. Evolution of Adaptive Control Algorithms and Products: A Critical Review and Evaluation. *IFAC Proceedings Volumes*, Elsevier, v. 22, n. 16, p. 1–8, 1989. Cited in page 35.

LEE, M. et al. Analytical design of multiloop PID controllers for desired closed-loop responses. *AIChE Journal*, v. 50, n. 7, p. 1631–1635, 2004. Cited 4 times in pages 38, 94, 101, and 114.

LEE, Y. et al. PID controller tuning for desired closed-loop responses for SI/SO systems. *AIChE Journal*, v. 44, p. 106–115, 1998. Cited in page 101.

LI, S.-Y. et al. Effective decentralized TITO process identification from closed-loop step responses. *Asian Journal of Control*, Wiley Online Library, v. 7, n. 2, p. 154–162, 2005. Cited 15 times in pages 15, 16, 19, 38, 39, 102, 103, 104, 105, 106, 107, 108, 109, 110, and 111.

LIU, T.; WANG, Q.-G.; HUANG, H.-P. A tutorial review on process identification from step or relay feedback test. *Journal of Process Control*, Elsevier, v. 23, n. 10, p. 1597–1623, 2013. Cited in page 39.

LIU, T.; ZHANG, W. D.; GU, D. Y. Analytical multiloop PI/PID controller design for two-by-two processes with time delays. *Industrial and Engineering Chemistry Research*, v. 44, p. 1832–1841, 2005. Cited in page 38.

LIU, T.; ZHANG, W. D.; GU, D. Y. Analytical design of decoupling internal model control (IMC) scheme for two-input-two-output (TITO) processes with time delays. *Industrial and Engineering Chemistry Research*, v. 45, p. 3149–3160, 2006. Cited in page 38.

LUYBEN, W. L. Simple method for tuning SISO controllers in multivariable systems. *Industrial and Engineering Chemistry Research*, v. 25, n. 1, p. 654–658, 1986. Cited 2 times in pages 38 and 103.

MARCHETTI, G.; SCALI, C.; ROMAGNOLI, J. A. Relay autotuning of multivariable systems: application to an experimental pilot-scale distillation column. In: *Preprints 15th IFAC World Congress*. Barcelona, ESP: [s.n.], 2002. Cited in page 37.

MATAUŠEK, M. R.; MICIC, A. D. A modified Smith predictor for controlling a process with an integrator and long dead-time. *IEEE Transactions on Automatic Control*, n. 41, p. 1199–1203, 1996. Cited in page 36.

MATAUŠEK, M. R.; RIBIĆ, A. I. Control of stable, integrating and unstable processes by the modified Smith predictor. *Journal of Process Control*, v. 22, p. 338–343, 2012. Cited 3 times in pages 36, 39, and 130.

MORARI, M.; ZAFIRIOU, E. *Robust Process Control*. Englewood Cliffs, NJ: Prentice Hall, 1989. Cited 2 times in pages 38 and 124.

NORMEY-RICO, J. E. *Control of dead-time processes*. [S.l.]: Springer Science & Business Media, 2007. Cited 3 times in pages 36, 39, and 99.

NORMEY-RICO, J. E.; CAMACHO, E. F. Unified approach for robust dead-time compensator design. *Journal of Process Control*, Elsevier, v. 19, p. 38–47, 2009. Cited 7 times in pages 36, 39, 62, 64, 73, 85, and 129.

NORMEY-RICO, J. E. et al. An automatic tuning methodology for a unified dead-time compensator. *Control Engineering Practice*, Elsevier, v. 27, n. 1, p. 11–22, 2014. Cited 6 times in pages 35, 36, 37, 47, 83, and 84.

ONO, M. et al. Discrete modified Smith predictor for an unstable plant with dead time using a plant predictor. *International Journal of Computer Science and Network Security*, v. 10, p. 80–85, 2010. Cited in page 39.

ONO, M. et al. Discrete modified Smith predictor based on optimal control method for a plant with an integrator. In: *2010 IEEE International Conference on Systems Man and Cybernetics (SMC)*. Istanbul: [s.n.], 2010. p. 630–635. Cited in page 39.

PALMOR, Z. J.; HALEVI, Y.; KRANSNEY, N. Automatic tuning of decentralized PID controllers for TITO processes. *Automatica*, v. 31, p. 1001–1010, 1995. Cited in page 37.

PEREIRA, R. D. O. et al. Automatic tuning of a dead-time compensator for stable, integrative and unstable processes. In: *2016 IEEE Biennial Congress of Argentina*. Buenos Aires, ARG: [s.n.], 2016. Cited 3 times in pages 35, 41, and 47.

PEREIRA, R. D. O.; TORRICO, B. C. New automatic tuning of multivariable PID controller applied to a neonatal incubator. In: *8th International Conference on Biomedical Engineering and Informatics (BMEI)*. Shenyang: [s.n.], 2015. Cited 2 times in pages 35 and 38.

PEREIRA, R. D. O. et al. Implementation and test of a new autotuning method for PID controllers of TITO processes. *Control Engineering Practice*, v. 58, p. 171–185, 2017. Cited 2 times in pages 35 and 41.

RIBIĆ, A. I.; MATAUŠEK, M. R. A dead-time compensating PID controller structure and robust tuning. *Journal of Process Control*, v. 22, p. 1340–1349, 2012. Cited 4 times in pages 39, 127, 128, and 133.

SANTOS, T. L. M.; BOTURA, P. E. A.; NORMEY-RICO, J. E. Dealing with noise in unstable dead-time process control. *Journal of Process Control*, n. 20, p. 840–847, 2010. Cited in page 36.

SEBORG, D. E.; EDGAR, T. E.; MELLICHAMP, D. A. *Process Dynamics and Control - 2nd edition*. USA: Wiley, 2004. Cited in page 100.

SHEN, S.-H.; YU, C.-C. Use of relay-feedback test for automatic tuning of multivariable systems. *AIChE Journal*, v. 40, p. 627–646, 1994. Cited in page 37.

SHINSKEY, F. G. *Feedback controllers for the process industries*. New York, NY: McGraw-Hill, 1994. Cited 2 times in pages 60 and 83.

SHIU, S.-J.; HWANG, S.-H. Sequential design method for multivariable decoupling and multiloop PID controllers. *Industrial and Engineering Chemistry Research*, v. 37, p. 107–119, 1998. Cited in page 37.

SKOGESTAD, S. Simple analytic rules for model reduction and PID controller tuning. *Journal of Process Control*, v. 13, p. 291–309, 2003. Cited 10 times in pages 46, 47, 48, 60, 62, 63, 64, 65, 98, and 102.

SKOGESTAD, S.; POSTLETHWAITE, I. *Multivariable Feedback Control*. Chichester: John Wiley & Sons, 1996. Cited in page 47.

SMITH, O. Closed control of loops with dead time. *Chemical Engineering Progress*, v. 53, n. 5, p. 217–219, 1957. Cited in page 36.

TAN, K.; LEE, T.; LEU, F. Predictive PI versus Smith control for dead-time compensation. *ISA Transactions*, v. 40, p. 17–29, 2001. Cited in page 39.

TORRICO, B. C. et al. Anti-windup dead-time compensation based on generalized predictive control. In: *2016 American Control Conference (ACC)*. [S.l.]: IEEE, 2016. v. 2016-July, n. July, p. 5449–5454. Cited in page 41.

TORRICO, B. C. et al. Simple tuning rules for dead-time compensation of stable, integrative, and unstable first-order dead-time processes. *Industrial & Engineering Chemistry Research*, American Chemical Society, v. 52, p. 11646–11654, 2013. Cited 2 times in pages 36 and 75.

TORRICO, B. C.; CORREIA, W. B.; NOGUEIRA, F. G. Simplified dead-time compensator for multiple delay siso systems. *ISA Transactions*, v. 60, p. 254–261, 2016. Cited in page 36.

VAZQUEZ, F.; MORILLA, F.; DORMIDO, S. An iterative method for tuning decentralized PID controllers. In: *Proceedings 14th IFAC World Congress*. Barcelona, E: [s.n.], 1999. Cited in page 38.

VERONESI, M.; VISIOLI, A. A technique for abrupt load disturbance detection in process control systems. In: *Proceedings of the 17th IFAC World Congress*. Seoul, ROK: [s.n.], 2008. p. 14900–14905. Cited in page 49.

VERONESI, M.; VISIOLI, A. Performance assessment and retuning of PID controllers. *Industrial and Engineering Chemistry Research*, v. 48, p. 2616–2623, 2009. Cited 10 times in pages 35, 36, 37, 38, 41, 47, 48, 60, 62, and 99.

VERONESI, M.; VISIOLI, A. An industrial application of a performance assessment and retuning technique for PI controllers. *ISA Transactions*, v. 49, p. 244–248, 2010. Cited 6 times in pages 35, 37, 38, 41, 47, and 60.

VERONESI, M.; VISIOLI, A. Performance assessment and retuning of PID controllers for integral processes. *Journal of Process Control*, v. 20, p. 261–269, 2010. Cited 7 times in pages 35, 36, 37, 38, 47, 60, and 61.

VERONESI, M.; VISIOLI, A. An automatic tuning method for multiloop PID controllers. In: *Preprints 18th IFAC World Congress*. Milan, ITA: [s.n.], 2011. Cited 4 times in pages 35, 37, 38, and 47.

VERONESI, M.; VISIOLI, A. A simultaneous closed-loop automatic tuning method for cascade controllers. *IET Control Theory and Applications*, v. 5, p. 263–270, Januar 2011. Cited 4 times in pages 35, 37, 38, and 47.

VERONESI, M.; VISIOLI, A. Performance assessment and retuning of PID controllers for load disturbance rejection. In: *Preprints IFAC Conference on Advances in PID Control*. Brescia, ITA: [s.n.], 2012. Cited 6 times in pages 35, 36, 37, 41, 47, and 48.

VISIOLI, A. *Practical PID Control*. [S.l.]: Springer, 2006. Cited in page 94.

WANG, Q.-G.; HUANG, B.; GUO, X. Auto-tuning of TITO decoupling controllers from step tests. *ISA Transactions*, v. 39, p. 407–418, 2000. Cited in page 37.

WANG, Q.-G.; NIE, Z.-Y. PID control for MIMO processes. In: *PID Control in the Third Millennium (R. Vilanova and A. Visioli eds.)*. London, UK: Springer, 2012. p. 177–204. Cited in page 37.

WANG, Q.-G. et al. *PID Control for Multivariable Processes*. [S.l.]: Springer, 2008. Cited in page 37.

WANG, Q.-G. et al. Auto-tuning of multivariable PID controllers from decentralized relay feedback. *Automatica*, v. 33, p. 319–330, 1997. Cited 3 times in pages 37, 38, and 39.

WOOD, R. K.; BERRY, M. W. Terminal composition control of a binary distillation column. *Chemical Engineering Science*, v. 28, n. 16, p. 1707–1710, 1973. Cited in page 103.

ZHANG, M.; JIANG, C. Problem and its solution for actuator saturation of integrating process with dead time. *ISA Transactions*, v. 47, p. 80–84, 2008. Cited in page 39.